N6-Methyladenosine Bimodal Peak Signature Mediates Acute and Selective Stress Translation by Specialized Cytoskeletal Ribosomes via a MARK4-FTO-PKR Axis

by

Bruno Saleme

A thesis submitted in partial fulfillment of the requirements for the degree of

Doctor of Philosophy

Department of Medicine

University of Alberta

Abstract

Cellular responses to stress are temporally-organized complex pathways designed to prioritize resources and adapt in order to promote repair and survival[1, 2]. In severe stress, the energetically demanding mRNA translation is mostly inhibited, but it is not known whether there is a universal mechanism that preserves the translation of acutely needed stress response proteins (SRPs)[1-6]. Here we show that the dynamic epitranscriptomic n6-methyladenosine (m6A) mRNA modification is used as an SRP mRNA marker, allowing for selective translation in microdomains consisting of specialized ribosomes (compatible with the recent discovery of ribosomal diversity[7-10]), the m6A demethylase FTO[11], and stress related kinases (MARK4 and PKR[12-15]), attached on the cytoskeleton (i.e. g tubulin). SRP mRNAs are characterized by a dual peak methylation pattern, downstream of their 3UTR segment, which hosts the eIF2a kinase PKR that inhibits their translation when they exit the nucleus. FTO, which also binds at the same site, is activated via a T6 phosphorylation by the stress kinase MARK4 and removes this dual peak methylation signature, removing the inhibitory effects of PKR, allowing the translation of SRPs. We describe a previously unrecognized, microtubule associated translation system for the translation of SRPs during the critical early stages of acute stress, when the translation of other proteins is mostly inhibited.

Preface

This thesis is an original work done by Bruno Saleme. No part of this thesis has been previously published as of the date of submission of this thesis.

Acknowledgements

This work, and all of my research work so far, would not have been possible for the mentorship, guidance, support, and friendship of the following people. First and foremost, Dr. Evangelos Michelakis, my mentor and supervisor, has provided me with timeless wisdom and tools that extend far beyond my academic career and has designed a rare environment at the lab to allow us to explore our limits. Dr. Gopinath Sutendra, my co-supervisor, mentor, and friend, has played an equally important role in my growth as a researcher and thinker. Dr. Richard Fahlman and Dr. Glen Jickling have provided me with great guidance and support in several critical experiments. Last but not least, I don't think journey would have been possible without the love and support of my friends and family.

Table of Contents

List of Figures

List of Abbreviations

Abbreviation	Meaning
2DG	2-deoxy-glucose
ALKBH5	AlkB family member 5, RNA demethylase
AMN	alpha-amanitin
AMPK	AMP-activated protein kinase
ATF4	Activating transcription factor 4
ATP	Adenosine triphosphate
CHOP	C/EBP homologous protein
CHX	Cycloheximide
CNT	control
COL	Colchicine
CS	Cytoskeletal
Cyto	Cytosolic
DAPI	4′,6-diamidino-2-phenylindole
eIF2a	eukaryotic Initiation factor 2a
ER	endoplasmic reticulum
ERK	extracellular signal regulated kinase
FTO	Fat mass and obesity associated protein, alpha-ketoglutarate dependent dioxygenase FTO
GCN2	general control nondepressible 2
GDP	guanosine diphosphate
GTP	guanosine triphosphate
HIF1a	hypoxia inducible factor 1a
HRI	heme-regulated eIF2a kinase
HS	heat shock
IF	Immunofluorescence
IP	immunoprecipitation
IRES	internal ribosome entry site
ITAF	IRES trans-acting factor
JNK	c-Jun N-terminal kinase
L-AHA	L-azidohomoalanine
lncRNA	long non-coding RNA
M6A	N-6 methyladenosine
MAMS	Microtubule-associated m6A-stress translation
MARK4	microtubule-associated protein(MAP)-microtubule affinity regulating kinase
meRIP	methylated RNA immunoprecipitation

Met	methionine (or methionine deprivation)
METTL14	N6-adenosine-methyltransferase 14
METTL3	N6-adenosine-methyltransferase 3
miRNA	microRNA
MT	microtubule
mTOR	mammalian target of Rapamycin
ng	nanogram
NT	Non-transfected
OPP	O-propargyl-puromycin
p (prefixed with protein name)	phospho-
PAR-CLIP	photoactivatable ribonucleoside-enhanced crosslinking and immunoprecipitation
PCR	polymerase chain reaction
PERK	protein kinase R-like ER kinase
PKR	protein kinase RNA-activated
PLA	Proximity ligation assay
qRT	quantitative reverse transcriptase PCR
RDB	RNA dotblot
Ribo-SEC	Ribosome size exclusion chromatography
Ribo-seq	Ribosome (mRNA) sequencing
RLP26	60S ribosomal protein L26
rRNA	ribosomal RNA
S6	S6 ribosomal protein
Scr	Scrambled siRNA
SG	Stress granule
siFTO	FTO siRNA
SILAC	stable isotope labelling of amino acids in cell culture
siMARK4	MARK4 siRNA
siMETTL3	METTL3 siRNA
siPKR	PKR siRNA
siScr	Scrambled siRNA
SRP	stress response protein
SRSF7	serine and arginine rich splicing factor 7
T6	threonine-6
T6A	threonine-6 mutation to alanine
TE	translation efficiency
TIAR	Nucleolysin TIAR
tRNA	transfer RNA
Tub	tubulin
uORF	upstream open reading frame

UTR	untranslated region
UV	ultraviolet radiation
VDAC	voltage-gated anion channel
VEH	vehicle
WB	western blot
YTH	YTH-domain

Chapter 1

Introduction

1.1.Introduction to protein synthesis.

Protein translation is the fruit of the central dogma as proteins carry out almost the entirety of biological functions. Not surprisingly, nature has evolved highly sophisticated machinery and the largest biological complex, the ribosome, to carry out this function[1]. Carrying out this task is no small feat, and it comes with several challenges, that I have summarized into 4 main challenges, that nature has solved in various ingenious ways, with an emerging fifth challenge that will be the focus of this work. **First challenge** is scalability; the translation machinery produces all proteins in cells and decides on *how much* protein to make, and since cells require millions of proteins at any given time, with constant production and degradation, protein synthesis becomes one of the most important jobs a cell has to do. Not surprisingly, some of the most potent toxic substances inhibit the ribosomes which would invariably result in cellular death[2]. Cells manage the scalability challenge by simply building a very large arsenal of ribosomes, which does the job but at a great cost, more on this in next section.

The **second challenge** revolves around *which* mRNAs to translate, and how much protein should ribosomes make from each mRNA? While this may seem trivial at first, it is one of the most crucial roles of the translation machinery. Some proteins are only required in finite amounts while others, such as structural proteins, are required in much more abundant amounts, with some single proteins comprising more than a third of all proteins made in the body, such as certain structural proteins[3]. An easy solution for this problem is to simply make more of the mRNAs that need to be translated more, relaying the regulation to the first step in the central dogma (transcription), and this is certain the case for several proteins[4]. However it is now evident that mRNA levels do not necessarily correlate with protein levels, and this remains a

very active area of research[4]. Advances in our knowledge in this field include mRNA regulatory elements, other regulatory RNAs (miRNAs, lncRNA), RNA modifications (both at the mRNA, tRNA, and rRNA levels), and ribosomal heterogeneity, along with myriads of RNA binding proteins and ribosomal binding and regulating proteins[1, 4-13]. All these systems, possibly among others, come together to contribute to solving this challenge; how much of each mRNA should be translated at a given time? These systems will be discussed in more detail in subsequent sections as well.

The **third challenge** the translation machinery has to solve is *where* to "print" each protein? The reason this is a challenge lies in the inherent diversity of proteins, and the diverse requirements to make optimal proteins. Proteins do the grunt of the work in the cell and the cell has lots of diverse microenvironments and functions that require very diverse proteins. Some of these diverse factors are protein folding, which may require special chaperones, protein modifications, which requires unique post translation modification systems, different pH or redox environments, among others[1, 6, 10, 12, 14-16]. This has naturally resulted in different pools of ribosomes to cater to these different protein needs, discussed in more detail in section 1.5, along with myriad of ribosome-associated proteins, known now as ribo-interactome[17].

Just like in physics, the **fourth challenge** of protein translation problem, or dimension, is time. The translation machinery needs to make decisions on *when* to make the proteins. The reason timing is also a critical challenge becomes apparent when emergencies happen. When a building catches fire, timing is of the essence and critical decisions have to be made to divert resources to minimize damage, put out the fair, and start repairs[18]. Similarly when cells get

infected with a virus, or when resources become low all of a sudden, or when a zap of DNA damaging agent wreaks havoc on your blue prints, critical decisions have to be made to minimize energy production, and divert resources to prioritizing life-saving emergency measures or else cell death would be eminent. While all four challenges are active areas of research, and lots of knowledge has been discovered to date, the fourth challenge remains more elusive[18-20]. This will be discussed in more detail in section 1.4. and 1.6 and will also be one of the main focuses of this thesis. A **fifth challenge** will emerge after discussing stress and cellular responses to stress which would incorporate elements of all four previous challenges discussed above to solve stress-unique translation problems. This fifth challenge will be the focus of this study and will be outlined in detail in section 1.7.

1.2.Translation Scalability and energy

It is estimated that cells have over 100 million proteins, all of which were made by hand, if you will, by ribosomes, one amino acid at a time[21]. The average rate of protein synthesis is 6-9 amino acids per seconds, or if we split the difference, 7.5 amino acids/seconds. The average length of proteins is around 300 amino acids. This means that it would take 225 billion seconds, or close to 6000 years, of translation time to make enough proteins for one cell. This challenge can obviously only be solved with numbers and brute force, so cells build a very large army of ribosomes, 10 million strong to carry out this task in the order of hours[10]. This comes at a great cost of consuming up to 50-60% of ATP energy in the cell however[10]. To put that in perspective, the United States of America, the country with the strongest and most expensive military in the world by a long shot, spends ~3.4% of its gross domestic product (GDP) on its military. The cost for cells is obviously justified as nature has evolved to be efficient and if there

was a less expensive way for cells to build ribosomes it likely would have appeared by now. The other intriguing thought is that a significant percentage of ribosomes in the cell will be making other ribosomes as ribosomes are protein-RNA complexes. This concept becomes highly critical when resources become limited such as in stress. Not surprisingly, ribosome biogenesis in intimately linked to energy production in the cell and the mTOR pathway[22]. Therefore solving the scalability of protein synthesis challenge (*challenge 1*) comes at a great price tag of being the single most expensive ticket item a cell needs to survive, a 50-60% tax on its total ATP production, a number that has great implications when resources become limited[23-25].

1.3 Translation Selectivity and the RNA world

After the cell has made the critical investment of spending half its ATP to make all the ribosomes, it now has to decide on which mRNAs to translate, and how much of each mRNA to translate. The simplest possible model is translating each mRNA that is available at a steady rate and at the same ratio as any other mRNA. This means that if a hypothetical cell requires 10 of very important protein (VIP) and 1 of very lonely protein (VLP), it has to transcribe 10 VIP mRNAs and 1 VLP mRNA and both mRNAs will be translated at the same rate making 10 VIPs and 1 VLP per time unit. While this model is certainly utilized for some mRNAs, it became very clear early on that lots of mRNA-protein levels do not correlate, and that mRNAs have different half lives in the cell[26]. This means that each VIP mRNA might actually make 10 proteins while the VLP mRNA might be degraded quickly, from loneliness perhaps, making no proteins, and we end up with 100 VIPs and 0 VLPs. These two concepts are addressed in translation efficiency and mRNA half-lives, which are the two main factors that fine tune solutions for

challenge 2. Delving deeper into those two factors, we find a lot of pathways and tools used by a cell to modulate the translation efficiency and half-live of an mRNA.

1.3.1. Translation Efficiency: A myriad of factors have been discovered so far that regulate mRNA translation efficiency[27, 28]. These factors can be further subdivided into factors endogenous to the mRNA itself, and factors external to the mRNA. *Endogenous mRNA factors* include 5' cap composition, sequence-specific elements such as 5'UTR elements (uORFs), exonic elements, 3'UTR elements, as well as poly(A) tail length, and most recently, mRNA epitranscriptomic modifications[11, 28-32]. All of these factors have been linked to regulating and varying the translation efficiency of an mRNA, or in other words, they help the translation machinery decide on how much protein to make from each mRNA. *Exogenous mRNA factors* are also very diverse and include mRNA binding proteins that may increase or decrease translation efficiency, RNA elements, such as lncRNA, translation machinery elements themselves via modifications, such as eIF2a phosphorylation, S6 phosphorylation, ribosomal availability, tRNA charging, tRNA modifications, or ribosomal RNA modifications, among others[8, 9, 18, 33-38].

1.3.2 mRNA half-life: If the mRNA is not present it cannot be translated so one of the main ways to fine tune challenge 2 is to regulate the mRNA half-life. Making mRNAs is also a significant energy expenditure to cells, so cells have to make just enough mRNAs, and keep around as long as needed but eventually they all have to be degraded due to damage, need to recycle for resources, changes in protein needs of the cell, among other reasons. mRNA half-life is also determined by similar elements that are involved in translation efficiency, such as the

5'UTR and 3'UTR, poly(A) tail, and epitranscriptomic modifications, but it is also regulated by other external factors such as miRNAs which are critical mRNA-sequence-specific regulatory elements[39-42]. Overall, mRNA half-life remains a critical component of translation regulation, almost as critical as mRNA transcription itself, as the two factor into the steady state and availability of mRNAs in cell.

1.3.4 Epitranscriptomics: One of the more recent discoveries in the mRNA world is the mechanism of some of the mRNA epitranscriptomic modifications, allowing researchers to study the dynamic nature of these modifications, and their implications on mRNA[43-46]. The most abundant mRNA modification is N-6-methyladenosine (or m6A), and although it was discovered back in the 70s, along with other modifications, it was not until recently that this field has gained traction with the discovery of the writers (METTl3 and METTL14 methyltransferase complex), and erasers (FTO and ALKBH5) resulting in myriads of discoveries implicating all aspects of mRNA, biological processes, and human disease[8, 11, 29, 39, 40, 43-54]. According to most recent discoveries, m6A modifications occur co-transcriptionally in the nucleus, with some evidence of extra-nuclear presence of the demethylase, FTO[44, 55]. The significance of one methyl tag is that it allows the binding of m6A-binding proteins, YTH domain containing family proteins, and possibly others as we'll see in this work, which can regulate mRNA half-life, location, binding proteins, and even translation[56]. The modification can also simply change the conformation and binding affinity of the nucleotides, as the N-6 position is in the binding domain and nucleotide recognition region of adenosine. The relevance of this modification to decision making by the translation machinery will be become very evident as it is the keystone of this thesis.

1.4 Location and Ribosomal Heterogeneity

Protein synthesis, while identical at its core, produces highly diverse products that have special requirements[1, 57]. Proteins destined to be outside the cell in a relative oxidizing environment, are made differently from proteins designed for a reducing environment. Similarly, proteins that live in membranes have to be made differently form proteins in cytosol[14, 15]. This diversity in protein synthesis conditions has resulted in challenge 3 discussed above which nature has solved by creating subcellular ribosomal pools. There are two main ribosomal pools known to date; one in the cytosol and one on the ER sheets giving the "rough ER" its descriptive name[15]. These two ribosomal pools are thought to carry out the entirety of protein translation.

1.4.1 ER. Vs Cytosolic ribosomes: The ER provides all the specialized tools required for many proteins, such as lipids for membrane-bound proteins, oxidizing potential for certain proteins (-S-S- disulfide bonds in secretory proteins for example), chaperones for assisted folding of specific domains and proteins (such as peptidyl-prolyl isomerases, assembly of subunits in multimeric proteins, packaging proteins for vesicle transport, and special protein modifications such as glycosylation[58, 59]. The cytosol provides a more reducing environment to make cytosolic free floating proteins and also provides the convenience of being everywhere in the cytosol so that proteins can be made at any required site within the cell[1, 10, 16, 35, 57]. Both ribosomal pools have extensive protein binding, and RNA binding, capacity, in what is known as the Ribo-interactome, a field of which we are only beginning to unravel[17, 60]. These binding proteins are predicted to be involved in ribosomal function, translation and protein modification and transport.

1.4.2. Ribosomal Heterogeneity by composition: An intriguing novel concept is emerging in ribosome biology now that suggests that the fine tuning of ribosomal function extends far beyond

the ribosomal location. Ribosomes are made up of two major units made up of ribosomal RNAs (rRNAs) and proteins. In eukaryotes, the 80S ribosomal protein is made up of a 60S large unit (has 28S, 6.8S, and 5S rRNA, along with 49 ribosomal proteins), and the 40S small unit (made up of 18S rRNA and 33 ribosomal proteins)[61, 62]. All together, the eukaryotic 80S ribosome has an astounding size of 3.5-4 MDa. While Ribosomal proteins are some of the most conserved proteins in evolution (some universally conserved across both prokaryotes and eukaryotes)[62, 63]. Given the large size of the ribosomal complex, and the number of protein and RNA elements making up the ribosome, it is not surprising that ribosomal heterogeneity has been predicted to be intrinsic to ribosomes as early as the 1950s, by Dr. George Palade, who first described the ribosomes[64, 65]. Compositional ribosomal heterogeneity, or heterogeneity in the components of a ribosome complex, have been described in every component of the ribosome; the ribosomal proteins (both in stoichiometric ratios, and in paralogues, or alternate proteins), protein modifications, ribosomal RNA and RNA modifications, and ribo-interactome (or ribosome binding proteins)[1, 10, 16, 35, 57].

Stoichiometry and tissue specific expression: Early examples of heterogeneity showed different ribosomal protein expression based on tissue proliferation in *Arabidopsis[65]*. Subsequent experiments confirmed that cells alter ribosomal protein stoichiometry and expression, there are tissue specific ribosomal protein expression such as RPL10L in testes and RPL3L in muscle[65]. It is now estimated that ~25% of ribosomal proteins are expressed in tissue specific manner, and several examples have been described to date showing switching of ribosomal protein paralogues under different conditions[66]. Intriguingly, work in polarised cells such as epithelial cells or neurons, shows ribosomal variation at the subcellular level for selective site-specific translation of proteins[65, 67].

Post Translational Modifications (PTMs): another layer of functional ribosomal heterogeneity emerges from post translational modifications of ribosomal proteins. Phosphorylation of RPeS6 is a characterized downstream effect of mTORC pathways[68, 69], and RPL26, a protein that has been shown to be required for acute translation of p53[70], is modified by UFMylation (ubiquitin fold modified 1), a form of ubiquitination[71, 72]. While the role of some of the modifications is still under investigation, the biological significance is clear as several PTMs are linked to human disease such as RPuS19 phosphorylation and Parkinson's[73].

rRNA diversity, modifications, and the Ribo-interactome: Similar to ribosomal protein diversity, ribosomal RNA, or rRNA, tissue-specific allele diversity has been described, with speculative functional roles to date[17]. Moreover, rRNA nucleotides have a very high post transcriptional modification rate or approximately 2%, or over 200 sites, with various modifications such as 2'-O-methylation, pseudouridylation, ribosylation, and methylation and acetylation on different sites of the base, among others[74-76]. All these RNA modifications may add yet another layer of diversity to ribosomal function. Last but not least, ribo-interactome, or proteins interacting with ribosomes, is an emerging area of translation regulation and ribosomal heterogeneity with the recent discovery of pyruvate kinase M2 (PKM2) as an important ribosomal interacting protein with preference for ER rather than cytosolic ribosomes[17]. All these areas of diversity present many unknowns about significance to ribosomal functions and human disease, but they do for sure shed a clear light about the heterogeneity of ribosomes in cells.

1.4.3. Ribosomal heterogeneity by location – while many of the previous examples of ribosomal heterogeneity are cell or tissue specific, there is yet another dimension of

subcellular ribosomal heterogeneity defined by subcellular ribosomal location[14]. The classic example is the cytosolic and ER distribution of ribosomes where, as mentioned above, provide some functional specialization for ribosomes in terms of the types of proteins they can make. For example ER ribosomes specialize in synthesizing membrane-bound proteins due to requirement of lipid bilayer co-translationally[1, 15, 57, 65]. There are however other examples that may suggest further subspecializing for ribosomes within the cell based on locations. One example is the sub-localization of ribosomes within polarized cells to produce micro-domain specific proteins such as in neurons and epithelial cells[67, 77]. Other examples include recently described mitochondrial-bound ribosomes whose function is yet to be characterized[78]. Lastly, there are very few examples hinting at association of ribosomes with cytoskeleton, such as F-actin-associated polysomes in HeLa cells, microtubule in sea urchin embryos, and intermediate filaments in myocardial Purkinje fibers[79-81]. While a lot more work is needed to prove the subcellular specialization of ribosomes based on location within a cell, beyond the cytosol and ER distinction, it would not be surprising if future studies prove that heterogeneity of ribosomes extends to different subcellular pools.

1.5. Cytoskeleton and mRNA

While the RNA *(1.3)* and ribosomal *(1.4)* heterogeneity address *Challenge 2* in the translation in combination, which is deciding which mRNA to translate, *Challenge 3,* or the location of translation, requires the introduction of additional players. In biology, we cannot discuss location of molecules without discussing the cytoskeleton which constitutes the main highways of transportation of all subcellular compartments, including mRNA. The cytoskeleton has three distinct, well integrated, components; the actin network (microfilaments), the

microtubules, and the intermediate filaments[80]. While all three components interact and have been linked to myriad of cellular processes and diseases, the details of the cytoskeletal systems are beyond the scope of this study, but we will focus on a very important part of the cytoskeleton for the purpose of translation regulation in this thesis, which is the microtubules, although other components of the cytoskeleton have strong links to the translational machinery[82].

1.5.1. F-Actin and translation: One of the strongest links to date between cytoskeleton and protein translation is between F-Actin and the translation machinery[80]. Early electron microscopy observations noted interaction between F-actin and polysomes and subsequent studies have shown strong evidence for the involvement of F-actin and bulk protein synthesis[83-92]. Drugs that disrupt F-actin (e.g. latrunculin and cytochalasin D) decreased bulk protein synthesis, as did genetic mutations in various cell lines[83-98]. Moreover, eEF1A (eukaryotic elongation factor 1A) has been shown to bind and crosslink F-actin has also been shown to be a major regulator of initiation of protein synthesis[99, 100]. Translation machinery is a very large complex and it requires the communication between various com[101-109]ponents at every stage of translation and F-actin is thought to be an important player in the communication process between various translation machinery components. Moreover, an important role for F-actin has emerged in supporting local translation within a cell, particularly in polar cells such as epithelial or differentiating cells, or large cells such as neurons[67, 77, 82, 110]. All together data so far suggest an important role for actin networks in the regulation of bulk protein synthesis of which clinical significance is only beginning to emerge.

1.5.2. Microtubules, mRNAs, and translation*:* While F-actin is emerging as the dominant cytoskeletal element regulating bulk protein synthesis, microtubules may play an equally important role in regulating mRNA translation despite some experiments suggesting that

they have no role in the bulk synthesis of protein[80, 111, 112]. Existing data so far point to a role for microtubules in localization and transport of specific mRNAs, especially in neurons[101, 107, 109]. However, given the unique properties of microtubules, we should not give up on a possible important regulatory role for microtubules in mRNA translation. Perhaps the unique properties of microtubules are better utilized in the *selective* translation regulation of mRNAs, rather than the general regulatory role for bulk protein synthesis by F-actin. Microtubules are the largest of the three cytoskeletal network systems in cells. Their large size, coupled with their dynamic nature, and the kinesis and Dynein motor transportation system make them the major highway system in cells, and the fastest way to get around the cell, which in the case of neurons can be vast travelling distances for biomolecules. Microtubules are also able to form complexes with ER tubules forming ER tubule-microtubule domains[113-120]. The reason why this would be highly useful for translation regulation is because it would be one of the very few locations, other than the ER, where translation machinery has access to lipid bilayer for synthesizing membrane-bound proteins. Having an alternate location for translating lipid-bound proteins could prove highly useful in situations of ER stress during which translation even at the ER sheets is stalled. Moreover, microtubules have their own microtubule associated proteins and kinases (known as MAPTs and MARKs, for microtubule associated proteins, and microtubule affinity related kinases, respectively) that have been shown to play very important regulator roles in protein homeostasis, cell survival and proliferation, and protein translation[121-127]. Lastly, although very scarce and weak in nature, there is some evidence suggesting that ribosomes may associate with microtubules, with stronger evidence showing binding of other translation machinery elements to microtubules such as RNA, ribosomal proteins, and translation factors[81, 128]. All together, these concepts can lay the foundation for a specialized role of microtubules in

regulating selective translation of mRNAs, perhaps under specific conditions where speed, efficient transportation, and selective regulation are required, such as during stress.

1.5.3. Microtubules and special proteins, i.e. p53 – While lots of proteins bind to microtubules during transport across the cell, there is strong evidence showing specific binding of specialized proteins to microtubules such as p53[129-131]. P53 is one of the first tumor suppressor proteins discovered and has been shown to be one of the major transcription factors in cells regulating up to 30% of mRNA transcription[132-134]. It's important role emerged into the research and clinical field with the discovery of pathogenesis of Li-Fraumeni syndrome, which predisposes patients to myriad of cancers at an early age, and has thus been dubbed since as the guardian angel protein[135]. The reason why this is important is because of the strong evidence between the association between p53 and microtubules, which has been shown to bind to and transport along the microtubule networks. P53 is a special protein because it is known that it is translated from pre-existing mRNA within 20 minutes of UV stress, and the protein transports to the nucleus in less than 30 minutes[70]. These would not be possible if it weren't for the microtubules facilitating the transportation. However is it possible that the role of microtubule extends beyond transportation in the case of p53? This intriguing question is important to ask because if this is true, p53 can simply be one of many specialized proteins that utilized an alternate translation coupled to microtubules to bypass distances and time when needed quickly. Therefore the unique roles of microtubule, and the possible links to the translation machinery make it especially adapted to play a specialized role in translation, a link that we will explore in detail in this thesis.

1.5.4. Microtubules and stress response- While the prominent role of microtubule in cell division, cellular structure, and trafficking, are well established, equally important might be the

increasingly recognized role of microtubules in stress signaling and responses. Microtubules are now known to be involved in sensing and being a part of the stress response for several major stresses via different mechanisms such as signaling responses, sequestration of stress proteins, remodeling, amongst others[130].

Microtubules as stress sensors: Microtubules mediate HIF1a translocation to the nucleus, and the microtubule associated proteins (MAPs) interact with mitochondrial and glycolytic proteins to regulate energetics during hypoxia, which along with dramatic structural remodeling, strongly implicate microtubules in hypoxic stress response[136-138]. Similarly, oxidative stress results in microtubule changes involving isoform changes and post translational modifications on cysteine regulating structure and signaling transforming the large networks into oxidative stress sensors[139-142]. Moreover, microtubules are also involved in sensing and responding to metabolic stresses by binding to and regulating the mitochondria including VDAC, along with glycolytic proteins, and various Kreb's cycle enzymes[143-149]. While the specifics of each interaction varies, it stands clear that microtubules are early sensors and mediators of metabolic stress. Similarly, important DNA damage sensors and repair enzymes are known to interact with microtubular proteins, which has been shown to have functional implications on DNA damage response as well[150]. While the outcomes of each relationship may be different, microtubules are thought to have a protective role against apoptosis due to sequestration of Bcl-2 and the interactions with mitochondrial VDAC[151-156].

Microtubules as signaling regulators: several important signaling pathways interact extensively with microtubules including the MAPK superfamily such as ERKs, JNK and p38 families, which sense a variety of stresses and mediate the major stress responses[157]. Their interaction with microtubules, estimated to encompass a third of the MAPK superfamily, plays

important roles in the initiation and execution of these cellular stress responses[130]. As mentioned earlier, various transcription factors and stress mediators such as p53 and HIF1a also rely on the interaction with microtubules placing microtubule networks at the centre of sensing and early response to stress, a role that will be of critical importance in translation regulation in stress as will be shown later on.

Stress Microtubule proteins and isoforms: It is also important to note that there are several isoforms of alpha and beta microtubules, several of which are associated with various disease, such as cancer[158-161]. Of note is beta-III tubulin, which is a downstream target of HIF1a, is involved with oxidative stress sensing, binding to and regulating metabolic proteins and apoptotic proteins, among others[130, 138]. These have unsurprisingly implicated beta-III tubulin in various solid cancers as a poor prognostic factor[130, 158-161]. Another important tubulin isoform is gamma tubulin, which forms the gamma-tubulin ring complexes (gTuRC) involving gamma tubulin and other proteins providing the centrosomal and non-centrosomal nucleation centres of microtubules[162]. Nucleation centres are where microtubules originate and they are the most stable end of microtubules[162]. They play critical roles in centrosomal function and chromosomal separation, but they also form non-centrosomal nucleation centres outside of mitosis, the "y-shaped" fork of microtubules, with poorly understood functions[162, 163]. Beyond it's role in forming the nucleation centres of microtubules, gamma-tubulin is strongly linked to DNA damage repair and checkpoints[164, 165]. DNA repair protein BRCA1 localizes to centrosomes and forms a complex with gamma tubulin prior to its transportation to the nucleus[164, 165]. Intriguingly, multiple DNA damage response pathway elements associated with the centrosomes placing gamma tubulin at the forefront of DNA damage sensing and repair pathways[162-165]. Together with the fact of having that gamma tubulin also forms

the most stable regions along the microtubule networks, makes us wonder whether its roles in extend far beyond what is currently known, possibly into being an important mediator of stress and translation.

1.6 Stress response stages

Living is very stressful; biological living that is. For cells to exist, they have to overcome various abiotic barriers such as UV, fluctuating temperatures, ion imbalances, pH disturbances, nutrient deficiencies, among many others, on a constant basis. As such, stress is one of the major driving forces of evolution and adaptation in biology that shapes cell development, survival, ageing, and disease[166]. One of the earliest stresses, UV, has shaped our DNA damage responses which is intimately linked to cancer and ageing. Similarly, oxidative stress and energy and metabolic limitation have been shaping our cells since the earliest ancestors, as do pathogens and infections. It is not surprising that many stress responses are universal in nature, almost immediate in their onset, and overarching with their effects[166-168]. Stress responses will be the major focus of this thesis, particularly the early translation-related stress responses.

1.6.1. Universal responses: Various universal stress responses have evolved to allow cells to either repair damage after stress and survive, or initiate cell death. These responses are organized temporally to prioritize resources and repair[168]. Just like in real emergencies and trauma, triaging helps to limit damage and maximize survival, and cells have their own version of triaging via interconnected stress response pathways. One of main universal responses to stress is inhibition of protein translation[19, 167]. As mentioned earlier, protein translation is the most energy consuming system in the cell and when stress occurs, energy must be preserved for

repair pathways, so protein translation is halted[19, 167]. This is done in various mechanisms discussed in section 1.6.2, but the implications of inhibition of translation

While stresses may vary in nature, such as UV, oxidative stress, metabolic deprivation, temperature fluctuations, etc, there are certain universal responses that cells undertake regardless of type of stress[169, 170]. This is because simply put, stresses damage cells, and cells need to prioritize repairing the damage, so they can survive. This damage repair prioritization and triaging is where the universal stress responses lie, and protein translation is a central component of these responses for two main reasons. Stress affects nearly every element in cells and tissues, such as transcription, cytoskeleton, metabolism, protein homeostasis, signaling, to name a few, yet protein translation is one of the most important stages where stress responses really matter [167, 168]. As mentioned earlier, protein translation machinery is the most energetically expensive task in the cell and just like in war time, resources become very limited and cells need to prioritize energy expenditure. For this reason, several pathways have been discovered to date that work together to shut down protein translation almost immediately after any stress. The details of these regulatory mechanisms will be discussed in section 1.6.2. Thus, turning off protein translation after stress has now diverted lots of energy away from protein synthesis and anabolic processes towards damage repair and adaptation. This leads us to the second reason of why translation is central in stress responses. Initiating repair and stress adaptive pathways often requires the synthesis of new specialized proteins[167, 168]. These are proteins that play very important roles during stress, but not at baseline conditions, or they may play other roles at baseline, and they may be needed in larger quantities to perform specific roles after stress. Whatever the case for each individual stress response protein (or SRP), cells must find a way to

make a lot of them immediately after stress when everything, including protein synthesis machinery, is shutting down. In such unstable and taxing moments, every second matters, and cells would not be able to afford the time to synthesize SRP starting with transcription; SRPs would theoretically be made immediately from pre-existing mRNAs that were prepared ahead of time for such times. Transcription takes on average several hours, and in the case of the Immediate Early Genes (IEGs), it can occur in the order of 5-20 minutes for a few select mRNAs, but whatever the case, whether it's IEGs as a best case scenario, or an average SRP mRNA, this is time that cells may not have[171, 172]. Therefore, while many studies have shed a lot of light on the regulation of transcription during stress, these programs, while critical for survival, tend to be more involved in the subacute *(hours)* to chronic *(days)* stress response stages after stress, which deal more with adaptation to stress. Therefore, it is more plausible that protein translation is the central player in reprogramming immediately after stress, in the hyperacute *(seconds)* to acute *(minutes)* stages after stress. As we will see in the studies conducted in this research program, translation is critical for the hyperacute and acute responses to stress in cells and all the various components discussed in the introduction will shed light on a novel system that is designed to solve the hyperacute selective stress-translation problem. Those two central translation-related responses, first being global protein synthesis shut down, and second being the hyperacute selective translation of SRPs, would be universal responses to stress that cells have to undertake, regardless of the nature of the stress, and the background on these two universal responses will be discussed in more detail below.

1.6.2. stress response and translation inhibition. Translation shutdown after stress is a highly conserved mechanism of survival from bacterial to humans[37]. Moreover, multiple mechanisms are in place to ensure efficient translation shutdown in cells, all pointing to the

importance of this universal step in the stress response pathway[173, 174]. Translation initiation is thought of as the rate limiting step in translation, during this step the mRNA and the ribosome come together, a process that is highly regulated and highly complex[174]. The mRNA is brought to the ribosome by the eIF4E complex which forms the eIF4F by binding eIF4G scaffold protein and eIF4A helicase[18, 174]. The other complex is the ternary complex which involves charged Met-tRNA and GTP-bound eIF2[18, 174]. This complex binds to the 40S ribosome small unit along with other factors forming the pre-initiation complex or PIC[18, 174]. The mRNA complex and PIC come together and start scanning the mRNA which marks the initiation process. While subsequent steps of translation, such as elongation and termination, are also regulated in stress, the majority of known regulation occurs at the initiation step[18, 174]. During stress, several stress kinases are activated via different mechanisms, these include JNK, p38, AMPK, and others[18, 19, 38, 167, 175]. Once stress kinases are activated, they inhibit both complexes of initiation via post-translational modifications of different regulatory nodes. The mRNA complex is inhibited by the binding of eIF4E-binding protein (4EBP) which completes with eIF4G[18]. This is inhibitory step is kept under control under normal conditions by mTORC1[18, 176, 177]. Moreover, the eIF2a subunit of the eIF2 complex in PIC is also a target for major regulation under stress. Four eIF2a kinases are known to phosphorylated it at S51 under a variety of stress. These kinases include PKR, activated by viral dsRNA, HRI, activated by heme deprivation, GCN2, activated by amino acid starvation and DNA damage, and PERK which is activated by unfolded proteins in ER[18, 38, 167, 176-179]. The S51 phosphorylation inhibits the GTP-GDP exchange effectively halting translation initiation[18, 179]. Multiple regulatory nodes are activated at the same time to effectively turn off translation during stress, this includes binding of 4EBP to eIF4F, eIF2a phosphorylation, along with elongation inhibition,

ribosomal modifications, such as S6 phosphorylation by S6 kinase (S6K), and mRNA and tRNA modifications[18, 38, 174, 175].

1.6.3. selective SRP translation: Despite all the inhibitory measures that are activated after stress, cells are still able to translate a few select SRPs. One of the known mechanism by which certain transcripts can bypass the translation inhibition is by using IRES, or internal ribosomal entry site, and ITAF, or trans-acting factors, partners[18, 178]. This was initially discovered in certain viruses where viral RNA was able to bind to ribosomes and translate the mRNA without the need of cap-binding proteins, with the help of an ITAF[30]. This IRES-ITAF system was found to help translate various endogenous mRNAs such as c-Myc, p53, XIAP, BCL2, and others, which were confirmed to have an IRES element in their 5'UTR[30]. Another system that allows mRNAs to bypass the inhibition is through having multiple start sites upstream (or uORFs) of the main start codon[180]. These start codons are either same as the canonical AUG, or can also be CUG. They act to generally inhibit translation at baseline, but can allow translation to proceed when eIF2a is phosphorylated due to leaking scanning[180, 181]. While uORFs have been shown to increase ribosomal loading on multiple mRNAs during stress, their abundance (50% of all mRNAs), and the exact mechanisms and contribution to selective translation in stress remain elusive[180, 181]. One well understood example is ATF4, which is increased dramatically, in a translation-dependent manner, after methionine deprivation. ATF4 contains uORFs which allow for its translation during methionine deprivation when eIF2a is phosphorylated by GCN2[182]. Recent discoveries linking mRNA modification, m6A, to ATF4 translation however suggests that the mechanism may not be as simple as predicted by experimental models[11].

1.6.4. the eIF2-a pathway and its kinases – central regulation nodes? Several lines of evidence suggests that eIF2a is a central translation regulatory node that orchestrates pathways after stress that determine cell fate. Firstly, phosphorylation of eIF2a at S51 occurs almost immediately downstream of any stress via four known kinases described above, GCN2, HRI, PERK, and PKR, with specialized functions designed to respond to different stresses[18, 176, 177, 179, 183]. This indicates that eIF2a phosphorylation is a part of a central universal response to stress given the intricate sensing systems that result in this modification, and the fact that it occurs downstream of every stress in a very timely fashion. Secondly, several studies have shown so far that eIF2a phosphorylation is a regulator of life and death post stress[168, 179, 184, 185]. eIF2a phosphorylation at S51 has a pro-survival role and pro-adaptive role after stress and decreasing its levels after stress results in stress sensitization and increased death downstream of various stresses such as glucose deprivation and oxidative stress[168, 177, 179, 184, 185]. While this shows some promise as a cancer therapeutic, it also points at the importance of the regulatory role this modification plays in life and death decision making after stress. Lastly, S51 phosphorylation, while mainly inhibitory to translation in nature, can have opposite roles on translation. One example is the ATF4 mRNA selective translation that is mediated, in part, by S51 phosphorylation[182]. Other examples include mRNAs like CHOP, IBTKa, among possible others[18, 38, 178, 182]. This suggests that while eIF2a phosphorylation acts to inhibit most translation, it also mediates the selective translation of certain mRNAs required to survival and adapt to stress to promote survival. While the molecular implications of eIF2a phosphorylation of slowing down the GTP-GDP exchange on eIF2B, is known, lots remains to be discovered by how this node mediates the selective translation of possibly a large group of SRP mRNAs. Altogether, the current discoveries so far point to a more complicated role of eIF2a

phosphorylation than a simple kill switch for translation, but they suggest that it is a highly sensitive, yet potent, regulator node of translation that is critical for life and death decision making post stress.

1.7. Study rational; Timing is of the essence.

The aim of this study to elucidate how cells selectively and acutely translate stress response proteins after stress. While stress-mediated translation inhibition is well established, and a few examples of acute selective translation of certain SRPs are described to date, a lot remains to be uncovered about a possible universal and potent SRP translation system that selectively and acutely (within seconds to minutes) translates dozens or possibly hundreds of SRP mRNAs after stress. To solve this challenge **fifth challenge**, cells have to incorporate solutions from all four challenges discussed in section 1.1. regarding scale, selectivity, location, and timing of translation. Nowhere is the need for an efficient solution for this challenge more evident than in times of stress when cells have to *selectively* translate SRP mRNAs *acutely* after stress. This selectivity and timely translation is what we will try and address in this study by proposing a novel translation pathway involving elements discussed throughout section 1. The importance of selective and acute translation is evident by the abundance and effect of stresses on our cells and the strong links this has to various human disease, such as cancer, and ageing.

1.8.1. The proposed SRP translation system and rational: In this study we will present data supporting a novel translation model that selectively and acutely translates SRP mRNAs while general translation remains inhibited. While we predict that cells translate a large number of SRPs acutely after stress, the exact extent of selective translation acutely after stress (within a

few minutes) has not been shown. In Chapter 3, we will first show using mass spectrometry and protein labelling that cells translate a large number of SRP within 20 minutes of stress, modeled with UV and 2DG, which mimics glucose deprivation. Moreover, using a modified RNA sequencing technique to detect mRNA modifications, we will show a unique tagging system for SRP mRNAs that correlates with the proteins that are acutely translated. This chapter will show that 1) SRP translation is more robust than previously thought, and that 2) SRP mRNAs share a unique tag involving posttranscriptional bimodal m6A tag which suggests that SRP mRNAs are tagged by cells prior to stress, likely for immediate and selective translation upon stress.

To explore the possible link between the bimodal m6A tag that marks SRP mRNAs and the mechanism of selective translation in stress, Chapter 4 will discuss the role of extranuclear demethylase, FTO, in the acute translation of two model SRP mRNAs, p53 and newly discovered SRSF7. FTO leaves the nucleus and is activated within minutes of stress resulting in the acute translation of SRPs. Chapter 4 will also introduce a novel link between microtubules and SRP translation as a possible microdomain for selective SRP translation.

To explore the mechanism further, Chapter 5 will show that FTO is phosphorylated at threonine-6, a previously undiscovered modification on FTO, by MARK4, a microtubule associated kinase. This phosphorylation results in the activation of FTO activity acutely after stress. Moreover, Chapter 5 will also show that microtubules are a novel microdomain for translation featuring newly discovered microtubule-associated ribosomes that are activated acutely after stress.

Last but not least, Chapter 6 will link the m6A-FTO-MARK4 and the microtubule-associated ribosomes to the translation machinery with the novel discovery of PKR-mediated control of SRP translation via m6A. While PKR is thought of as a sentinel kinase for viral

infections, we will see that is regulated by m6A and it plays a critical role in the selective translation of endogenous SRP mRNAs acutely after stress.

Altogether, this thesis will propose a novel translation system for selective and acute translation of SRPs in stress providing a more comprehensive model for the pathway-level selective translation that is critical for life and death decisions post stress, effectively providing a novel solution for the fifth challenge of translation discussed above.

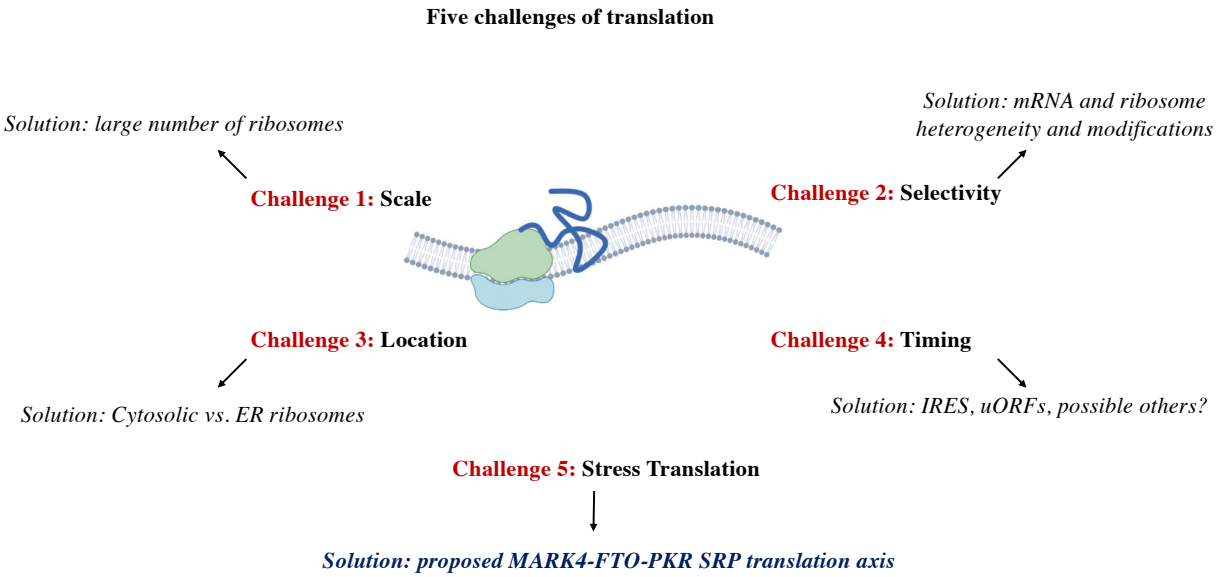

Figure A. ***Challenges of protein translation:*** diagram outlining the 5 main challenges of translation and the current and proposed solutions for these challenges as outlined in section 1. Translation scalability is solved by building a large number of ribosomes, the selective translation challenge is solved by ribosomal heterogeneity, RNA binding proteins, RNA modifications and elements. The location challenge is solved by having specialized cytosolic and ER ribosomes. The timing challenge, or selectively translating certain mRNAs is currently solved by a few unique examples of selective translation involved RNA elements such as IRES or uORFs. Challenge five is a proposed challenge with a novel proposed solution, a universal system for selective translation of SRPs acutely in stress, solved by a new MARK4-FTO-PKR axis involved microtubule-associated ribosomes and a bimodal SRP mRNA m6A tag.

Chapter 2

Materials and Methods

Cell Culture: A549 (ATCC), MEF (ATCC), HFF-1 (ATCC) were cultured in Dulbecco's Modified Eagle's Medium (DMEM, Gibco) with 10% FBS, 1% PSF at 9% CO_2. All cell lines tested negative for mycoplasma contamination using LookOut Mycoplasma PCR Detection Kit (Sigma).

Reagents and Antibodies: *Antibodies:* p53 (Cell Signaling 9282, Lot 4) was used at 1:1000 for immunoblots (IB). FTO (Abcam ab92821) and METTL3 (Abcam ab195352), SRSF7 (Cedarlane A303-773A-T), NDUFB8 (Abcam ab192878), ATF4 (NEB 11815), MEK1 (Cell Signaling 2352), Grp78 (Santa Cruz sc-1051), SP1 (Santa Cruz sc-14027), S6 (Cell Signaling 2217), RLP26 (Cell signaling 5400), Lamin A/C (Cell Signaling 4777), Emerin (Abcam ab54996), Nup98 (Cell Signaling 2598), Fibrillarin (Abcam ab5821), pH2AX (Cell Signaling 5438), g-Tubulin (Sigma T5326), b-tubulin (Cell signaling 2128, Sigma T8328), m6A (Synaptic Systems 202111), pT6-FTO (GenScript, custom antibody), MARK4 (Cell signaling 4834), PKR (Abcam ab184257), pT446-PKR (Abcam ab32036) , pS51-eIF2a (Cell Signaling 9721, Abcam ab32157), eIF2a (Cell Signaling 5324), Flag (Cell Signaling 2368), cCas3 (Cell Signaling 9661, 9663). *siRNA:* METTL3 (Life Technologies 32142), FTO (Life Technologies 35512), MARK4 (Thermo Fisher Am51331, ID1089), PKR (Thermo Fisher AM16708). *Primers:* p53 (), ATF4 (Thermo Fisher Hs00909569), METTL3 (Thermo Fisher Hs00219820). *Drugs:* Cycloheximide (10μg/ml), A-Amanitin (5μg/ml), 2-deoxyglucose (50mM), Colchicine (5μM), OTSSP167 (1-10μM), C16/PKRi (10μM).

Plasmid Transfections: Cells were plated at 70% confluency 24 hrs prior to transfection in antibiotic-free media. Lipofectamine 2000 (Thermofisher) was used to transfect 1 μg of DNA per 6 well . Cells were washed after 6 hours and transfection was assayed 24-48 hours later. Wildtype human FTO (Origene RC215889) was used for FTO overexpression and mutagenesis experiments.

Site Directed Mutagenesis: QuickChange II XL Site-Directed Mutagenesis Kit (Agilent) was used along with custom-made primers (sequences are available in Supplementary Table 1) to mutate the residues on human FTO.

Immunoblots: Cells were lysed in RIPA (Santa Cruz) supplemented with protease inhibitor cocktail, PMSF and sodium orthovanadate for 30 min on ice with frequent vortexing. Lysates were spun down at 10,000 RPM at 4˚C. Pierce BCA protein Assay (Thermofisher) was used to measure concentrations and samples were prepared in 2x Laemmli (Sigma) and boiled for 7 min at 100˚C. Proteins were separated on SDS-PAGE and transferred onto nitrocellulose membranes, blocked at room temperature for 1h in 5% non-fat dry milk in TBST (0.1% Tween-20) and incubated with primary antibodies overnight at 4˚C. Membranes were then washed for 30' in TBST, incubated with horseradish peroxidase-coupled secondary antibodies (Santa Cruz) at room temperature for 1 hr and visualized with enhanced chemiluminescence (Pierce, Thermofisher). Tissues were prepared by sonication with RIPA on ice.

Immunoprecipitation: Co-Immunoprecipitations were done using the Dynabeads Co-IP kit (Thermofisher 14321D), Dynabeads ProteinA (Thermofisher 10002D) and Pierce IP lysis buffer (Thermofisher 87787) as per manufacturer's recommendations. Briefly, cells were rinsed and scraped with ice cold PBS followed by lysis with IP buffer. 50 mg equivalent of cell pellet volume were added to 1 μg of antibody or the appropriate IgG conjugated to beads and incubated at either 4˚C for 2 hrs (for Flag IPs) or overnight at 4˚C (for other IPs). Beads were then washed, eluted and boiled in 4x Laemmli buffer (Biorad). Flag immunoprecipitation: anti-Flag M2 Magnetic beads (Sigma M8823) were used.

RNA isolation and qRT-PCR: RNA was isolated using Trizol reagent. Taqman RNA-to-CT 1 step (Applied Biosystems 4392938) was used as recommended for quantitative RT-PCR.

Immunofluorescence: Cells/tissue on glass slides were fixed with 2% PFA at 37˚C for 15 min, permeabilized with 0.5% Triton X-100 for 15 min, followed by PBS washes and blocking in Image-iT FX Signal Enhancer (Thermofisher I36933) for 30 min at room temperature. Primary antibodies were then added in primary diluent (Dako) overnight at 4˚C. Alexa Fluor secondary antibodies (Molecular Probes) were then added in secondary antibody diluent (Dako) at 1:1000 at room temperature for 1 hr in the dark. Slides were then washed with PBS for 20 min and DAPI was added at room temperature for 10 min, prior to mounting in ProLong Gold (Thermofisher) for 24 hrs at room temperature. Imaging was done with a Zeiss LSM 710 confocal microscope. Investigators were blinded to all in vivo imaging and analysis.

Mass Spectrometry: In-gel trypsin digestion was performed on samples. Briefly, excised gel bands were de-stained twice in 100 mM ammonium bicarbonate/acetonitrile (50:50). The samples were then reduced (10 mM BME in 100 mM bicarbonate) and alkylated (55 mM iodoacetamide in 100 mM bicarbonate). After dehydration, trypsin (6 ng/μl) was added to just cover the gel pieces and the digestion was allowed to proceed overnight (~16 hrs) at room temperature. Tryptic peptides were first extracted from the gel using 97% water/2% acetonitrile/1% formic acid followed by a second extraction using 50% of the first extraction buffer and 50% acetonitrile. Fractions containing tryptic peptides were resolved and ionized by using nanoflow HPLC (Easy-nLC II, Thermo Scientific) coupled to an LTQ XL-Orbitrap hybrid mass spectrometer (Thermo Scientific). Nanoflow chromatography and electrospray ionization were accomplished by using a PicoFrit fused silica capillary column (ProteoPepII, C18) with 100 μm inner diameter (300 Å, 5 μm, New Objective). Peptide mixtures were injected onto the column at a flow rate of 3000 nL/min and resolved at 500 nL/min using linear gradients from 0 to 45% v/v aqueous ACN in 0.2% v/v formic acid over 45 minutes. The mass spectrometer was operated in data-dependent acquisition mode, recording high-accuracy and high-resolution survey Orbitrap spectra using external mass calibration, with a resolution of 30 000 and m/z range of 400–2000. The fourteen most intense multiply charged ions were sequentially fragmented by using collision-induced dissociation, and spectra of their fragments were

recorded in the linear ion trap; after two fragmentations all precursors selected for dissociation were dynamically excluded for 60 s. Data were processed using Proteome Discoverer 1.4 (Thermo Scientific) and a Uniprot (uniprot.org) human database was searched using SEQUEST (Thermo Scientific) to find binding p53 binding partners or searched against the PKM2 sequence using SEQUEST (Thermo Scientific) (to find modified cysteine). Search parameters included a precursor mass tolerance of 10 ppm and a fragment mass tolerance of 0.8 Da.

AHA labelling: Cell were plated in100mm dishes at 40% confluency, and transfected with either scrambled or METTL3 siRNA. 48 hours post transfection, cells are rinsed once in PBS, and twice in methionine free DMEM, and incubated in methionine-free DMEM (supplemented with dialyzed FBS) for 40 minutes. They were then either treated with UV, and fresh media supplemented with L-AHA (Invitrogen C10102 at 100μM) and incubated for another 20 minutes. They were then scraped in cold PBS and lysed in 570μL of urea supplemented with proteinase and phosphatase inhibitors. Click iT protein enrichment capture kit (Thermo Fisher C10416) was then used to purify AHA-modified peptides for mass spec analysis as per manufacturer's recommendations.

SILAC: Thermo Fisher kit A33972 for SILAC protein quantification was used. Briefly, cells were cultured in heavy or light media for 6 passages after which they were split into T500 plates and treated with either UV or 2-DG for 20 minutes and scraped in cold PBS. 90% of cells were kept for RNA sequencing experiments, and 10% were kept for SILAC protein analysis via mass spec as per manufacturer's recommendations.

meRIP: *Step1 RNA isolation and fragmentation:* 90% cells cultured and treated for SILAC experiment underwent cellular fractionation to isolate nuclei, followed by RNA isolation (with 3M sodium acetate precipitation and isolation). 5% is kept as input, and the rest is then fragmented with 10x fragmentation buffer (Thermofisher AM8740) and incubated at 90˚C for 5 min followed by neutralization with EDTA and precipitation and purification of RNA using 3M sodium acetate (1/10th the volume) and 2.5 volumes of ethanol incubated overnight at -80˚C. RNA is then pelleted and resuspended in water the next day. *Step 2 m6A immunoprecipitation:* RNA volume is first adjusted to 755μL with water, 200μL of 5X IP buffer (details are in m6A immunoprecipitation step), 5μL of RNaseOUT, and 12.5μg of m6A antibody are added and incubated at 4˚C for 2 hours rotating. In the meantime, 200μL of protein A beads are washed with 2X IP buffer and incubated with BSA (0.5mg/ml) for 2 hours to block. Beads are then washed twice with 1X IP buffer and split into 2 tubes (m6A and IgG IP). RNA-antibody mixture is then added to the beads and are incubated together at 4˚C for 2 hours rotating. Beads are then collected and washed 5x with 1ml of 1X IP buffer and are eluted in 100μL of elution buffer (90μL of 5X IP buffer, 150μL of 20mM of m6A (10mg in 1.3 ml, Carbosynth NM10586), 7μL of RNAse inhibitor, and 203μL of water, with final m6A concentration of 6.7mM) incubated at 4˚C for 1 hour. Beads are then collected, rinsed three times with 100μL of 1X IP buffer and the eluent is kept (400μL in total). RNA is then collected by sodium acetate precipitation (3M at pH 5.2). RNA is then pelleted and resuspended in water and cDNA libraries are made using SMART-Seq Stranded kit (Takara 634442) as per manufacturer's recommendations and libraries are sequenced on Illumina Hiseq platform.

Cellular Fractionation: subcellular fractions were obtained either with protein fraction kit (Thermo Fisher 78840) as per manufacturer's recommendations, or from an adapted sequential detergent extraction protocol [186]. Sequential detergents are first prepared as per protocol (permeabilization buffer, wash buffer, and lysis buffer), with an additional cytoskeletal buffer (1ml of 400mM potassium acetate, 125μL 25mM potassium HEPES pH 7.2, 150μL magnesium acetate, with final concentration of 1mM DTT, 1mM PMSF, 40U/ml RNAseout (added fresh), and 5μM colchicine in a total volume of 10 ml) Cells are cultured in 100mm dishes and treated with vehicle, drugs, or stress as per experiment. They are then rinsed in 4˚C PBS, and first permeabilized with ice cold permeabilization buffer (2ml) for 5 min on a rocker, the solution is kept as the cytosolic fraction, they are then washed in 5ml of wash buffer which is aspirated, and 2ml of lysis buffer is added for 5 min at 4˚C on rocker. The lysis buffer solution is kept as the ER fraction, and 2ml of CS buffer is added to each dish and cells are scraped with a cell lifter and pipetted 3-5 gently using a 1ml pipette to separate the cytoskeletal fraction from the remaining nuclei. The solution is then spun down at 400g at 4˚C for 3 minutes, and the supernatant is kept as the CS fraction, remaining pellet is the nuclear fraction. All three lysates (cytosolic, ER, and CS) were then cleared by spinning down at 14000g for 12 minutes at 4˚C.

RNA Dot blots: 500-1000ng of RNA are first treated with 1μL DNAse-I (Invitrogen AM2222) for 30 minutes are 37˚C and heat inactivate at 75˚C for 5 min. RNA is then suspended in RNA dot blot buffer (RDB) made by mixing 675μL formamide, 210μL 37% formaldehyde, and 133μL of 10X MOPs solution. RNA is then denatured at 65˚C for 5 min and placed on ice, and an equal volume of 20X SSC is added to each sample. In the meantime a piece of Nylon Zeta probe membrane (Bio-Rad 1620165) is rinsed in water and 10X SSC buffer and fixed on the pre-

rinsed dot blot apparatus (Bio-rad 1703938) with 2 pieces of filter paper (Bio-Rad 1620161) connected to a vacuum filter. Once membrane is fully dry RNA samples are added onto wells using filtered tips, and once membrane is dry again, apparatus is disassembled, the upper left corner of membrane is marked with a pencil, and membrane is cross linked with UV crosslinker (UVP CL1000, 254nm) at 5000J/m^2. Membrane is then blocked in 5% dry milk in TBST for 1 hour at room temperature and incubated with m6A antibody at 1:1000 in TBST overnight at 4˚C and developed the next day as other immunoblots.

RNA gels: 0.8-2% agarose gels were prepared and poured (agarose in 1X TBE buffer) in a horizontal nucleic acid gel apparatus, and RNA (100-500ng) were dissolved in 2-5 volumes of 100% formamide and 5X loading buffer (Sigma R1386) and run at 150V in 1X TBE buffer. Gels were then stained with SYBR green II RNA stain (Thermo Fisher S7568) and developed on a Bio-Rad ChemiDoc apparatus.

M6A immunoprecipitation: total RNA is first isolated from cells (cultured in T175 flask or larger) using Trizol (in 3-6 ml as required). 300-500μg of total RNA is mixed with 5X IP buffer (made by mixing 0.5ml of 1M TrisHCl pH 7.4, 1.5ml of 5M NaCl and 0.5ml 10% NP40 and 7.5ml of RNAse free water) and RNAse free water to make 1X IP buffer in a total volume of 500-800μL. 10μg of m6A antibody is added to the RNA-IP solution, and incubated for 2 hours at 4˚C. In the meantime, 100μL of Dynabeads ProteinA (Thermofisher 10002D) are washed twice in 800μL of 1X IP buffer and blocked in 5% BSA for 1 hour in 1X IP buffer. The beads are then rinsed twice in 1X IP buffer and the RNA-antibody complex is added to the beads and incubated for an additional 2 hours at 4˚C on a rotator. The beads are then removed and washed 3x in

800μL of 1X IP buffer and the supernatant of the IP solution is kept as the "eluted fraction". The beads are either eluted in elution buffer (made by mixing 90μL of 5X IP buffer, 150μL of 20mM m6A, 7μL of RNAsin Plus and 203μL of water), or mixed directly with 1ml of Trizol to isolate RNA. RNA is precipitated with 1/10 volume of 3M sodium acetate pH 5.2 and 2.5 volumes of 100% ethanol incubated at -20 for 1 hour or longer, and spun down at 15000 g for 12 min. The pellet is then rinsed twice in 70% ethanol and resuspended in water.

Ribosome isolation: Cells are cultured in T175 flasks and treated according to experiment. They are then fractionation as per fractionation protocol above (with cyclohexide added to all used solutions at 100μg/ml) to collect a cytosolic, ER, and CS fraction which are loaded gently onto 5-6 ml of ice cold mammalian sucrose cushion (50mM Tris HCl pH 7.5, 5mM MgCl2, 25mM KCl, 2M sucrose (filtered with 0.22μg filter), 100μg of cycloheximide). They are then spun in a fixed angle type rotor type Ti90 rotor at 54,000RPM for 2.5 hours at 4˚C, with wall side marked with a marker to aid in pellet detection. The sucrose layer is removed gently, and the ribosomal pellet (clear hard pellet at the bottom) is resuspended in 1ml of Trizol to isolate RNA.

HPLC RIBO SEC: Ribosome profiling using HPLC was done on Agilent SEC-5 2000Å (7.8x300mm) column using a modified previously published protocol. First cells were cultured in 100mm dishes and treated with UV or left untreated for 20 minutes. Cycloheximide (CHX) was then added at 100μg/ml for 3 minutes and cells were then rinsed in cold PBS containing CHX as same concentration and then fractionated using chemical cellular fraction to obtain a cytosolic, ER, and CS fraction, each in 2ml of buffer, as described in the cellular fractionation section, with the addition of cycloheximide to all buffers at 100μg/ml. They were then injected

into the HPLC and run at 4˚C with a flow rate of 0.8ml/min. Polysomal peaks were observed around 7.5-8.5 min mark.

Ribosome Sequencing: *Step 1 ribosomal isolation:* Cells were cultured in T500 dishes and cellular fractions (cytosol, ER, and CS) were collected as per fractionation protocol above. Lysates were then treated with 16μL of RNAse I for 45 minutes at RT, followed by reaction inhibition with superNasein at 20μL per tube. They were placed on ice and layered on top of 6ml of sucrose cushion (prepared as per ribosome isolation protocol above) and spun down at 54000 RPM in Ti90 rotor for 2.5 hours at 4˚C. The sucrose layer is then gently removed and the ribosomal pellet is resuspended in Trizol for RNA isolation. *Step 2 mRNA fragments isolation:* RNA gels (15% polyacrylamide TBE-Urea gel (4.8g of urea, 3.75ml of 40% Acrylamide (29:1), 33μL 30% APS, 4μL TEMED, 1ml of 10X TBE buffer, topped up to 10ml with water)) are first pre-run for 20 minutes at 400 V in 1x TBE, and isolated RNA in step 1 is mixed with 2X loading buffer (98% formamide v/v with 10mM EDTA and 300μg/ml bromophenol blue) to isolate the protected mRNA fragments and are denatured at 80˚C for 90 seconds and cooled on ice prior to running on gel for 65 minutes at 200V with a 100Da marker. The gel is then stained with SYBR green II RNA stain (Thermo Fisher S7568) for 3 minutes and bands corresponding to 26-40 nt are excised and cut up into small pieces with a 21 gauge needle. 360μL of RNAse free water is added to the gel debris and incubated at 70˚C for 10 min. The water/gel solution is then spun down at full speed for 2 min and the liquid filtrate is removed and transferred to a new tube to precipitate the RNA. 40μL of 3M sodium acetate (pH 5.2) is added to the filtrate along with 2.5 volumes of 100% ethanol. The solution is incubated at -80 overnight and spun down at 14000g for 15 minutes to precipitate the RNA pellet. RNA is then rinsed twice in 70% ethanol and is

resuspended in 30μL of water. *Step 3 library preparation:* RNA samples are first topped up to 43μL with water and are denatured at 80˚C for 90 seconds and are then cooled down to 37˚C slowly. To each tube, 5μL of 10X T4 PNK buffer and 1μL of T4 PNK (10U/μL) (NEB M0201) are added along with 1μL of SUPERNaseIn (20U/μl). The solution is incubated for 1 hour at 37˚C and is heat inactivated at 70˚C for 10 min. This allows for dephosphorylation of RNA fragments in preparation for cDNA library synthesis. rRNA is then blocked with rRNA kit (Qiagen 334386) as per manufacturer's recommendations, and cDNA libraries are prepared using Smarter smRNA-seq kit from Takara bio (635029). Samples are then sequenced on Illumina Hiseq system with Novogene.

PAR-CLIP: Previously published protocol [187] was followed and modified slightly to perform PAR-CLIP analysis of FTO and PKR. Cells are cultured in 2 T500 dishes (per sample) at 80% confluency transfected with flag-FTO 48 hours prior to collection day. 4-thiouridine (4SU) is added 24 hours prior to collection at 150μM. On day of experiment, cells are treated with UV (25J/m^2) or left untreated as control, incubated for 20 minutes are then cross-linked at 3000J/m^2 with a 365nm crosslinker. Then cells are rinsed with cold PBS and are scraped with a cell lifter and collected, and lysed with 1ml of 1X NP40 buffer (50mM HEPES pH 7.5, 150mM KCl, 2mM EDTA, 1mM NaF, 0.5% v/v NP40, 0.5mM DTT supplemented with EDTA-free protease inhibitor cocktail) for 10 min on ice, and cleared at 12000g for 10 min. Lysates are then incubated with RNAse T1 at 1U/μL for 15 min at RT and 80μL of washed M2 flag beads (per T500) are added and incubated for 4 hours rotating at 4˚C. Beads are then taken out and rinsed 5x with 1X NP40 buffer and are then resuspended in 1ml of 1X NP40 buffer and incubated with 1U/μl of RNAseT1 for 15 min at RT. Beads are then collected and rinsed twice in 500μL of 1X

NP40 and eluted in 0.1M Glycine pH 2.6 for 5 min at RT and is then neutralize with Tris after removal from beads, and resuspended in 67μL of SDS loading buffer (10% glycerol v/v, 50mM Tris HCl pH 6.8, 2mM EDTA, 2% SDS w/v, 100mM DTT, 0.1% bromophenol blue) and boiled at 100˚C for 4 min and loaded on precase 4-12% polyacrylamide gel. Gel was then rinsed in TBST and stained in SYBR green II to detect RNA fragments. Gel was then transferred for onto a nitrocellulose membrane which was blocked with 5% milk and probed with flag antibody to detect bands corresponding to immunoprecipitated FTO or PKR. These bands were then cut from the membrane and were incubated with 200μL of 2X proteinase K buffer (100mM Tris HCl pH 7.5, 150mM NaCl, 12.5 mM EDTA, 2% w/v SDS), topped up to 400μL with water, and 5μL of proteinase K at 55˚C for 1 hour. The tube is then spun down and the solution is removed to a clean tube and RNA is precipitated using 3M sodium acetate (pH 5.2) and ethanol. cDNA libraries are then prepared using SMART-seq Stranded kit (Takara 63442) as per manufacturer's recommendations, and sequenced on Illumina Hiseq platform.

FTO Activity assay: Cells are cultured in T75 flasks and FTO is pulled down either with and FTO antibody (endogenous FTO), or with flag beads of flag-FTO overexpressing cells using the immunoprecipitation procedure (eluted with flag peptide (Sigma F3290) competition added at 1.5ng/μL). The protein is then incubated with the Epigenase m6A Demethylase assay kit (EpiGentek P-9013) for 4-6 hours at 37˚C following manufacturer's recommendations.

FTO MARK4 kinase assay: endogenous FTO was immunoprecipitated from cultured cells as outlined above, and IP product was concentrated in 10KDa spin columns (Abcam ab93349) for 1 hour at 11000 g at 4˚C to 50μL, 5 volumes of kinase reaction buffer (Abcam ab138879), they

were then splint into 2 tubes and 15μL of recombinant human MARK4 (Abcam ab105211) were added. The protein mixture was incubated at 37˚C for 15 minutes followed by 1 hour incubation at RT. Proteins were then either used to run immunoblots, mass spectrometric analysis or were used in FTO demethylase assay as outlined above.

PKR Kinase assay: flag-PKR was overexpressed in cells (cultured in T175 flasks), and flag immunoprecipitation was carried out as outlined above and was eluted with flag peptide competition (Sigma F3290 added at 1.5ng/μL) to isolate purified PKR protein. IP product was then run on 10KDa filter for 1 hour at 10000 g at 4˚C. In the meantime, m6A was pulled down from total RNA as outlined above. Kinase assay ELISA kit (Abcam ab138879) was used to carry out the PKR kinase reaction as per manufacturer's recommendations. Purified PKR +/- RNA and PKRi were added to different wells and incubated at 37˚C for 15 min followed by a 30 min incubation at RT. The sensor buffer and the sensor were then added as per recommendations and fluorescence was read after 4 min. Proteins were then removed from the well using RIPA lysis buffer and immunoblots were done to quantify protein levels.

siRNA knockdown: cells are plated into 6 well plates at 50% confluency. siRNA transfection is done using Lipofectamine RNAiMax as per manufacturer's recommendations. Cells are treated and collected 48 hours after siRNA transfection.

OPP staining: Cells are plated either into glass bottom confocal dishes, or onto glass coverslips in 6 well plates at 40% confluency. On day of experiment, cells are incubated with OPP reagent A (Thermo Fisher C10458) at 1:1000 for 20 min and are then fixed in 37˚C 2% PFA for 10 min.

They are then rinsed with PBS and permeabilized with 0.25% Triton-X for 10 minutes at 37˚C, followed by 3 additional rinses in PBS. ClickIT reaction is then carried out as per kit recommendations, and cells are blocked with 10% serum (matching the host of DAKO secondary antibodies used) for 1 hour at 37˚C, and are then rinsed once in PBS and incubated with primary antibodies overnight at 4˚C as outlined in immunofluorescence protocol section above.

Electron microscopy: Cells were fresh thin-slices (50 micrometer) prepared with a vibrotome and snap frozen (-80 C). 1x1 mm pieces or thin slices of cells were transferred immediately into ice-cold modified Karnovsky fixative solution (2% paraformaldehyde, 2% glutaraldehyde in 0.1 M sodium Cacodylate buffer) and incubated on ice overnight. The next day, samples were rinsed with sodium cacodylate 3x. Secondary fixation was in 1% cold osmium tetroxide for 1 hour followed by incubation overnight with uranyl acetate 2% at 4˚C. The next day, 70%, 90% and pure ethanol were used followed by two propylene oxide treatments for dehydration, prior to overnight incubation with embed 812/resin (50/50) overnight and under vacuum. Samples were transferred to beem capsules and cured at 60˚C for 48 hours. Couple of days later, the resin blocks were sectioned (70 nanometer thin) using a Leica EM UC6 and imaged with JEM-2100 using 200KV to capture images.

PLA staining: Same protocol outlined in "immunofluorescence staining and OPP staining" was followed for PLA staining along with the PLA kit manufacturer's recommendations (Sigma DUO92004, DUO92002, DUO92008)

M6A detection using BST-MRT RT-PCRs: Previously published protocol [188] was followed to detect methylation regions in p53 and SRSF7 mRNA transcripts along with DreamTaq polymerase for the subsequent PCR step.

Bioinformatics analysis: RNA seq: Sequences were aligned with STAR to human genome GRch38.100, and indexed and converted to bam files with samtools. Transcript compilation and expression estimation was done using StringTie and differential expression was measured using Ballgown in R. Metascape was used for pathway analysis.

Bioinformatics: meRIP seq: Sequences were and trimmed with Trimmomatic and aligned with STAR to human genome GRch38.100, and indexed and converted to bam files with samtools. M6A peaks were then analyzed with MeTDiff package in R. HOMER was then used annotate the peaks using annotatePeaks function. Rstudio used used to plot peaks locations and measure distance from 3'UTR using biomaRt.

Bioinformatics: Ribo-seq: Sequences were aligned with STAR to human genome GRch38.100, and indexed and converted to bam files with samtools. Transcript counts was then measured and normalized using StringTie and differential expression analysis was done using Ballgown in R. Metascape was used for pathway analysis.

Bioinformatics: PAR-CLIP: Sequences were and trimmed with Trimmomatic and aligned with STAR to human genome GRch38.100, and indexed and converted to bam files with samtools. dCLIP package was then used in R to measure and compare RNA peaks between control and stress using dclip function. Peaks were then annotated with HOMER using the annotatePeaks function.

Bioinformatics: SILAC: MaxQuant was used to analyze all protein mass spectrometry data and find significantly different hits.

Tables of Sequences:

Mutation primers for FTO: Mutagenesis was done by Vector Biolabs using the given sequences below.

FTO wildtype:

GGTACCGAGGAGATCTGCCGCCGCGATCGCCATGAAGCGCACCCC

GACTGCCGAGGAACGAGAGCGCGAAGCTAAGAAACTGAGGCTTCT

TGAAGAGCTTGAAGACACTTGGCTCCCTTATCTGACCCCCAAAGA

TGATGAATTCTATCAGCAGTGGCAGCTGAAATATCCTAAACTAAT

TCTCCGAGAAGCCAGCAGTGTATCTGAGGAGCTCCATAAAGAGGT

TCAAGAAGCCTTTCTCACACTGCACAAGCATGGCTGCTTATTTCG

GGACCTGGTTAGGATCCAAGGCAAAGATCTGCTCACTCCGGTATC

TCGCATCCTCATTGGTAATCCAGGCTGCACCTACAAGTACCTGAA

CACCAGGCTCTTTACGGTCCCCTGGCCAGTGAAAGGGTCTAATAT

AAAACACACCGAGGCTGAAATAGCCGCTGCTTGTGAGACCTTCCT

CAAGCTCAATGACTACCTGCAGATAGAAACCATCCAGGCTTTGGA

AGAACTTGCTGCCAAAGAGAAGGCTAATGAGGATGCTGTGCCATT

GTGTATGTCTGCAGATTTCCCCAGGGTTGGGATGGGTTCATCCTA

CAACGGACAAGATGAAGTGGACATTAAGAGCAGAGCAGCATACAA

CGTAACTTTGCTGAATTTCATGGATCCTCAGAAAATGCCATACCT

GAAAGAGGAACCTTATTTTGGCATGGGGAAAATGGCAGTGAGCTG

GCATCATGATGAAAATCTGGTGGACAGGTCAGCGGTGGCAGTGTA

CAGTTATAGCTGTGAAGGCCCTGAAGAGGAAAGTGAGGATGACTC

TCATCTCGAAGGCAGGGATCCTGATATTTGGCATGTTGGTTTTAA

GATCTCATGGGACATAGAGACACCTGGTTTGGCGATACCCCTTCA

CCAAGGAGACTGCTATTTCATGCTTGATGATCTCAATGCCACCCA

CCAACACTGTGTTTTGGCCGGTTCACAACCTCGGTTTAGTTCCAC

CCACCGAGTGGCAGAGTGCTCAACAGGAACCTTGGATTATATTTT

ACAACGCTGTCAGTTGGCTCTGCAGAATGTCTGTGACGATGTGGA

CAATGATGATGTCTCTTTGAAATCCTTTGAGCCTGCAGTTTTGAA

ACAAGGAGAAGAAATTCATAATGAGGTCGAGTTTGAGTGGCTGAG

GCAGTTTTGGTTTCAAGGCAATCGATACAGAAAGTGCACTGACTG

GTGGTGTCAACCCATGGCTCAACTGGAAGCACTGTGGAAGAAGAT

GGAGGGTGTGACAAATGCTGTGCTTCATGAAGTTAAAAGAGAGGG

GCTCCCCGTGGAACAAAGGAATGAAATCTTGACTGCCATCCTTGC

CTCGCTCACTGCACGCCAGAACCTGAGGAGAGAATGGCATGCCAG

GTGCCAGTCACGAATTGCCCGAACATTACCTGCTGATCAGAAGCC

AGAATGTCGGCCATACTGGGAAAAGGATGATGCTTCGATGCCTCT

GCCGTTTGACCTCACAGACATCGTTTCAGAACTCAGAGGTCAGCT

TCTGGAAGCAAAACCCACGCGTACGCGGCCGCTCGAGCAGAAACT

CATCTCAGAAGAGGATCTGGCAGCAAATGATATCCTGGATTACAA

GGATGACGACGATAAGGTTTAAACGGCCGGCCGCGG

FTO T6A:

GGTACCGAGGAGATCTGCCGCCGCGATCGCCATGAAGCGCACCCC

GgccGCCGAGGAACGAGAGCGCGAAGCTAAGAAACTGAGGCTTCT

TGAAGAGCTTGAAGACACTTGGCTCCCTTATCTGACCCCCAAAGA

TGATGAATTCTATCAGCAGTGGCAGCTGAAATATCCTAAACTAAT

TCTCCGAGAAGCCAGCAGTGTATCTGAGGAGCTCCATAAAGAGGT

TCAAGAAGCCTTTCTCACACTGCACAAGCATGGCTGCTTATTTCG

GGACCTGGTTAGGATCCAAGGCAAAGATCTGCTCACTCCGGTATC

TCGCATCCTCATTGGTAATCCAGGCTGCACCTACAAGTACCTGAA

CACCAGGCTCTTTACGGTCCCCTGGCCAGTGAAAGGGTCTAATAT

AAAACACACCGAGGCTGAAATAGCCGCTGCTTGTGAGACCTTCCT

CAAGCTCAATGACTACCTGCAGATAGAAACCATCCAGGCTTTGGA

AGAACTTGCTGCCAAAGAGAAGGCTAATGAGGATGCTGTGCCATT

GTGTATGTCTGCAGATTTCCCCAGGGTTGGGATGGGTTCATCCTA

CAACGGACAAGATGAAGTGGACATTAAGAGCAGAGCAGCATACAA

CGTAACTTTGCTGAATTTCATGGATCCTCAGAAAATGCCATACCT

GAAAGAGGAACCTTATTTTGGCATGGGGAAAATGGCAGTGAGCTG

GCATCATGATGAAAATCTGGTGGACAGGTCAGCGGTGGCAGTGTA

CAGTTATAGCTGTGAAGGCCCTGAAGAGGAAAGTGAGGATGACTC

TCATCTCGAAGGCAGGGATCCTGATATTTGGCATGTTGGTTTTAA

GATCTCATGGGACATAGAGACACCTGGTTTGGCGATACCCCTTCA

CCAAGGAGACTGCTATTTCATGCTTGATGATCTCAATGCCACCCA

CCAACACTGTGTTTTGGCCGGTTCACAACCTCGGTTTAGTTCCAC

CCACCGAGTGGCAGAGTGCTCAACAGGAACCTTGGATTATATTTT

ACAACGCTGTCAGTTGGCTCTGCAGAATGTCTGTGACGATGTGGA

CAATGATGATGTCTCTTTGAAATCCTTTGAGCCTGCAGTTTTGAA

ACAAGGAGAAGAAATTCATAATGAGGTCGAGTTTGAGTGGCTGAG

GCAGTTTTGGTTTCAAGGCAATCGATACAGAAAGTGCACTGACTG

GTGGTGTCAACCCATGGCTCAACTGGAAGCACTGTGGAAGAAGAT

GGAGGGTGTGACAAATGCTGTGCTTCATGAAGTTAAAAGAGAGGG

GCTCCCCGTGGAACAAAGGAATGAAATCTTGACTGCCATCCTTGC

CTCGCTCACTGCACGCCAGAACCTGAGGAGAGAATGGCATGCCAG

GTGCCAGTCACGAATTGCCCGAACATTACCTGCTGATCAGAAGCC

AGAATGTCGGCCATACTGGGAAAAGGATGATGCTTCGATGCCTCT

GCCGTTTGACCTCACAGACATCGTTTCAGAACTCAGAGGTCAGCT

TCTGGAAGCAAAACCCACGCGTACGCGGCCGCTCGAGCAGAAACT

CATCTCAGAAGAGGATCTGGCAGCAAATGATATCCTGGATTACAA

GGATGACGACGATAAGGTTTAAACGGCCGGCCGCGG

FTO T6D:

GGTACCGAGGAGATCTGCCGCCGCGATCGCCATGAAGCGCACCCC

GGACGCCGAGGAACGAGAGCGCGAAGCTAAGAAACTGAGGCTTCT

TGAAGAGCTTGAAGACACTTGGCTCCCTTATCTGACCCCCAAAGA

TGATGAATTCTATCAGCAGTGGCAGCTGAAATATCCTAAACTAAT

TCTCCGAGAAGCCAGCAGTGTATCTGAGGAGCTCCATAAAGAGGT

TCAAGAAGCCTTTCTCACACTGCACAAGCATGGCTGCTTATTTCG

GGACCTGGTTAGGATCCAAGGCAAAGATCTGCTCACTCCGGTATC

TCGCATCCTCATTGGTAATCCAGGCTGCACCTACAAGTACCTGAA

CACCAGGCTCTTTACGGTCCCCTGGCCAGTGAAAGGGTCTAATAT

AAAACACACCGAGGCTGAAATAGCCGCTGCTTGTGAGACCTTCCT

CAAGCTCAATGACTACCTGCAGATAGAAACCATCCAGGCTTTGGA

AGAACTTGCTGCCAAAGAGAAGGCTAATGAGGATGCTGTGCCATT

GTGTATGTCTGCAGATTTCCCCAGGGTTGGGATGGGTTCATCCTA

CAACGGACAAGATGAAGTGGACATTAAGAGCAGAGCAGCATACAA

CGTAACTTTGCTGAATTTCATGGATCCTCAGAAAATGCCATACCT

GAAAGAGGAACCTTATTTTGGCATGGGGAAAATGGCAGTGAGCTG

GCATCATGATGAAAATCTGGTGGACAGGTCAGCGGTGGCAGTGTA

CAGTTATAGCTGTGAAGGCCCTGAAGAGGAAAGTGAGGATGACTC

TCATCTCGAAGGCAGGGATCCTGATATTTGGCATGTTGGTTTTAA

GATCTCATGGGACATAGAGACACCTGGTTTGGCGATACCCCTTCA

CCAAGGAGACTGCTATTTCATGCTTGATGATCTCAATGCCACCCA

CCAACACTGTGTTTTGGCCGGTTCACAACCTCGGTTTAGTTCCAC

CCACCGAGTGGCAGAGTGCTCAACAGGAACCTTGGATTATATTTT

ACAACGCTGTCAGTTGGCTCTGCAGAATGTCTGTGACGATGTGGA

CAATGATGATGTCTCTTTGAAATCCTTTGAGCCTGCAGTTTTGAA

ACAAGGAGAAGAAATTCATAATGAGGTCGAGTTTGAGTGGCTGAG

GCAGTTTTGGTTTCAAGGCAATCGATACAGAAAGTGCACTGACTG

GTGGTGTCAACCCATGGCTCAACTGGAAGCACTGTGGAAGAAGAT

GGAGGGTGTGACAAATGCTGTGCTTCATGAAGTTAAAAGAGAGGG

GCTCCCCGTGGAACAAAGGAATGAAATCTTGACTGCCATCCTTGC

CTCGCTCACTGCACGCCAGAACCTGAGGAGAGAATGGCATGCCAG

GTGCCAGTCACGAATTGCCCGAACATTACCTGCTGATCAGAAGCC

AGAATGTCGGCCATACTGGGAAAAGGATGATGCTTCGATGCCTCT

GCCGTTTGACCTCACAGACATCGTTTCAGAACTCAGAGGTCAGCT

TCTGGAAGCAAAACCCACGCGTACGCGGCCGCTCGAGCAGAAACT

CATCTCAGAAGAGGATCTGGCAGCAAATGATATCCTGGATTACAA

GGATGACGACGATAAGGTTTAAACGGCCGGCCGCGG

FTO T6E:

GGTACCGAGGAGATCTGCCGCCGCGATCGCCATGAAGCGCACCCC

GGAGGCCGAGGAACGAGAGCGCGAAGCTAAGAAACTGAGGCTTCT

TGAAGAGCTTGAAGACACTTGGCTCCCTTATCTGACCCCCAAAGA

TGATGAATTCTATCAGCAGTGGCAGCTGAAATATCCTAAACTAAT

TCTCCGAGAAGCCAGCAGTGTATCTGAGGAGCTCCATAAAGAGGT

TCAAGAAGCCTTTCTCACACTGCACAAGCATGGCTGCTTATTTCG

GGACCTGGTTAGGATCCAAGGCAAAGATCTGCTCACTCCGGTATC

TCGCATCCTCATTGGTAATCCAGGCTGCACCTACAAGTACCTGAA

CACCAGGCTCTTTACGGTCCCCTGGCCAGTGAAAGGGTCTAATAT

AAAACACACCGAGGCTGAAATAGCCGCTGCTTGTGAGACCTTCCT

CAAGCTCAATGACTACCTGCAGATAGAAACCATCCAGGCTTTGGA

AGAACTTGCTGCCAAAGAGAAGGCTAATGAGGATGCTGTGCCATT

GTGTATGTCTGCAGATTTCCCCAGGGTTGGGATGGGTTCATCCTA

CAACGGACAAGATGAAGTGGACATTAAGAGCAGAGCAGCATACAA

CGTAACTTTGCTGAATTTCATGGATCCTCAGAAAATGCCATACCT

GAAAGAGGAACCTTATTTTGGCATGGGGAAAATGGCAGTGAGCTG

GCATCATGATGAAAATCTGGTGGACAGGTCAGCGGTGGCAGTGTA

CAGTTATAGCTGTGAAGGCCCTGAAGAGGAAAGTGAGGATGACTC

TCATCTCGAAGGCAGGGATCCTGATATTTGGCATGTTGGTTTTAA

GATCTCATGGGACATAGAGACACCTGGTTTGGCGATACCCCTTCA

CCAAGGAGACTGCTATTTCATGCTTGATGATCTCAATGCCACCCA

CCAACACTGTGTTTTGGCCGGTTCACAACCTCGGTTTAGTTCCAC

CCACCGAGTGGCAGAGTGCTCAACAGGAACCTTGGATTATATTTT

ACAACGCTGTCAGTTGGCTCTGCAGAATGTCTGTGACGATGTGGA

CAATGATGATGTCTCTTTGAAATCCTTTGAGCCTGCAGTTTTGAA

ACAAGGAGAAGAAATTCATAATGAGGTCGAGTTTGAGTGGCTGAG

GCAGTTTTGGTTTCAAGGCAATCGATACAGAAAGTGCACTGACTG

GTGGTGTCAACCCATGGCTCAACTGGAAGCACTGTGGAAGAAGAT

GGAGGGTGTGACAAATGCTGTGCTTCATGAAGTTAAAAGAGAGGG

GCTCCCCGTGGAACAAAGGAATGAAATCTTGACTGCCATCCTTGC

CTCGCTCACTGCACGCCAGAACCTGAGGAGAGAATGGCATGCCAG

GTGCCAGTCACGAATTGCCCGAACATTACCTGCTGATCAGAAGCC

AGAATGTCGGCCATACTGGGAAAAGGATGATGCTTCGATGCCTCT

GCCGTTTGACCTCACAGACATCGTTTCAGAACTCAGAGGTCAGCT

TCTGGAAGCAAAACCCACGCGTACGCGGCCGCTCGAGCAGAAACT

CATCTCAGAAGAGGATCTGGCAGCAAATGATATCCTGGATTACAA

GGATGACGACGATAAGGTTTAAACGGCCGGCCGCGG

Chapter 3

Bimodal m6A peaks tag SRP mRNAs

3.1. Introduction and Summary:

Modeling acute stress and acute stress responses requires a stress-adaptive cell along with a potent, yet conservative and biologically relevant stress. Moreover, since experiments will be focusing on the acute stress responses, within a few minutes after a stress exposure, the stress would also ideally be highly reproducible with minimal variability, and quick administration to cells. For those reasons we started our experiments with a simple model of A549 non-small cell lung cancer treated with a defined dose of UV exposure. Cancer cells are highly adaptive to stress, particularly DNA damage, which is also one of the most ancient stresses which resulted in several conserved repair mechanisms to evolve in mammalian cells[175, 189, 190]. Treatment of UV can be done with a simple and quick procedure that produces almost identical stress exposure in a matter of few seconds, a timeline that is ideal to minimize variability in treatments and standardize stress response measurements. One of the first objectives we had was to establish a model that results in the acute and selective translation of a highly conserved SRP protein that is known to be responsive to UV stress. We focused on p53, an important tumor suppressor, as it has been shown previously to be induced acutely within 20 minutes of a low UV dose, in a translation-dependent manner via unknown mechanisms[70]. This provided a great model to test our SRP translation hypothesis as we predicted that an important protein such as p53, that is induced by a conservative stress, such as UV, would most likely be part of the larger SRP translation system we are hypothesizing. To test this, we first verified the p53 translation-dependent induction in our laboratory, within 20 minutes of UV dose, and then we started building our theory around this central SRP translation. First we show that p53 induction is part of a larger SRP translation system that encompasses hundreds of previously unidentified SRPs,

and that N6-methyl adenosine (m6A) mRNA epitranscriptomic modifications is critical for this comprehensive acute translation system. We predicted that an mRNA tag would likely be an SRP signature, since it was recently discovered that m6A is the most common modification on mRNAs, and the diverse locations along the mRNA regions, along with the highly dynamic nature of these epitranscriptomic tags, made m6A our first choice as an SRP tag candidate. Moreover, we then show using global protein labelling that hundreds of proteins are selectively translated after stress, in an m6A-dependent manner. This strongly suggested two important observations, firstly being that the acute translation response to stress is much larger than previously thought, and that m6A modifications play an important role in this comprehensive translation system.

To investigate this further, we then search for a unique m6A tag for SRP mRNAs that can help us distinguish them from non-SRP mRNAs using a specialized mRNA sequencing technique called methylated RNA immunoprecipitation sequencing (or meRIP-seq). These experiments showed us that SRP mRNAs do in fact share a previously unidentified m6A tag characterized by a bimodal peak distribution along the 3'UTR. This was the first epitranscriptic universal SRP tag discovered to date that is common to diverse SRP mRNAs. Using these experiments we were to verify some of the newly discovered and predicted SRPs, and we confirm the bimodal peak distribution along p53 and one of the newly discovered SRPs using a PCR-based m6A-detection technique, that is distinct from meRIP-seq.

3.2. Results

3.2.1. M6A-dependent p53 translation is part of a large translation program occurring within minutes of UV stress

Among all cells, cancer cells are highly adaptive to stress[175, 191], particularly DNA damage, one of the most ancient stresses with conserved repair mechanisms[192]. We focused on studying a classic model of this stress response (ie UV irradiation) in A549 cancer cells, a widely studied cancer cell line. We also studied additional classic models of non-genomic stress like the metabolic stresses induced by lack of glucose, using 2DG, or culture media lacking the essential amino acid Methionine. All these are serious cellular stresses in which the first few minutes are essential in determining whether the cell can adapt and proceed with a hyperacute repair process, or fail and proceed to apoptosis or necrosis. Thus, we focused on events within a very short period of time post stress, for example within 20 minutes post a moderate dose of UV irradiation. This is important since these initial repair processes lead to cascades of additional layers of responses, e.g. transcriptional, epigenetic, cell trafficking or metabolic responses, among others, which have been much better studied[9, 11, 18-20, 29, 36, 37, 167, 178, 193-195]. We first studied p53, a conserved protein that plays a critical roles in DNA damage response[70, 196]. Within 20 minutes of UV, we found a predictable global suppression in protein translation, detected by Met-S35 labelling of newly translated proteins (Fig. 1-1), while, in contrast, p53 protein levels increased significantly (Fig. 1-2). The increase in p53 levels is maintained with the transcription inhibitor alpha-Amanitin (Fig. 1-3) but completely blunted with the ribosome inhibitor cycloheximide (Fig. 1-2) suggesting a transcription-independent and selective translation-dependent increase. Coupled with the concurrent global translation inhibition

measured with Met-S35 labelling, the acute selective p53 translation post UV stress provided an ideal model for investigating out theory. We next wanted to test the first element of our theory, which is that SRP mRNAs likely have a unique signature that helps cells distinguish them from non-SRP mRNAs, especially during stress, to be selectively and acutely translated. Due to the abundant and dynamic nature of RNA methylation, particularly m6A [8, 11, 29, 40, 44-46, 50-54, 194, 197], we predicted that m6A tags may provide a unique tagging system that allows detection and selective translation of SRP mRNAs immediately after stress. Moreover, the dynamic nature of m6A modifications, and the diversity in m6A tags locations along mRNA regions, made this particular modification a highly likely candidate to mark the SRP mRNAs via a unique signature, which we predicted could be marked by quantity of methylation, or by location along the mRNA, or a combination of both.

We first wanted to test if m6A tags are required for SRP translation, regardless of the possible unique signature they may mark SRP mRNAs with, so we knocked down the previously established m6A writers METTL3, or METTL14 [45], and eraser, FTO. Since this methylation system is the only one discovered to date to methylated mRNAs with m6A tags, and since it is predicted to be the major methylation system for this tag in cells, we predicted that inhibiting one of the essential components using siRNA knockdown would be more than sufficient to test our theory. Knockdown of METTL3 and METTL14 resulted in a robust blunting of p53 translation within 20 minutes of UV, and ATF4 within 30 min of methionine deprivation (Fig. 1-4, Fig. 1-5, Fig. 1-6), lasting at least 2 hours post stress, but not at 24 hours after stress, with a clear time-dependent decrease in effect on translation efficiency with maximal effect within one hour (Fig. 1-7), implicating m6A tagging in the hyperacute, but perhaps not the normal translation mechanism of p53 following acute stress. This robust finding strongly indicated that m6A

tagging is in fact required for SRP translation, or at least for the selective and acute p53 translation. Intriguingly, the same result was seen when the demethylase, FTO, was knocked down. Acute p53 induction post UV was lost in the absence of the demethylase FTO. The fact that both a methyltransferase (METTL3) and demethylase (FTO) were involved in the acute translation of p53 post UV stress suggested that dynamic m6A regulation may be required for of SRP mRNA selection and translation. While the need for the demethylase was not apparent at first, this finding was still significant and it more strongly linked the m6A tagging system to acute SRP translation. While this may seem counterintuitive, we predicted that this may solve both challenges of having a universal SRP translation system; a methylation tag to mark the SRP mRNAs which at the same could provide translation control, or inhibition, when not needed in stress, and an activation signal when needed after stress. This may be supported by the observation that while METTL3, the methyl transferase, remains exclusively nuclear after stress (Fig. 1-8), FTO, the demethylase appears to translocate outside the nucleus within 20 minutes of UV (Fig. 1-9) acting perhaps as an SRP translation activation signal.

Next we wanted to see if cells translate a large number of unique proteins after stress, as part of a more universal comprehensive SRP translations system, of which p53 may be a part of. To test this, we first labelled and purified the newly synthesized proteins 20 minutes after UV stress using L-azidohomoalanine (AHA)-labelling, an amino acid mimetic that incorporates into newly synthesized proteins, followed by mass spectrometry (Fig. 2-1, Fig. 2-2). Differential analysis revealed over 600 significantly enriched proteins in the UV-treated group compared to control cells (Fig. 2-3, Fig. 2-4), confirming the possible presence of universal SRP translation system that orchestrates translation of hundreds of SRPs acutely. Due to the large number of proteins that are translated acutely within the same time frame, while general translation is suppressed,

suggests that a common translation system is perhaps orchestrating the selective batch translation. Moreover, pathway analysis revealed that RNA processing, p53 pathways, and metabolic pathways were the most significantly enriched (Fig. 2-4) and analysis of the upstream regulators of translated proteins in our model, revealed the TP53 gene is regulating the largest network amongst the most significant hits (Fig. 2-5) among others involved in cancer biology and tissue damage/repair (Fig. 2-6), confirming the important role that p53 plays in the acute stress response post UV. To confirm the involvement of m6A tagging in the selective and batch translation of the newly discovered SRPs, we knocked down METTL3, the main m6A methyltransferase for mRNA, using siRNA. This resulted in a significant decrease in all the major SRPs pathways detected using AHA labelling and mass spectrometry after 20 minutes of UV, with less than 30 proteins remaining significantly higher in the UV group, compared to over 600 in the scrambled siRNA control group, indicating that an m6A methylation system mediates the selective and comprehensive acute translation of large groups of SRPs immediately after stress (Fig. 2-3, Fig. 2-4). All together these data confirm that 1) cells translate large number of proteins acutely after stress, which we term as SRPs in this thesis, and 2) m6A tagging of mRNAs is critical for this selective batch translation.

3.2.2. SRP mRNAs share a unique 3'UTR bimodal m6A-peak pattern

We then we sought out to look for a unique methylation signature that may mark the SRP mRNAs. To do this, we utilized stable isotope labelling by amino acids in cell culture (SILAC), which compares heavy labelled peptides to light labelled peptides, to quantify and group proteins into decreased, maintained, and increased groups. We also did RNA sequencing and meRIP-seq, an m6A antibody pulldown sequencing technique, on extra-nuclear RNA from the same cells

treated with UV, 2-deoxyglucose (2-DG) or control (Fig. 3-1). These techniques in combination will allow us to elucidate the unique m6A signature that marks the SRPs. By quantifying global proteins into decreased, maintained, and increased, post stress, we can simplify and group proteins into three domains. The m6A signatures of the mRNAs of all the proteins within each group can then be grouped into a single density plot, normalized to individual RNA length, to result in three simple m6A peak signatures, one for each protein group (decreased, maintained, and increased). By comparing the three m6A peak signatures, we would be able to very easily visualize how the m6A tags are different, in terms of location along the mRNAs, of the SRPs compared to other mRNAs in the cell. Since previous studies[8, 11, 29, 40, 50, 54, 198] showed acute nuclear changes in RNA modification systems and transcription post stress, we excluded nuclear RNA from the sequencing using cellular fractionation to minimize confounding nuclear co-transcriptional changes that would not be involved in the immediate translation processes out of the nucleus, and protein levels were factored based on SILAC ratios as decreased, maintained, and increased. The mRNA methylation peaks were then factored based on the SILAC protein ratios as decreased, maintained, and increased "peak patterns" to detect methylation signatures common to SRPs (i.e. unique to "increased" group). While the majority of proteins remained unchanged within 20 minutes of stress (maintained group), several hundred proteins were decreased (decreased group), either from decreased translation or from degradation, and a few hundred were significantly increased in stress (increased group), which predictably correlated poorly to RNA levels indicating transcription-independent activation of translation (Fig. 3-2, Fig. 3-3, 3-4). Quantitative analysis of the m6A peaks count of the RNA transcripts in each protein group revealed that the increased protein group (i.e. the SRPs), had the fewest number of peaks per transcript, likely the result of active extranuclear demethylation, since nuclear RNA

was excluded from sequencing (Fig. 3-5). Interestingly, the increased proteins also seemed to have shorter 3'UTRs when compared to maintained or decreased proteins suggesting the presence of common 3'UTR features between the SRP mRNAs (Fig. 3-6). Plotting the location of m6A peaks along the transcripts of increased, maintained, and decreased protein groups, normalized to the transcript length to decrease variability, showed clustering of peaks around the 3'UTR, as previously shown in other studies [45, 46, 50, 194](Fig. 3-7, Fig. 3-8). The increased proteins (SRPs) showed a unique bi-modal peak distribution downstream of the 3'UTR start sites when compared to maintained or decreased protein groups (Fig. 3-7, Fig. 3-8). While m6A methylation is relatively common in mRNA transcripts, and serves various functions and regulatory roles, a unique bimodal peak distribution downstream of the 3'UTR appears to be a previously unrecognized common signature for acutely translated SRPs. All together these results confirm that SRP mRNAs share a few common features that differentiate them from non-SRP mRNAs such as shorter 3'UTR lengths, decreased total m6A peak counts, and more importantly, a bimodal m6A peak distribution along their 3'UTRs.

The SILAC-meRIP experiment predicted several previously unrecognized SRPs, two of which are SRSF7, a protein involved in RNA binding and splicing regulation[38], and NDUFB8, the levels of which were confirmed to be increased acutely after stress (Fig. 3-9). Knockdown of METTL3 and FTO resulted in the loss of induction of SRSF7 and NDUFB8 after UV, confirming the requirement of methylation to tag SRP mRNAs for acute and selective translation after stress (Fig. 3-10), just as we saw with p53, suggesting that all these proteins share common translation activation mechanisms in stress, and confirming the findings of the sequencing experiments.

In order to understand the role of the bimodal m6A peak distribution in the acute translation of SRPs, we first confirmed the location of methylation peaks on p53 mRNA using a Bst-MRT RT enzyme system, which uses differential affinity of RT enzymes to methylated or non-methylated sites to quantify methylation peaks using RT-PCR[188]. By measuring the difference in reverse-transcription rate of the same RNA region using two different RT enzymes (BST and MRT) with one showing decreased activity, and one showing unchanged activity, in the presence of m6A, we are able to quantify and localize m6A peaks in a sequencing and antibody-independent manner. We designed primers against the entire 3'UTR of both p53 and SRSF7mRNAs and detected two regions of methylation along the 3'UTR of both transcripts, and based on previously published consensus m6A sites, the regions were predicted to contain a single methylation site. This confirmed the presence of bimodal methylation peaks downstream of p53 and SRSF7 3'UTR (Fig. 3-7). All together, these data suggest that a unique methylation peak pattern in the 3UTR of SRP mRNAs marks the SRP mRNAs for acute translation in stress (Fig. 3-12).

3.3. Figures

Figure 1

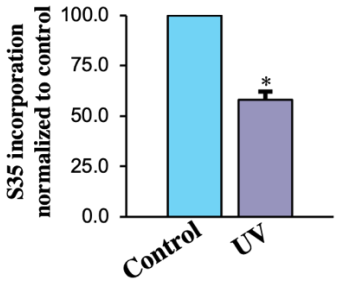

Fig. 1-1. To measure global translation after stress, newly translated proteins were radioactively labelled with Methionine S35, at baseline and 20 minutes after 25 J/m^2 UVB dose and run on SDS PAGE and radioactive proteins were quantified using immunoblots. Mean data of S35 signal normalized to Ponceau signal and SEM are shown, n=3, *p<0.05 compared to control.

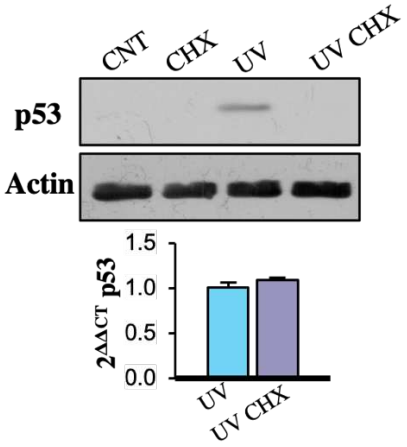

Fig. 1-2. P53 levels were measured after UV treatment in the presence and absence of cycloheximide (CHX), using immunoblots and qRT-PCR. Actin and 18S were used as loading controls for immunoblots and qRT-PCR, respectively.

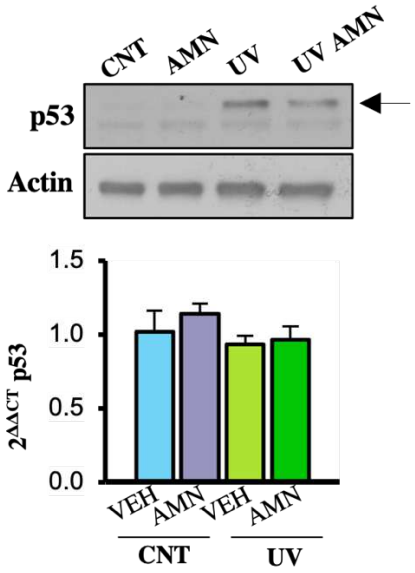

Fig. 1-3. P53 levels were measured after UV treatment in the presence and absence of alpha-amanitin (AMN), using immunoblots and qRT-PCRActin and 18S were used as loading controls for immunoblots and qRT-PCR, respectively.

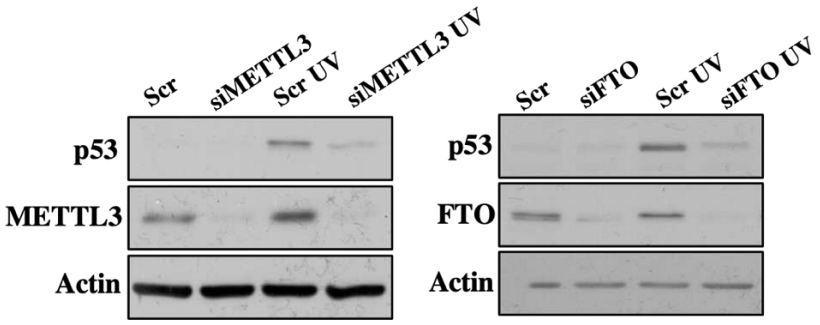

Fig. 1-4. P53 levels were measured after UV treatment in the presence and absence of siRNA for METTL3 (left blot), and FTO (right blot), using immunoblots. Actin was used as loading control.

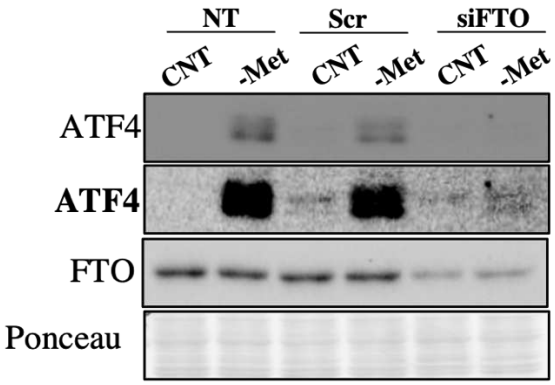

Fig. 1-5. ATF4 levels were measured after methionine deprivation in the presence and absence of siRNA for FTO, using immunoblots. Actin was used as loading controls for immunoblots.

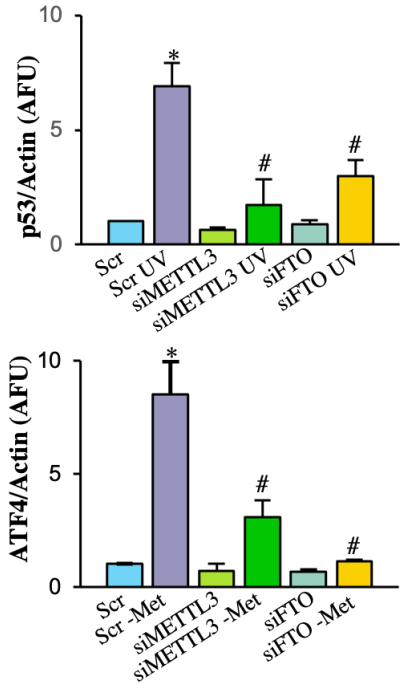

Fig. 1-6. Mean data of p53 and ATF4 protein levels normalized to Actin in the presence and absence of siFTO and siMETTL3 in control and UV treated cells (top chart), or methionine deprivation and ATF4 levels (bottom chart) showing an inhibition of SRP protein increase in the presence of siFTO and siMETTL3. n=3, *p<0.05 to control (non-UV treated group), #p<0.05 to Scr UV group.

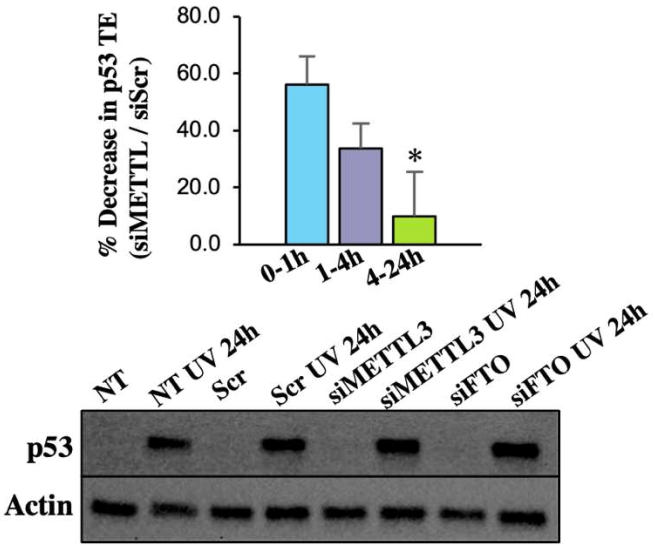

Fig. 1-7. Mean data of percent decrease in translation efficiency of with siMETTL3 as a timecourse after UV stress showing decreased effect on translation efficiency with time, with largest effect within 1 hour, and lowest effect 4-24 hours after stress (top chart). Immunoblots at the bottom show p53 protein levels in the presence and absence of siRNA for FTO and METTL3 in cells treated with UV for 24 hours showing the blunting of the increase after 24 hours. Actin is used as a loading control. n=3, *$p<0.05$ to 0-1h group.

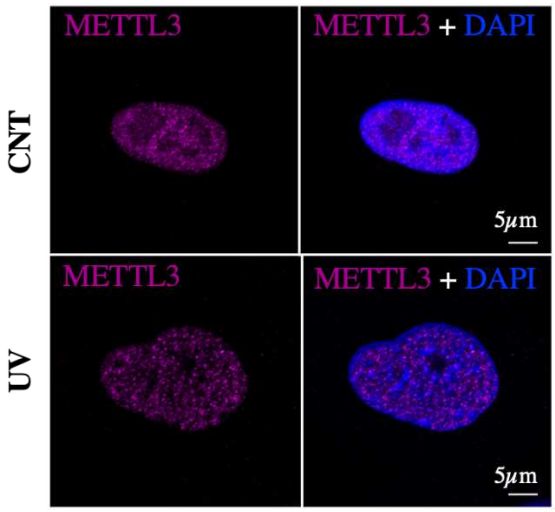

Fig. 1-8. Immunofluorescence staining showing METTL3 (purple) and DAPI (blue) in control and UV treated cells showing exclusively nuclear signal for METTL3 in control and UV treated cells.

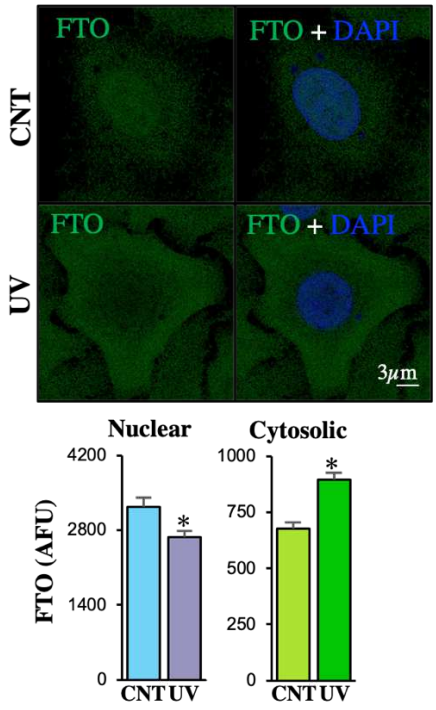

Fig. 1-9. FTO immunofluorescence staining showing FTO in green, in the nucleus and outside the nucleus in control and UV treated cells. DAPI nuclear stain shows nuclei in blue. Mean data below shows significantly lower FTO nuclear levels and higher Cytosolic FTO levels 20 minutes after UV treatment, suggestive of stress-induced acute FTO export from nucleus to cytosol. Mean data and SEM are shown, n=3, *p<0.05 to control (CNT).

Figure 2:

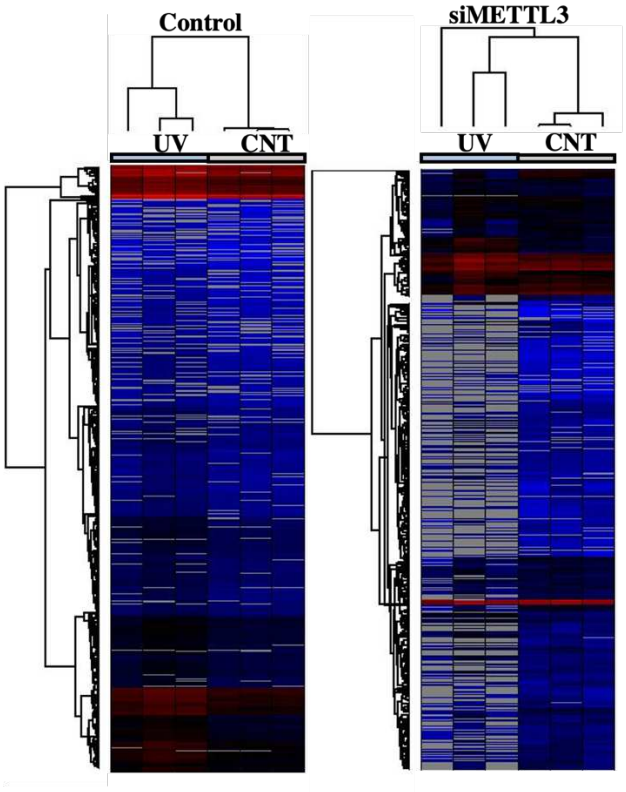

Fig. 2-1. Heatmap clustering of control and UV samples (n=3) in the presence and absence of METTL3 siRNA.

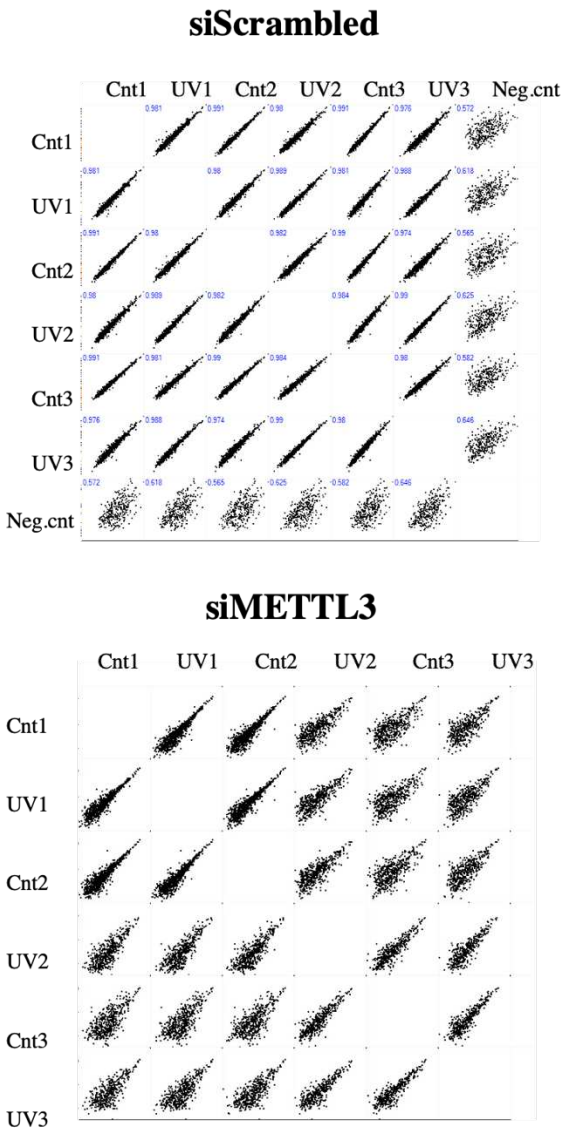

Fig. 2-2. Scatter plots of protein hits in the AHA mass spectrometry experiment of all groups (control and UV treated cells) in the siScrambled and siMETTL3 showing correlation between samples within the same group

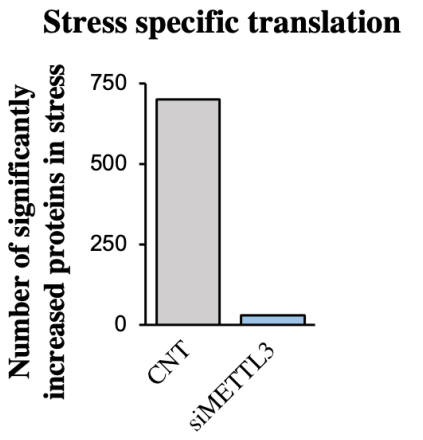

Fig. 2-3. Quantification of significantly increased proteins in UV compared to control treated cells in the siScr control and siMETTL3 groups.

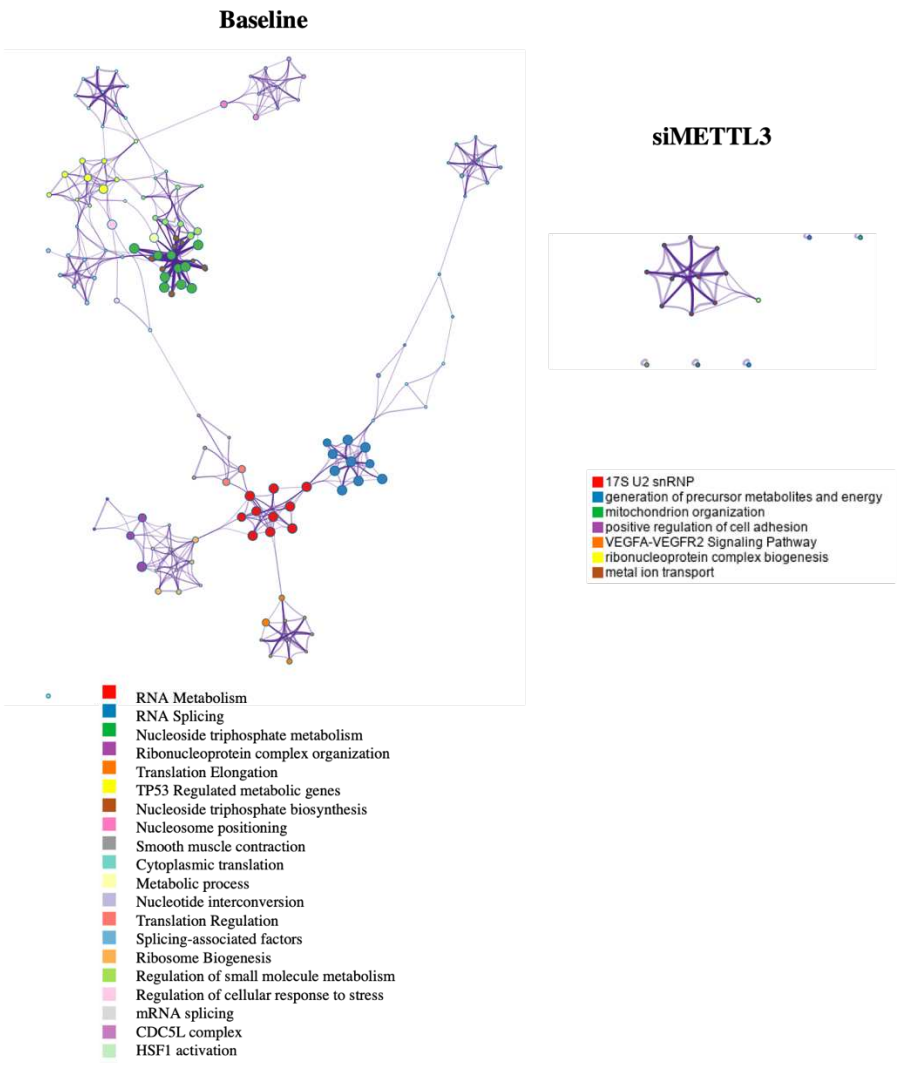

Fig. 2-4. Visual representation of pathway analysis of the significantly increased proteins in the UV treated cells compared to control treated cells. Peptides are labelled with L-AHA and detected with mass spectrometry.

Upstream Regulator	Predicted Activity	Activation Z-score	P-value of overlap	Mechanistic Network
MYC	+	8.863	2.78E-73	454
LARP1	-	-7.612	2.25E-64	
MYCN	+	4.19	1.33E-59	376
MLXIPL	+	7.298	1.47E-43	
TP53	+/-	0.932	2.31E-43	463
YAP1	+	3.52	1.72E-38	372

Fig. 2-5. Analysis of upstream regulators of the proteins significantly increased after 20 minutes of UV, as detected by L-AHA labelling, showing p53 protein as a major regulator of the acutely increased proteins after 20 minutes of UV.

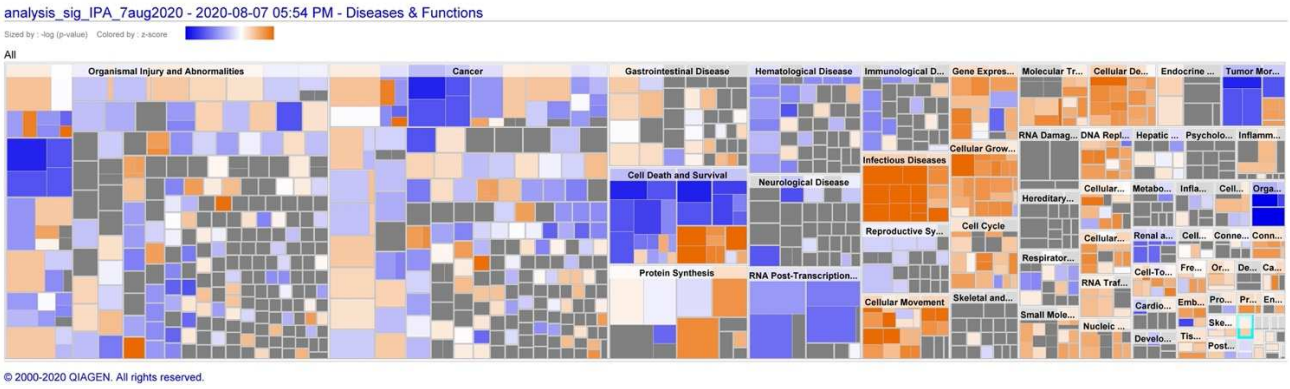

Fig. 2-6. Disease pathway analysis of the significantly increased proteins in UV treated cells, as measured with AHA labeling of peptides and mass spectrometry.

Figure 3:

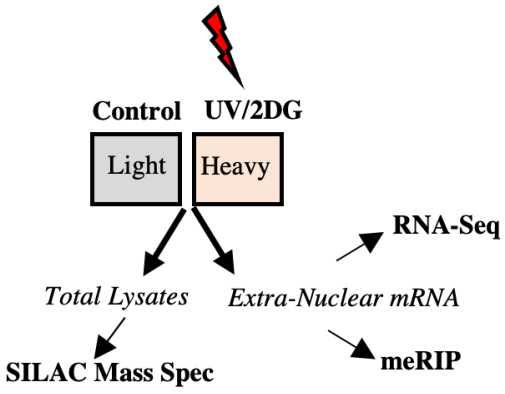

Fig. 3-1. Experimental design of the SILAC-meRIP experiment. Cells are labelled with light or heavy amino acids for 6 passages. They are then split into control or stress (UV

or 2DG) groups, treated for 20 minutes, and cells are then collected and split for protein and RNA analysis. Protein analysis is done via mass spectrometry to measure the H/L ratios, and meRIP-seq and RNA-seq are done on extra-nuclear RNAs.

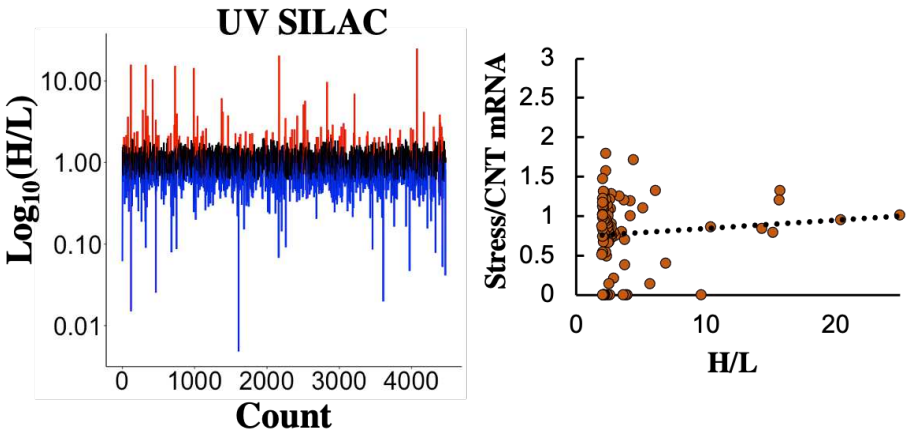

Fig. 3-2. Line plot of total protein levels in UV (heavy labelled) compared to control (light labelled) cells, expressed as H/L ratio. Correlation plot of RNA levels, measured using RNA-seq, of the top increased hits in SILAC shows no correlation between increased proteins and their RNA levels.

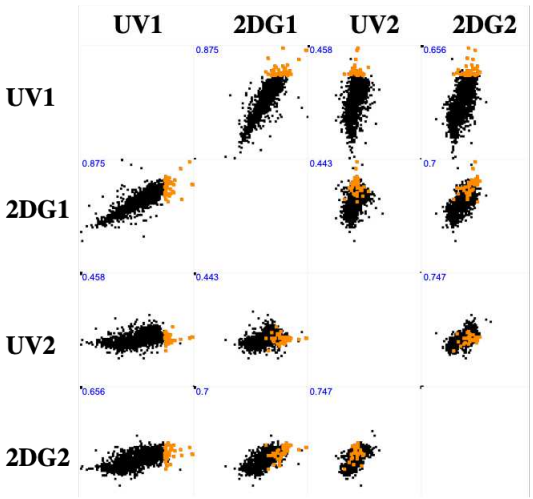

Fig. 3-3. Scatter plot analysis UV and 2DG stress groups levels normalized to their controls as H/L ratios highlighting the "increased" protein groups in orange in all 4 groups.

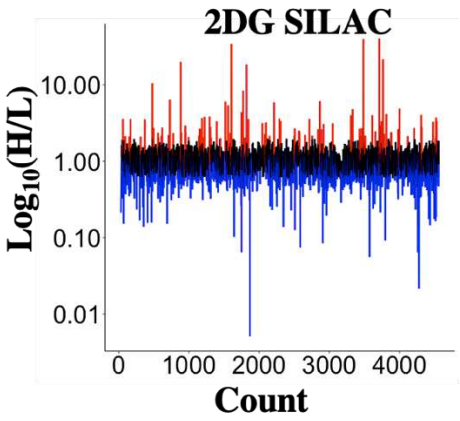

Fig. 3-4. Line plot of total protein levels in 2DG (heavy labelled) compared to control (light labelled) cells, expressed as H/L ratio.

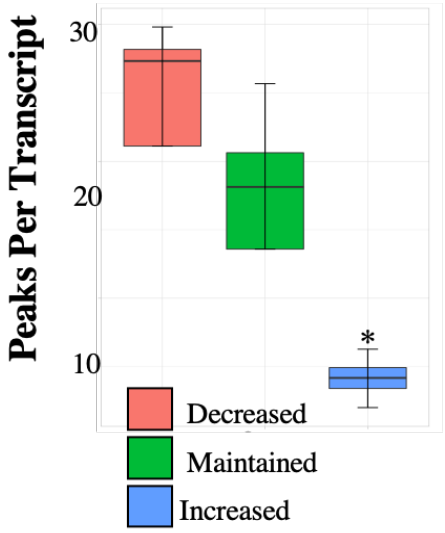

Fig. 3-5. Average number of methylation peaks per transcript quantified using meRIP-seq, factored based on protein levels measured using SILAC as decreased, maintained, or increased, showing decreased total number of peaks in the increased group compared to decreased or maintained groups. *p<0.05 compared to Decreased and Maintained groups.

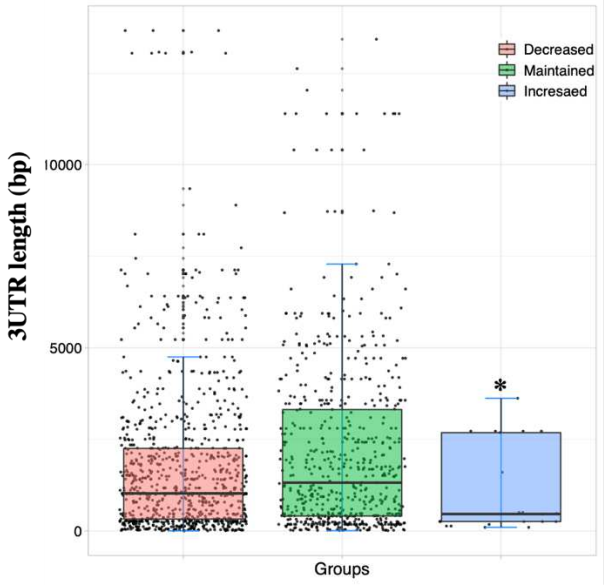

Fig. 3-6. Boxplot representation of the total length of 3'UTR based on protein levels of decreased, maintained, and increased groups showing decreased 3'UTR length of the increased protein group. *p<0.05 compared to decreased and maintained 3'UTR lengths.

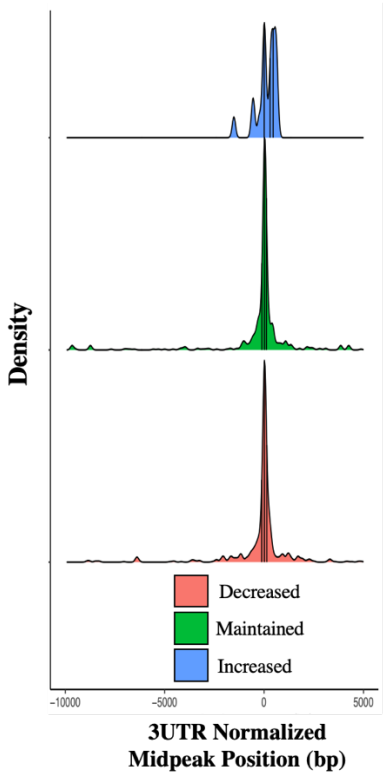

Fig. 3-7. Pooled M6A peak locations from 3UTR of the increased, maintained, and decreased protein groups showing bimodal peak distribution downstream of the 3UTR of the increased protein groups.

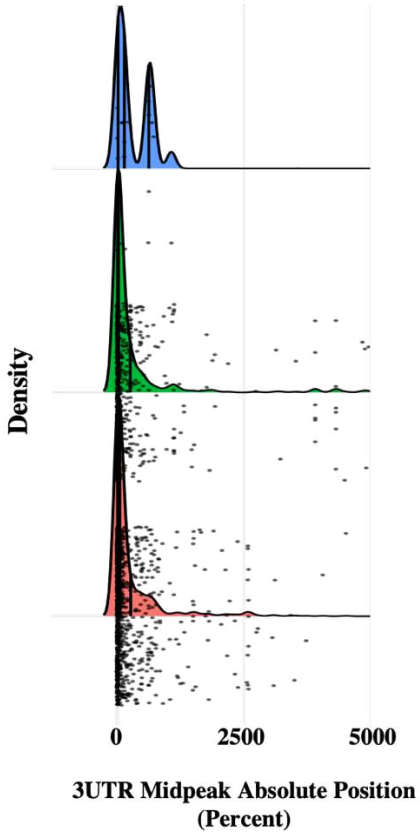

Fig. 3-8. Location of the m6A peaks represented in relationship to the 3'UTR, as an absolute percentage, normalized to length of individual mRNAs, showing bimodal peak distribution further away from the 3'UTR start site in the increased, but not the maintained or decreased protein groups.

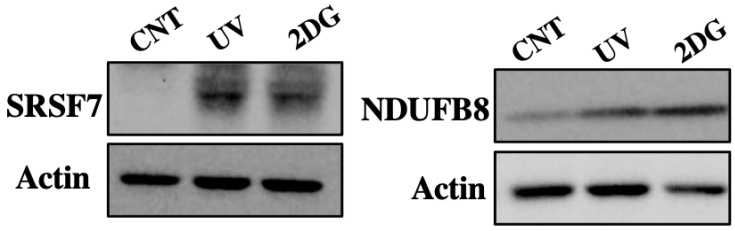

Fig. 3-9. Immunoblots of SRSF7 and NDUFB8 proteins showing the increase in their levels after 20 minutes of UV, as predicted by the SILAC-meRIP experiment. Actin is used as a loading control

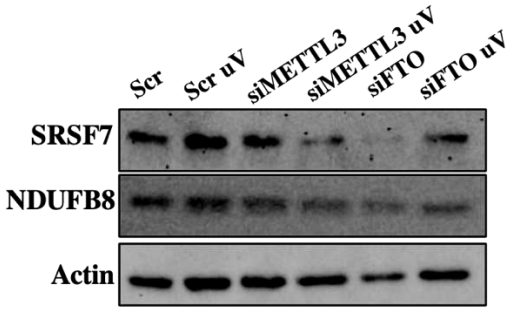

Fig. 3-10. Immunoblots of SRSF7 and NDUFB8 proteins showing the increase in their levels after 20 minutes of UV, and loss of increase in the presence of siRNA for FTO or METTL3. Actin is used as a loading control

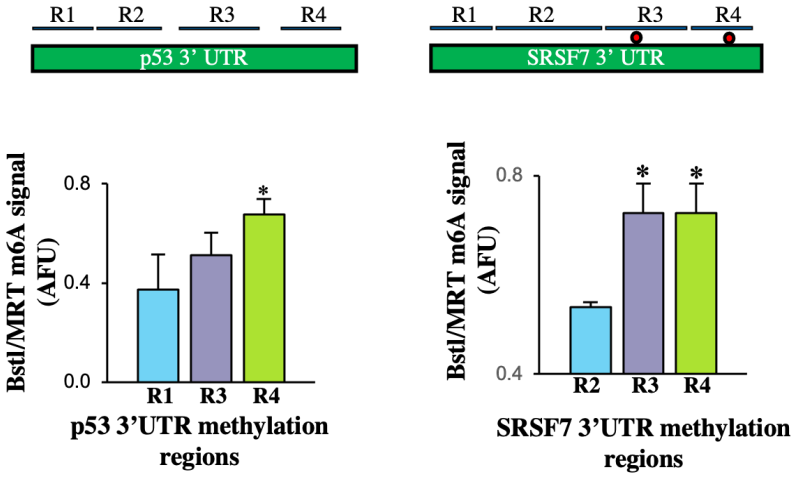

Fig. 3-11. Representation of the regions probed, and m6A peaks detected in p53 and SRSF7 3'UTR using BST-MRT qRT enzyme assay for m6A detection. Mean data of methylated regions are show in charts below. n=3, *p<0.05 to non methylated region. (R1 for p53, and R2 for SRSF7).

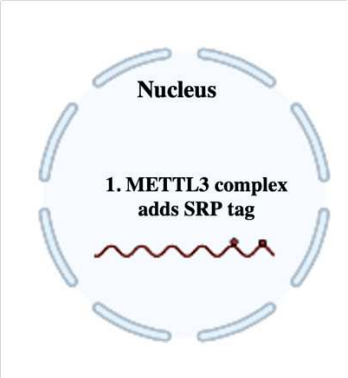

Fig. 3-12. Schematic summarizing findings of figure 1. Methylation complex adds an SRP tag (bimodal m6A peaks in the 3'UTR of SRP mRNAs), in the nucleus.

Chapter 4

Cytoskeletal FTO mediates acute demethylation of SRP mRNAs post stress

4.1. Introduction and Summary:

Chapter 3 established the presence of m6A-mediated stress translation system that is responsible for the selective translation of hundreds of proteins acutely after stress. To investigate the mechanism of this translation system, we started with two pieces of evidence that emerged from early experiments, which led to an exciting discovery about novel specialized translation locations within the cell, and the involvement of a major cellular component, the microtubules.

Firstly, we knew that m6A tagging is required for the selective SRP translation. This suggested that SRP mRNAs likely have a unique m6A features along their mRNAs that distinguish them, and mark them for selective translation. We saw from sequencing experiments that this is likely the bimodal m6A peaks in the 3'UTRs. The second piece of evidence that helped us elucidate the mechanism further was the surprising finding that FTO was also required to translate certain model SRPs, such as p53, ATF4, and the newly discovered SRSF7 and NDUFB8. Since FTO is a demethylase, it suggests that at some point during the life of the SRP mRNA, possibly after the stress, there is some selective FTO-mediated demethylation that may act as an activation signal for translation. We therefore looked first measured FTO activity to see if it is activated acutely after stress, and in fact we see that it's activity increased significantly acutely after 2DG and UV stresses suggesting that acute demethylation is likely taking place. Intriguingly we see that this demethylation is also occurring in the cytoskeletal fraction of cells, bringing the cytoskeleton into the forefront of our mechanism as a possible selective site of translation for SRPs during stress. Using several experiments, we see that microtubules are acting as a site for SRP translation, a finding that provides exciting novel insight into location-mediate selectivity of translation in cells, beyond the classic ER-Cytosolic ribosomal divide, and

elucidating the second element of selectivity in SRP translation, first being the bimodal m6A signature, and second being the site-specific translation along the microtubules.

4.2. Results.

4.2.1. Acute stress results in m6A demethylation within the cytoskeletal cell comportment

To solve the fact that the SRP translation in stress requires both a methyltransferase system (METTL3/14) and the demethylase, FTO, we predicted that a possible dynamic regulatory mechanism may be providing two critical functions for SRP translation and the demethylation could allow it to switch from one function to another. Going back to *challenge 5* of translation in section 1, translating SRPs would require two elements. First the SRP mRNAs should be prevented from being translated at baseline prior to stress, and secondly the SRP mRNA should be selectively translated in a highly efficient manner immediately after stress. The requirement of both the methyltransferase and the demethylase suggested that m6A likely fulfills both elements in marking the SRP mRNA and preventing translation at baseline prior to stress, and inducing the translation acutely after stress. So we predicted that FTO likely serves as the activation signal for SRP translation by demethylating an inhibitory m6A SRP tag that serves to mark SRP mRNAs and prevent their translation when not needed. We found that while METTL3 remained exclusively within the nucleus at both baseline and after UV, FTO appears to exist the nucleus within 20 minutes of UV, likely closer to the translation sites[44, 55]. (Fig. 1-8, Fig. 1-9). This suggests that while methylation may occur in the nucleus (perhaps tagging potential SRPs, an acute extranuclear demethylation may be required for the selective SRP translation, and that demethylation could be the “activation signal” for SRP translation under stress. This is supported by the observation that the mRNAs of proteins that go up within 20 minutes of UV

and 2-DG stress show decreased methylation levels when compared to mRNAs of proteins that do not go up (Fig. 3-5). To test whether FTO activity is also dynamically regulated in stress, we measured FTO activity within 20 minutes of stress (UV and 2-DG) and found a significant acute increase in it's m6A demethylation activity suggesting an acute (within 20 minutes of stress exposure) activation of FTO outside of the nucleus (Fig. 4-1). Using RNA dot blots, we found that this was associated with a concurrent decrease in total RNA methylation acutely after several stresses (UV, methionine deprivation, as well as an additional stress, i.e. heat shock, suggesting perhaps a universal stress response) (Fig. 4-2, Fig. 4-3) in agreement with the increase in FTO m6A demethylase activity after stress. This suggests that the acute demethylation is likely a conserved and universal response to stress that encompasses a large group of mRNAs. Knockdown of FTO using siRNA resulted in the loss of methylation decrease after UV stress (Fig. 4-4), suggesting that FTO is mediating the large scale acute demethylation after diverse stresses. While stress may decrease co-transcriptional methylation of RNA, blocking RNA transcription, using α-amanitin, resulted in a surprising increase in RNA methylation at baseline and after stress, suggesting that the stress-induced decrease in methylation is likely due to the increase in demethylation activity of FTO (Fig. 4-5), and is not the result of acute nuclear changes in co-transcriptional mRNA methylation.

To address the mechanism of selective translation further, we then looked at where the m6A tagged RNA localize within the cell, and where the demethylation is occurring post stress as we predicted that it is possible for SRP translation to be sequestered in certain microdomains of translation that are spared from the global translation suppression after stress. Using cellular fractionation, we found an extra-nuclear decrease in methylation in the cytoskeletal (CS) fraction in UV (Fig. 4-7) suggesting that acute demethylation of SRP mRNAs may be occurring in the

CS fraction. Cellular fractionation also revealed a large amount of methylated RNA in the CS fraction at baseline (Fig. 4-6), suggesting a role for the cytoskeletal fraction in the acute translation of SRPs and more specifically that the increase in FTO activity occurs within the cytoskeletal fraction. We utilized several markers for each compartment to ensure adequate separation of subcellular components, including cytosolic markers (MEK1), ER markers (Grp78), and Nuclear and Ribosomal markers (Fig. 4-8- Fig. 4-10).

The association between the cytoskeleton and m6A-tagged mRNAs warranted investigating the cytoskeleton as a possible microdomain of SRP translation in stress. We then looked at whether FTO associates with the cytoskeleton, and high resolution immunofluorescence staining of FTO outside of the nucleus reveals a colocalization with a microtubular (MT) pattern suggesting that FTO possibly associates closely with the MT network (Fig. 4-11). Mass spectrometric analysis to immunoprecipitated FTO showed a strong enrichment in MT-associated proteins (Fig. 4-12). All together, these data suggest that after exiting the nucleus microtubule-associated FTO is activated acutely after stress leading to selective m6A demethylation in the CS fraction, which may be a previously unrecognized microdomain for selective SRP translation in stress. The surprising role the microtubule network appears to play in the FTO-m6A mediated SRP translation could solve the second main challenge in a universal SRP translation system; selective sparing of ribosomes from universal translation inhibition after stress by providing microdomains for SRP translation. In addition, translating SRPs close to the MT network could result in rapid shipping of translated proteins to all parts of the cell via the microtubule networks. This warranted further experiments to look into the role of microtubule networks into the selective SRP translation in stress.

4.2.2. m6A-mediated SRP translation occurs in microtubule-associated foci

Since the cytoskeleton has been implicated in RNA localization, and stress responses, and RNA is known to translocate within the cell along microtubules [79, 81, 128, 130, 199, 200], we speculated that the microtubule portion of cytoskeleton may be involved in the acute translation of m6A-SRPs, beyond it's possible role in mRNA translocation. As such, treating cells with microtubule destabilizers (colchicine and nocodazole) 1-2 minutes prior to UV stress exposure, a timeline that would predictably affect the microtubule translation role more than the translocation role of mRNA, significantly decreased p53 translation efficiency over 20 minutes suggesting that microtubule stability may be required for acute translation of m6A-SRPs (Fig. 4-13). We then imaged newly synthesized proteins using O-propargyl puromycin (OPP), a fluorescent amino acid mimetic that incorporates into newly synthesized proteins allowing for visualization of translation, along with m6A and beta-tubulin after 20 minutes of stress to visualize the relationship between m6A signals and translational changes in stress. While total translation was predictably decreased within 20 minutes of UV and 2DG stresses (Fig. 4-14), dense OPP translation foci, or granules, appeared to increase significantly after UV and 2DG stress, as early as 5 min (Fig. 4-15, Fig. 4-16, Fig. 4-17). Furthermore, co-staining of m6A, microtubules (beta tubulin), and ribosomes (S6) revealed co-localization with the stress-induced translation foci (Fig. 4-18, Fig. 4-19). These imaging studies suggested that microtubules likely provide a platform for m6A-mediated selective translation in stress.

We noticed that the co-localization sites followed a "Y" shaped microtubule pattern reminiscent of gamma-tubulin and the augmin complex which provides a branching point for microtubules and has previously been linked to stress response [162-165, 201] (Fig. 4-19). We

further investigated the possibility of gamma tubulin, or microtubule branching points, as the site of selective SRP translation as these are the most stable points along the microtubule networks. Co-staining of OPP and FTO and gamma-tubulin using proximity ligation assay (PLA), a technique that combines antibody binding specificity with DNA probe amplification which allow sensitive colocalization detection within 30 nm. We saw that FTO and gamma-tubulin associate with each other within 30nm and more importantly these association sites showed a near perfect colocalization with the OPP translation foci that increase after stress (Fig. 4-20). This suggests that the active SRP translation, predicted to occur in the OPP translation foci, is occurring at FTO-gamma tubulin sites. Furthermore, m6A-pulldown showed a microtubule and RLP26 ribosomal protein binding (Fig. 4-21). All together these data suggest an important role for microtubule-associated units with the acute translation of m6A-tagged SRPs, presumably in translation foci on the microtubule networks along gamma-tubulin branching points.

While stress granules made of RNA-protein complexes are known to form acutely after stress [20], the observed translation foci appear to be distinct cellular complexes due to the absence of stress granule marker TIAR and the presence of active translation detected with OPP staining (Fig. 4-22). Overall, we observe an acute demethylation on SRP mRNAs at microtubule junctions (or gamma-tubulin branching points), which is likely the activation signal of SRP translation, and the microdomain site for selective SRP translation (Fig. 4-23).

4.3. Figures.

Figure 4:

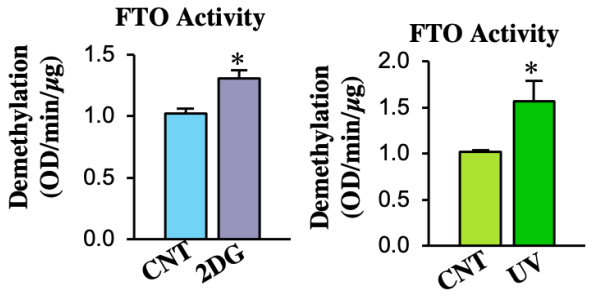

Fig. 4-1. Mean data of FTO activity measured using an m6A demethylase antibody based assay of immunoprecipitated FTO from control and 2DG or UV treated cells. n=3-4, *p<0.05 compared to control (CNT).

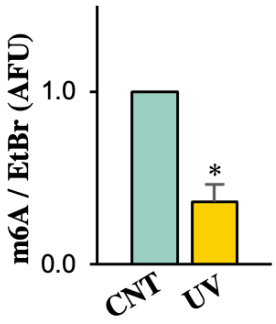

Fig. 4-2. Mean data of m6A levels measured using RNA dot blots and an m6A-specific antibody from control and UV treated cells. n=8, *p<0.05 compared to control (CNT).

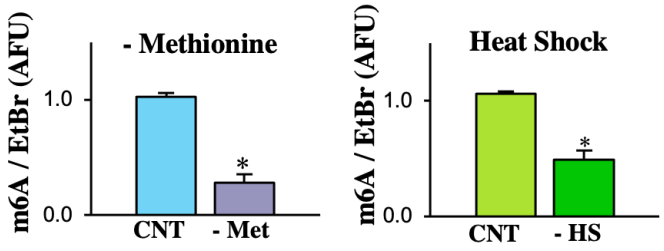

Fig. 4-3. Mean data of m6A levels measured using RNA dot blots and an m6A-specific antibody from control and methionine deprived, or heat shock treated cells. n=6, *p<0.05 compared to control (CNT).

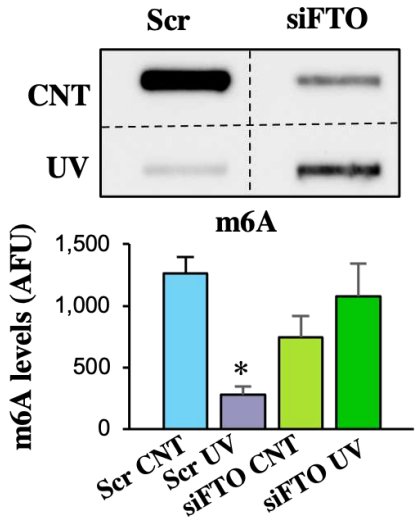

Fig. 4-4. RNA dot blot showing m6A levels from control and UV treated cells in the presence and absence of Scrambled or FTO siRNA. Mean data shown underneath of m6A levels normalized to RNA gels. n=3, *p<0.05 compared to scrambled siRNA control (Scr CNT).

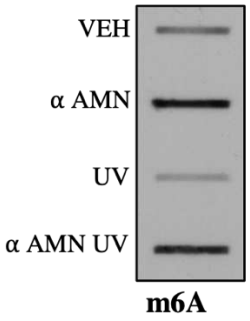

Fig. 4-5. RNA dot blot showing m6A levels from control and UV treated cells in the presence and absence of alpha-amanitin transcription inhibitor.

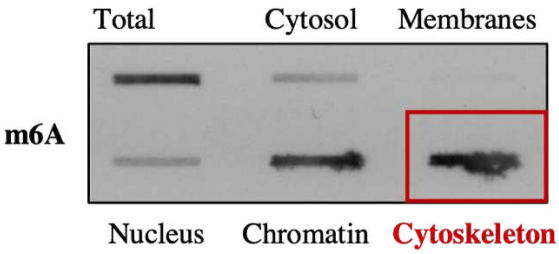

Fig. 4-6. RNA dot blot showing m6A levels at baseline in different cellular fractions. Shown in red box is m6A amounts in the cytoskeletal fraction indicating the presence of significant amounts of m6A-tagged mRNAs in the cytoskeletal fraction.

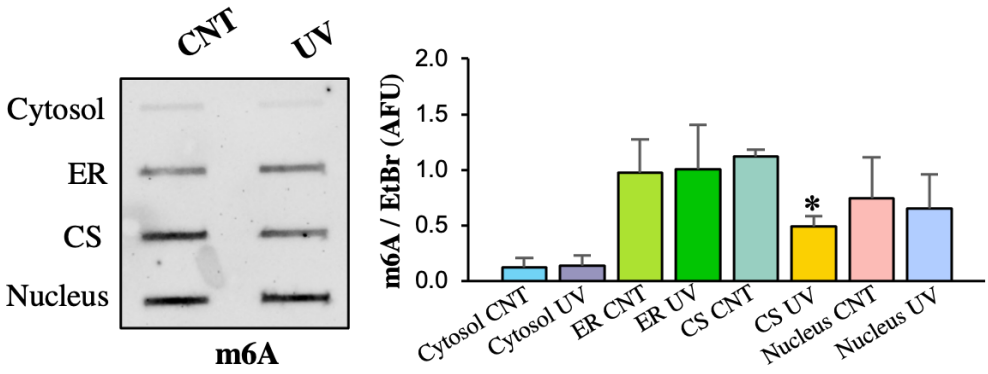

Fig. 4-7. RNA dot blot showing m6A levels of different cellular fractions (cytosol, ER, CS, and nuclear) from control and UV treated cells. RNA gel of the same RNA samples stained with ethidium bromide shows RNA loading and quality of samples in the middle. Mean data of m6A levels, normalized to RNA levels measured in RNA gels, showing the decrease in m6A levels in the CS fraction only in UV treated cells compared to control. n=3, *p<0.05 compared to CS control (CNT).

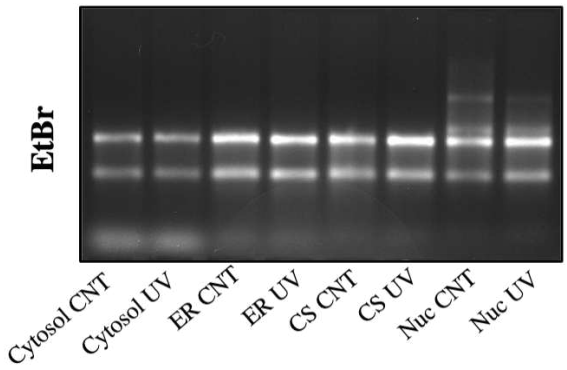

Fig. 4-7. RNA gel stained with ethidium bromide showing RNA levels and patterns of total RNA isolated from Cytosolic, ER, Cytoskeletal (CS), or nuclear fractions in control and UV treated cells. The RNA gels are used to normalize RNA amounts loaded onto RNA dot blots (in Fig. 2C).

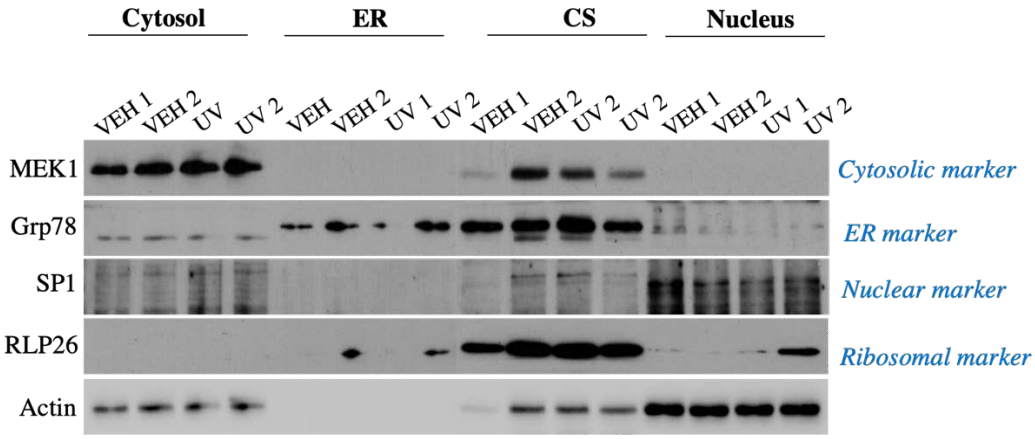

Fig 4-8. Immunoblots showing fractionation purity of cytosolic, ER, cytoskeletal (CS), and nuclear fractions with specific markers for fraction (indicated in blue font on the side) from control and UV treated cells.

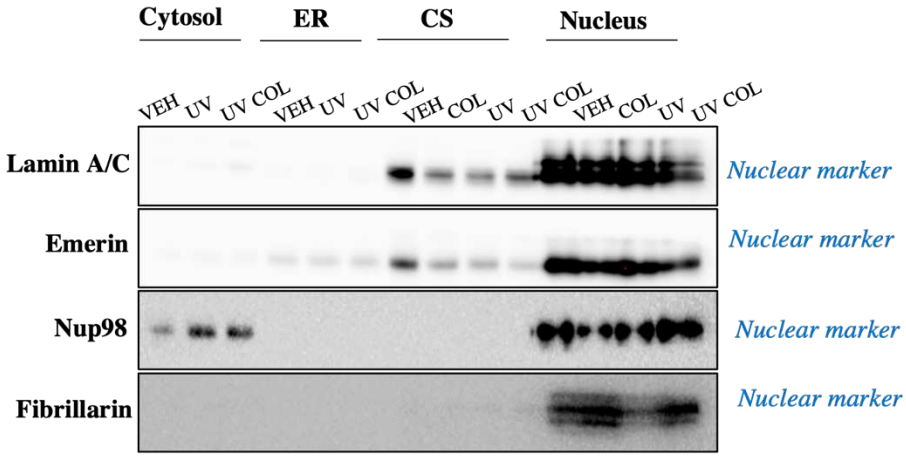

Fig. 4-9. Immunoblots showing fractionation purity of cytosolic, ER, cytoskeletal (CS), and nuclear fractions with additional nuclear specific markers showing the distinct separation in the CS and nuclear pools.

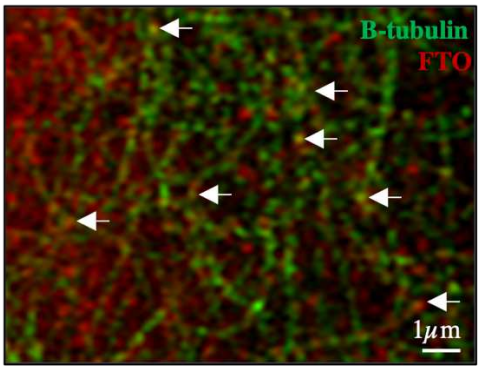

Fig. 4-10. Immunofluorescence staining of FTO (red) and beta tubulin (green) showing microtubular colocalization patterns.

FTO Binding partners Clustering (DAVID 6.7)

Top Cluster (score 16.79)

Analysis	Pathway	Count	p Value	Benjamini
INTERPRO	Tubulin/FtsZ, 2-layer sandwich domain	14	9.90E-26	1.60E-23
INTERPRO	Tubulin, conserved site	14	2.30E-25	1.90E-23
INTERPRO	Tubulin/FtsZ, C-terminal	14	2.30E-25	1.90E-23
INTERPRO	Tubulin, C-terminal	14	2.30E-25	1.90E-23
INTERPRO	Tubulin	14	4.90E-25	2.70E-23
KEGG_PATHWAY	Pathogenic Escherichia coli infection	17	8.90E-25	7.50E-23
INTERPRO	Tubulin/FtsZ, GTPase domain	14	1.00E-24	4.20E-23
GOTERM_MF_DIRECT	structural constituent of cytoskeleton	20	3.50E-24	6.60E-22
SMART	SM00865	14	8.70E-24	4.20E-22
SMART	SM00864	14	4.30E-23	1.00E-21
GOTERM_BP_DIRECT	microtubule-based process	13	1.20E-19	6.10E-17
UP_KEYWORDS	Cytoskeleton	31	2.20E-16	6.90E-15
INTERPRO	Beta tubulin	8	1.40E-15	4.40E-14
INTERPRO	Beta tubulin, autoregulation binding site	8	1.40E-15	4.40E-14
KEGG_PATHWAY	Gap junction	14	1.80E-15	7.50E-14
GOTERM_BP_DIRECT	cytoskeleton organization	15	5.60E-14	1.40E-11
KEGG_PATHWAY	Phagosome	15	9.30E-14	2.60E-12
UP_KEYWORDS	Microtubule	16	1.10E-12	2.40E-11
GOTERM_CC_DIRECT	microtubule	17	1.20E-12	2.30E-10
GOTERM_MF_DIRECT	GTPase activity	14	2.40E-10	1.50E-08
INTERPRO	Alpha tubulin	6	9.10E-10	2.50E-08
UP_SEQ_FEATURE	nucleotide phosphate-binding region:GTP	14	1.10E-09	3.30E-07
UP_KEYWORDS	GTP-binding	14	2.70E-09	3.30E-08
UP_KEYWORDS	Nucleotide-binding	26	8.80E-08	9.70E-07
GOTERM_MF_DIRECT	GTP binding	14	9.20E-08	3.50E-06

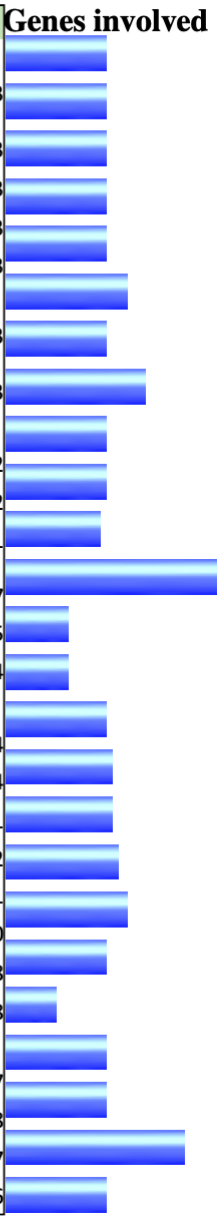

Fig. 4-11. Chart showing FTO binding partners detected using FTO immunoprecipitation (at baseline) and mass spectrometry. Microtubule-related proteins are highlighted in blue font, and blue bars on side show the relative number of genes involved.

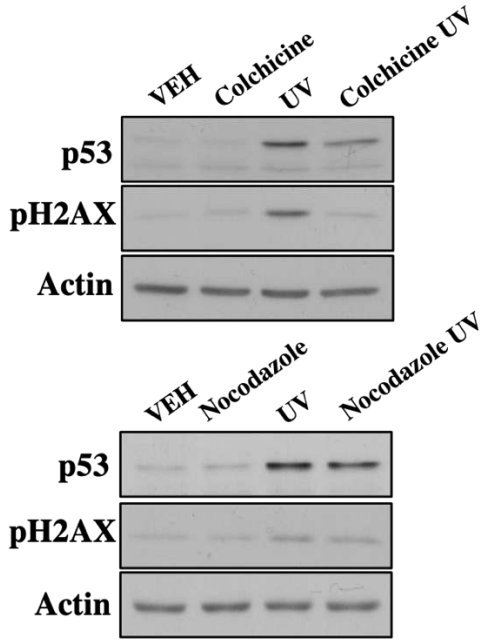

Fig. 4-12. Immunoblots showing p53 levels, and DNA damage response marker (pH2AX) in control and UV treated cells in the presence and absence of microtubular destabilizer colchicine (top blot), and nocodazole (bottom blot). Actin is used as a loading control.

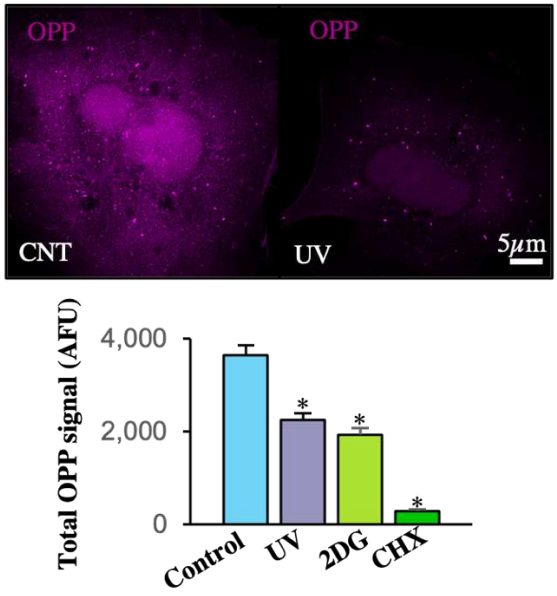

Fig. 4-13. Immunofluorescence staining showing OPP (purple) and beta microtubules (green) showing the dense translation foci colocalization with microtubular patterns. n=3, *p<0.05 compared to control.

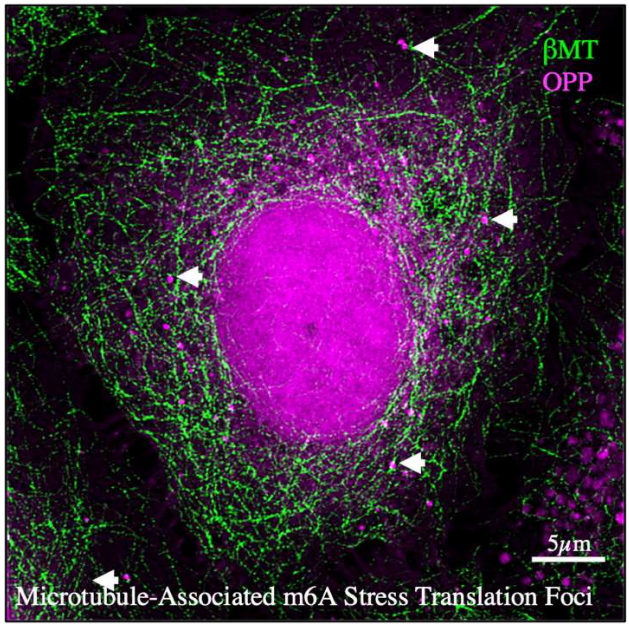

Fig. 4-14. Immunofluorescence staining of translation measured using OPP dye (in purple) that incorporates into newly synthesized proteins in control and UV treated cells. Chart underneath is mean data showing total fluorescence detected in control, UV, 2DG, and cycloheximide (CHX) treated cells, showing decreased translation levels in stress and a near complete loss of fluorescence in presence of CHX.

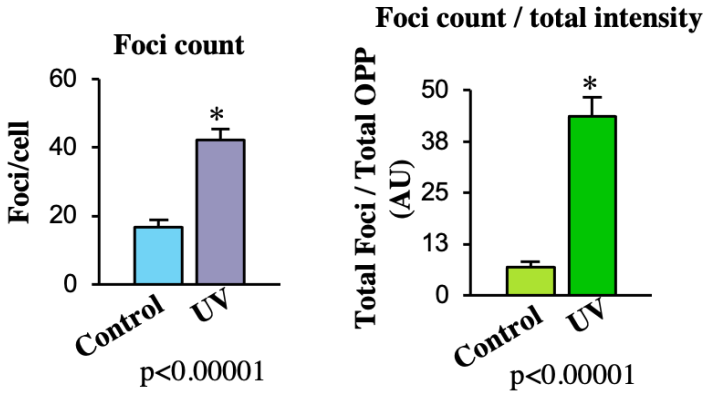

Fig. 4-15. Mean data quantifying the dense translation granules (count per cell) in control and UV treated cells showing significant increase in the foci after 20 minutes of UV.

Chart on right shows the number of foci normalized to total OPP intensity in control and UV treated cells. n=3, *p<0.05 compared to control.

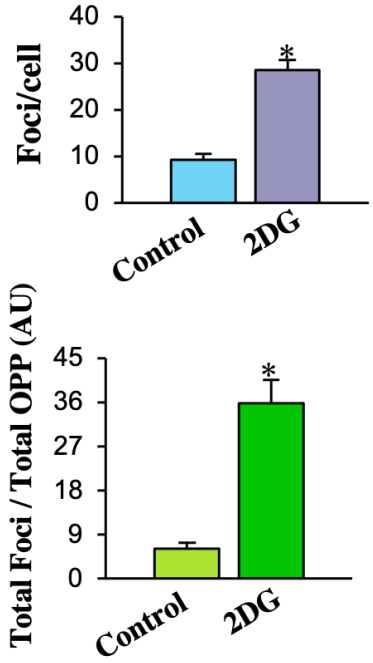

Fig. 4-16. Mean data quantifying the dense translation granules (count per cell) in control and 2DG treated cells showing significant increase in the foci after 20 minutes of 2DG treatment. Chart on right shows the number of foci normalized to total OPP intensity in control and UV treated cells. n=3, *p<0.05 compared to control.

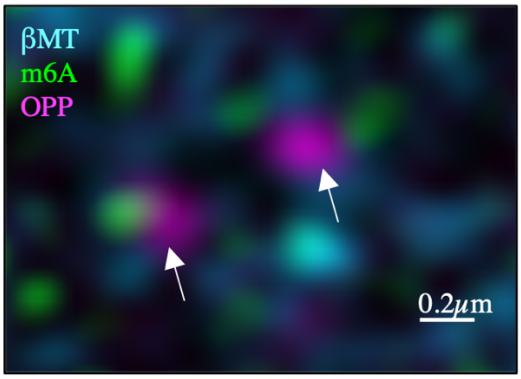

Fig. 4-17. Immunofluorescence staining showing OPP (purple), beta microtubules (blue), and m6A (green) showing colocalization between all three components.

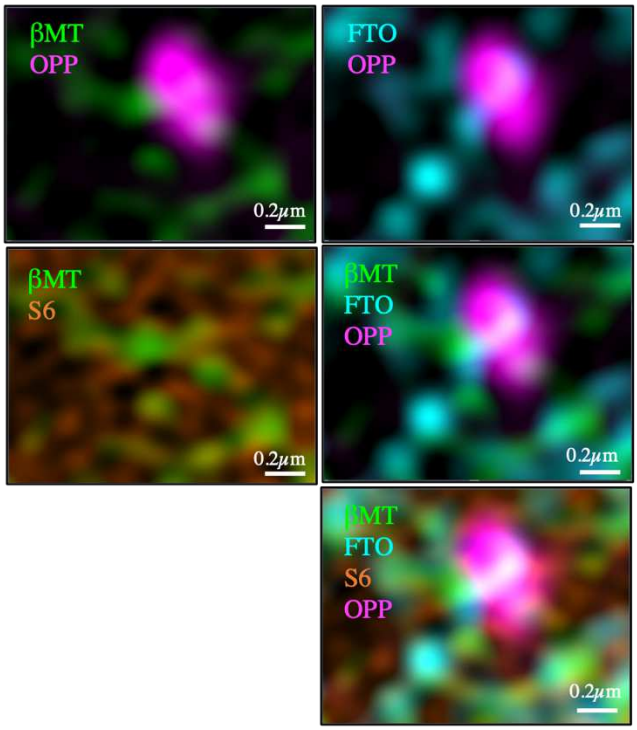

Fig. 4-18. Immunofluorescence staining showing OPP (purple), beta microtubules (green), FTO (blue) and S6 (orange) showing colocalization between all four components.

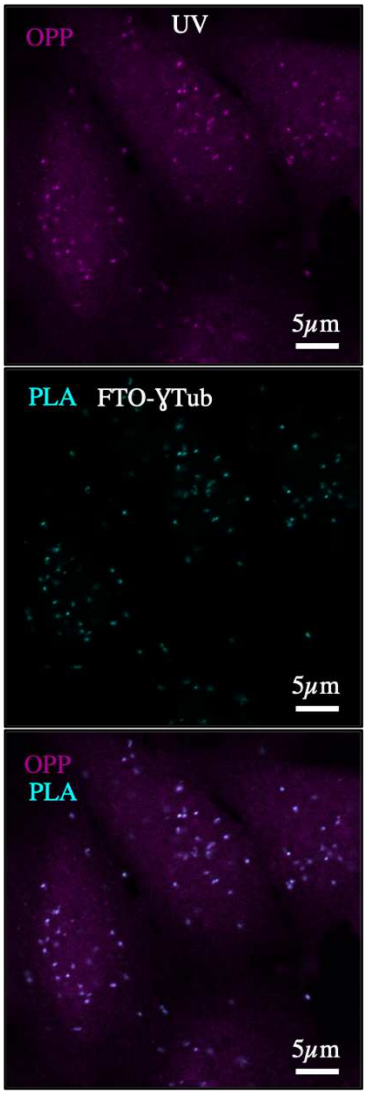

Fig. 4-19. Immunofluorescence staining of OPP (in purple) and PLA between FTO and gamma tubulin (in teal) in control and UV treated cells showing colocalization in the PLA signal and the dense translation foci that increase in UV.

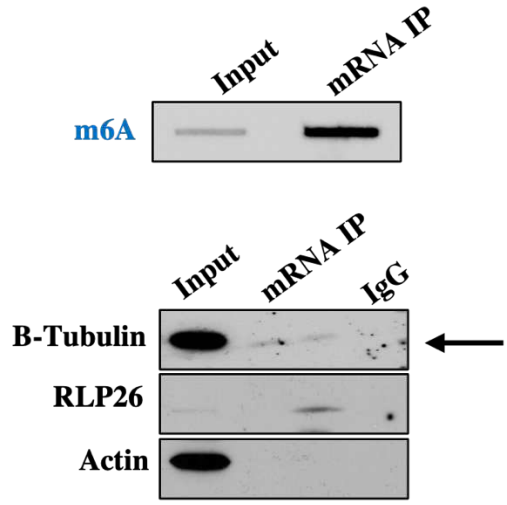

Fig. 4-20. RNA dot blot (top) showing m6A levels in mRNA IP using for co-immunoprecipitation detection of beta-tubulin, and RLP26 proteins (shown in immunoblots below). Actin is used as a control for non-mRNA binding proteins and to show IP purity.

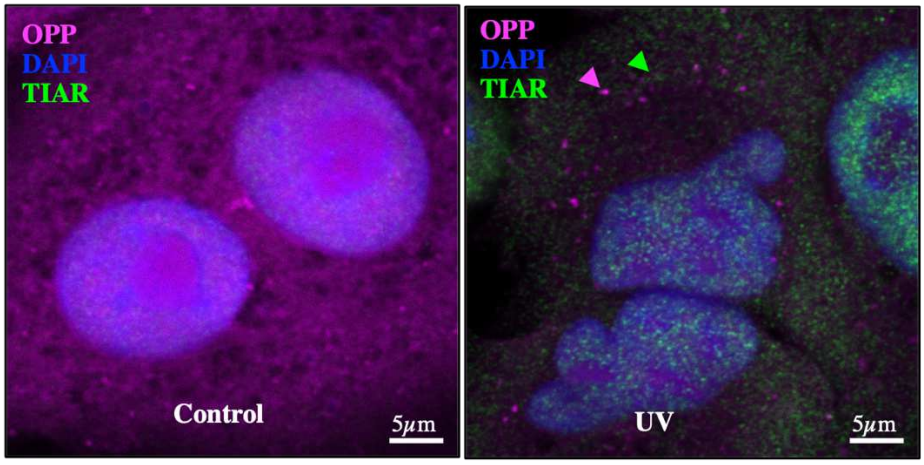

Fig. 4-21. Immunofluorescence staining of OPP (purple), DAPI (blue), and TIAR stress granule marker (green) in control and UV treated cells showing no colocalization between the dense translation foci induced after UV and the stress granule marker TIAR.

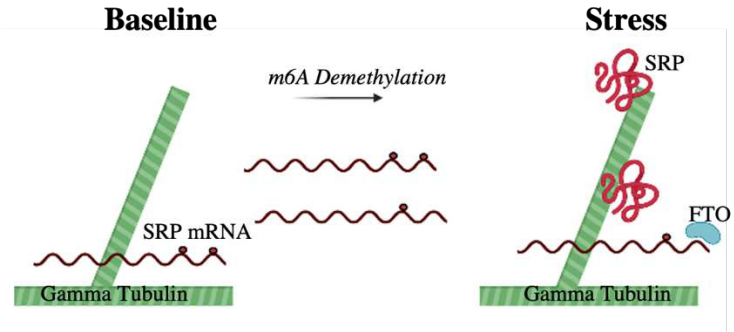

Fig. 4-22. Schematic summarizing findings of figure 2. SRP tagged mRNAs (with the bimodal methylation peaks), associates with gamma tubulin on the cytoskeleton where microdomain specialized stress induced translation occurs. The likely "activation signal" is the demethylation the bimodal peak.

Chapter 5

Cytoskeletal Ribosomes translate SRP mRNAs

5.1. Introduction and summary:

While Chapter 4 shed some important light on the mechanism of SRP translation in stress and brought to the forefront the microtubule network, in particular gamma tubulin branching points of the network, along with FTO demethylation activity, lots of important questions remained unanswered. Firstly, how is FTO activated as this activation signal will be upstream of FTO and downstream of the stress sensor and is likely to be a major regulator of stress responses. Secondly, if branching points of microtubules can act as translation centres for SRPs, does this mean that actively translating ribosomes are sequestered there? Answers to these questions would further expand the links between the SRP translation and the sensors of stress, and the downstream ribosomes that carry out the selective translation.

In this chapter we explore those links in detail. We first show that FTO is activated by a phosphorylation tag on a highly mobile loop in its N terminus at threonine-6 (T6). This phosphorylation strongly activates the demethylation activity of FTO. We then show that MARK4, a microtubule associated kinase, phosphorylates FTO at T6 and activates it acutely after stress, and that MARK4 is important for translating model SRPs like p53 and ATF4. While this elucidates the mechanism upstream of FTO activity further, we then investigate the possibility of having actively translating ribosomes along the microtubule networks. To address this we use a combination of methods and techniques such as cellular fractionation followed by HPLC ribosomal profiling, ribosomal sequencing, and other imaging and antibody-based experiments. We show that the cytoskeletal fraction (CS) does in fact have an actively translating ribosomal pool which increases in activity acutely after stress, and using ribosomal sequencing we see that the mRNAs translated in this pool strongly matches the SRPs detected in chapter 3. Similarly we find other distinguishing features of the CS ribosomal pool that set it apart from ER

and cytosolic ribosomal pools such as enrichment of RLP26, and a lower level of p-eIF2a in stress.

5.2. Results.

5.2.1. FTO is activated by phosphorylation on threonine-6 by microtubule-associated kinase MARK4.

To assess the mechanism of translation activation further, we focused on FTO as we have that it's activity increases acutely in stress, it is required to translate SRPs, and because we saw acute demethylation on mRNAs after stress that coincides with SRP mRNAs having less m6A tags than other mRNAs. We predicted that it's activation signal would shed light on the upstream pathways that sense stress and mediate acute responses to stress, including FTO activation. As with most signaling pathways, we turned our attention to protein post translational modifications and we measured the changes in acute post-translational modifications on extranuclear FTO, using mass spectrometry. We detected a phosphorylation in FTO on threonine-6 (T6) within 20 minutes of UV stress (Fig. 5-1), suggesting that an upstream kinase is phosphorylating FTO in response to stress. To test whether T6 phosphorylation results in FTO activation, we mutated this residue to phosphorylation mimetic and to non-phosphorylating mimetics but changing it to conservative mutations that mimic phosphorylated and non-phosphorylated threonine. Alanine is similar to non-phosphorylated threonine, and when we mutated threonine-6 to alanine-6, FTO demethylation activity decreased mimicking the non-phosphorylated threonine suggesting that non-phosphorylated T6 FTO at baseline has decreased activity. We then mutated T6 to phospho-threonine mimetics, aspartic acid (D) and glutamic acid (E), which are conservative in size and charge to phosphor-threonine and this increased FTO activity independent of stress (Fig. 5-2, Fig. 5-3) confirming that phosphorylation of FTO at T6 post stress is an important activation

signal. Moreover, we generated an antibody specific to phospho-T6 on FTO which showed a significant increase in FTO T6 phosphorylation within 20 minutes of UV further confirming that acute phosphorylation of FTO at that site (Fig. 5-4) using an independent technique. We predicted that, given the location of FTO and its association with microtubule-proteins and networks, a microtubule-associated kinase, such as the MARK family may be responsible for the acute T6 phosphorylation in stress [202]. Due to recent discoveries implicating MARK4 in various diseases that have also been linked to FTO [47, 49, 203-206], we predicted that MARK4 and FTO could be linked in similar pathways. To test this, we first incubated purified FTO protein with MARK4 and measured FTO activity. MARK4 resulted in significant increase in FTO activity which was inhibited with the selective kinase inhibitor OTSSP167, previously shown to inhibit MARK4 (Fig. 5-5) [207], and mass spectrometry further confirmed FTO phosphorylation at T6 mediated by MARK4 in the in-vitro kinase assay (Fig. 5-6). This confirms that MARK4 phosphorylates FTO at T6 which increases its demethylation activity. To see if MARk4 plays a role in SRP translation in cells, we treated cells with OTSSP167 in the presence of UV stress which resulted in complete inhibition of acute p53 translation in stress (Fig. 5-7, Fig. 5-8), and selective knockdown of MARK4 using siRNA resulted in the same inhibition in translation for both p53 and ATF4, which are previously described SRPs (Fig. 5-7, Fig. 5-9, Fig. 5-10). Moreover, knocking down MARK4 with siRNA resulted in decrease in FTO phosphorylation at T6 as detected by the pT6-FTO specific antibody (Fig. 5-11) in cells confirming that MARK4 mediates FTO phosphorylation at T6 in cells. Lastly, loss of both FTO and MARK4 prevented the increase in the OPP stress translation foci that increase acutely after UV further confirming the role of MARK4-FTO axis in functional translational units along the microtubule networks (Fig. 5-12) that were previously described in Chapter 4. All together, these

data suggest that the acute phosphorylation of FTO at T6 by MARK4 kinase increases its demethylation activity and this is required for the SRP translation activation after stress. The fact that a microtubule-associated kinase phosphorylates FTO and appears to play an important role in activating SRP translation post stress further strengthens the role of microtubules in the selective SRP translation.

5.2.2. Microtubule-associated ribosomal units act as translation centres for SRP mRNAs acutely after stress

The second important question that emerged from Chapter 4 deals with the possibility of microtubule-associated ribosomes with distinct function from the well characterized ER and cytosolic ribosomes. Actively translating ribosomes are known to be mainly free floating in cytosol or embedded in ER sheets, with recent reports of ribosomal sub-pools localizing to mitochondrial membranes [78], however our data so far predict that there may be a different pool of active ribosomes, along microtubules, that serves a unique role in stress. While our understanding of ribosomal heterogeneity is improving [1, 5, 10, 12, 16, 17, 35] and few reports have suggested binding of ribosomes directly to microtubules, there has been no evidence to date of specialized active ribosomes on microtubules [79, 81, 128, 208].

Having actively translating ribosomes along the microtubules would serve two functions at least for SRP translation, one being providing offering a secluded site for translation that could easily bypass the global suppression during stress, and secondly is offering a highway for exporting newly made SRPs through the cell in a timely fashion. To test this we first did immunofluorescence (IF) co-staining of microtubules, OPP, FTO, and ribosomal protein S6 to look for associations between microtubules and the SRP translation system elements. IF staining

reveals significant overlap along the translation foci suggesting the presence of microtubule-associated ribosomes (Fig. 5-13). Moreover, PLA staining between S6 ribosomal protein and gamma tubulin, and OPP translation stain reveals near perfect overlap in signal along the translation foci in UV suggesting that microtubule-associated ribosomes are present at the site of the stress translation foci (Fig. 5-14). While these imaging studies show close association between ribosomes and SRP translation along microtubules, functional analysis were required to prove that actively translating ribosomes exist along the microtubules. To address this, we then utilized and adapted an established protocol [209] to fractionate cells and isolate ribosomes from cytosolic (Cyto), ER, and cytoskeletal (CS) fractions (Fig. 5-15). Markers for cytosol (MEK1), ER (Grp78), Cytoskeletal (Actin), and nuclear fractions (SP1, Lamin A/C, Nup98, Fibrillarin, Emerin) reveal a distinct separation in the compartments using the fractionation protocol (Fig. 4-8, Fig. 4-9). Unlike all other fractions, the CS fraction appears to be rich in RLP26 ribosomal protein and Grp78 confirming that it is a unique fraction from the Cytosolic, ER and nuclear fractions. RNA gel analysis reveals significant presence of processed ribosomal RNA in isolated ribosomes from the Cytosol, ER, and CS fractions and an expected unprocessed rRNA in the nuclear fraction confirming the purity of the cellular fractionation, with clear ribosomal RNA detection in all three extra-nuclear fractions (cytosol, ER, and CS) (Fig. 5-16), all together suggesting the presence of a ribosomal pool in the CS fraction. Since total ribosomal isolation detects all ribosomes present, active or otherwise, we utilized ribosomal profiling using HPLC [210] to quantify the actively translating ribosomes in different conditions from the three cellular fractions by measuring the polysomal peak distribution; the actively translating ribosomes (Fig. 5-17, Fig. 5-15). Ribosomal profiling using HPLC reveals active translation in both Cytosol, ER, and CS fractions which decreases in the cytosolic fraction, remains relatively unchanged in the

ER fraction, and increases significantly in the CS fraction 20 minutes after UV. This suggests an increase in active translation minutes after stress in the CS fraction mainly while the cytosolic ribosomal fraction is inhibited and ER ribosomal fraction remains unchanged (Fig. 5-17). This differential response to stress in terms of ribosomal activity provides a great example of the utility of having a distinct ribosomal pool in a cellular fraction such as the microtubules. P-eIF2a levels, (a translation initiation protein that decreases translation when phosphorylated after stress [9, 19, 37, 178]), were highest in the cytosolic ribosomal fraction, and lowest in the CS ribosomal fraction post UV corresponding to the HPLC active translation quantification (Fig. 5-18), suggesting that the translation initiation elements are regulated different in the ribosomal pools post stress, with the CS fraction have less levels of peIF2a after stress. Moreover, previous studies have shown a unique role for RLP26 in the acute and selective translation of p53 20 min post UV [70], and an analysis of relative RLP26 levels normalized to S6 core ribosomal protein shows a significant enrichment in the CS fraction compared to the cytosolic and ER ribosomal fractions (Fig. 5-18), that correlated with an increase in p53 mRNA levels in the CS fraction only after UV (Fig. 5-19) suggesting that p53 is translated acutely in the CS ribosomal fraction.

Moreover, m6A levels show acute demethylation in the CS ribosomal fraction while they remain relatively unchanged in the Cytosolic and ER ribosomal fractions within 20 minutes of UV stress suggesting that dynamic m6A changes, predicted to be related to SRP translation, occur in the CS ribosomal fraction (Fig. 5-20). All together, these experiments confirm that a distinct ribosomal pool in the CS fraction is regulated differently from other ribosomal fractions acutely after stress.

In order to see which ribosomal pools the SRPs detected in proteomics studies (Chapter 3) come from, we did ribosomal-sequencing where only the mRNA fragments protected by

bound ribosomes in each fraction were sequenced [211]. Interestingly, cytosolic ribosomes showed the greatest number of differentially decreased genes after 20 minutes UV while the ER ribosomal pool showed little change, the CS ribosomal pool had the largest differential increase in number of transcripts bound to ribosomes (Fig. 5-21) confirming the increased translation on the CS ribosomal pool detected in the polysome profiling experiment (Fig. 5-17). When we analyzed the pathways of the proteins that are either differentially upregulated in each ribosomal pool, or were specific to each ribosomal pool (CS enriched, or Cytosol and ER enriched), the CS enriched genes matched closely the pathways detected in the AHA labelling mass spectrometry experiment suggesting that the newly translated SRPs within 20 minutes of UV came from the CS ribosomal pool (Fig. 5-22, Fig. 5-23). All together, these data suggest an active role for m6A-tagged SRP selective translation in the CS fraction mediated by previously unrecognized unique ribosomal fraction along the gamma tubulin branching networks. Lastly, due to the limitation in resolutions of immunofluorescence staining which is currently is around 180-200nm, or 30nm in the case of PLA staining, we next utilized transmission electron microscopy (TEM), we were able to observe dense ribosome-sized particles, on microtubule branching points further confirming the findings (Fig. 5-24).

Overall, our data suggest that acutely after stress, MARK4 activates the demethylation of SRP mRNAs at the CS ribosomes via cytosolic FTO.

5.3. Figures.

Figure 5:

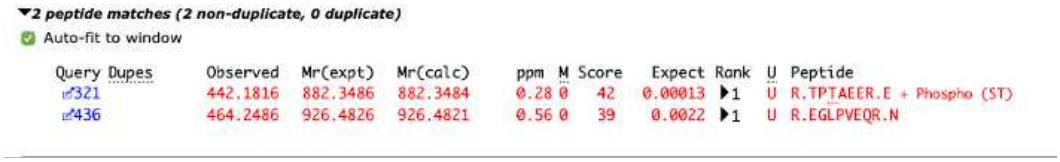

▼2 peptide matches (2 non-duplicate, 0 duplicate)

Auto-fit to window

Query	Dupes	Observed	Mr(expt)	Mr(calc)	ppm	M	Score	Expect	Rank	U	Peptide
321		442.1816	882.3486	882.3484	0.28	0	42	0.00013	1	U	R.TPTAEER.E + Phospho (ST)
436		464.2486	926.4826	926.4821	0.56	0	39	0.0022	1	U	R.EGLPVEQR.N

Fig. 5-1. Mass spectrometric data of post translational modifications detected in immunoprecipitated endogenous FTO in UV treated cells, showing a significant presence of T6 phosphorylation.

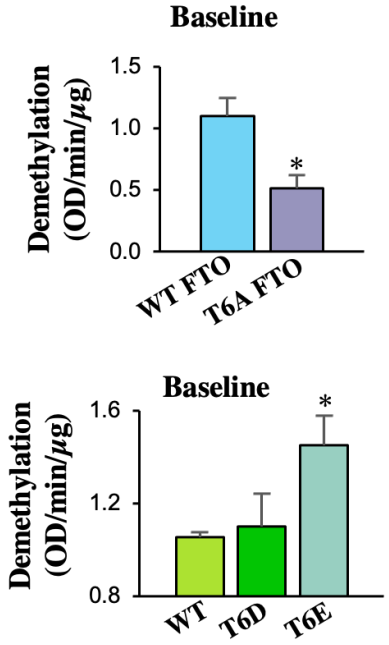

Fig. 5-2. Mean data of FTO activity measured using an m6A demethylase antibody-based assay of immunoprecipitated wildtype, T6A, T6D, or T6E FTO showing decreased FTO demethylase activity when T6 is mutated to Alanine, a non-phosphorylated threonine mimetic, and increased FTO demethylase activity when T6 is mutated to aspartic, or glutamic acid, a phosphorylated-threonine mimetic. n=3, *p<0.05 compared to wildtype (WT) FTO.

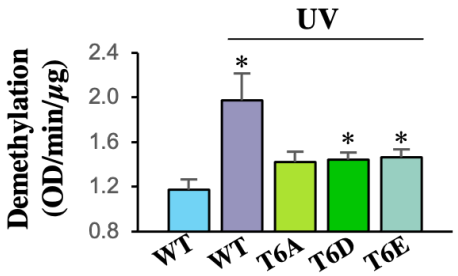

Fig. 5-3. Mean data of FTO activity measured using an m6A demethylase antibody-based assay of immunoprecipitated wildtype or T6A, T6D or T6E FTO in UV treated cells showing increased FTO activity in WT FTO after UV treatment, but not in T6 mutated-FTO. n=3, *p<0.05 compared to wildtype (WT) FTO.

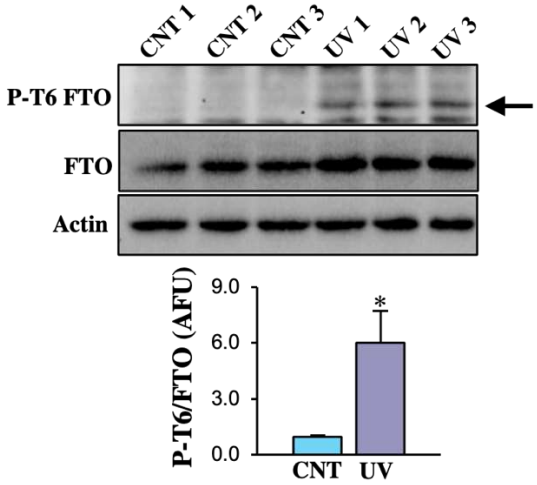

Fig. 5-4. Immunoblots showing increased FTO-T6 phosphorylation after 20 min of UV treatment using a phospho-T6 specific antibody in 3 different experiments. Actin is used as a loading control. Mean data are shown in chart below. n=3, *p<0.05 compared to control (CNT).

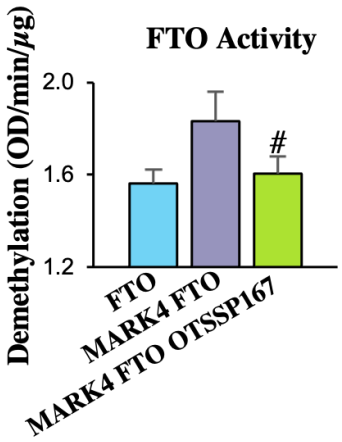

Fig. 5-5. Mean data of FTO activity measured using an m6A demethylase antibody-based assay of immunoprecipitated FTO incubated with recombinant MARK4 protein, alone or with OTSSSP167 kinase inhibitor. n=3, *p<0.05 compared to FTO alone, #p<0.05 compared to MARK4 FTO.

Mass Spectrometry verification (pT6)

Accession	Description	Score	Coverage	# Proteins	# Unique Peptides	# Peptides	# PSMs	# AAs	MW [kDa]	calc. pI				
Q9C0B1	**FTO**	**11.60**	**1.39**	**1**	**1**	**1**	**140**	**505**	**58.2**	**5.22**				
	A3	Sequence	# PSMs	# Proteins	# Protein Groups	Protein Group Accessions	Modifications	ΔCn	XCorr	Probability	Charge	MH+ [Da]	ΔM [ppm]	RT [min]
	High	tPTAEER	140	1	1	Q9C0B1	T1(Phospho)	0.0000	1.26	0.00	2	883.35735	1.82	6.21

Fig. 5-6. Mass spectrometric data of post translational modifications detected in immunoprecipitated FTO incubated with MARK4 in-vitro in a kinase assay, showing a significant presence of T6 phosphorylation in FTO incubated with MARK4.

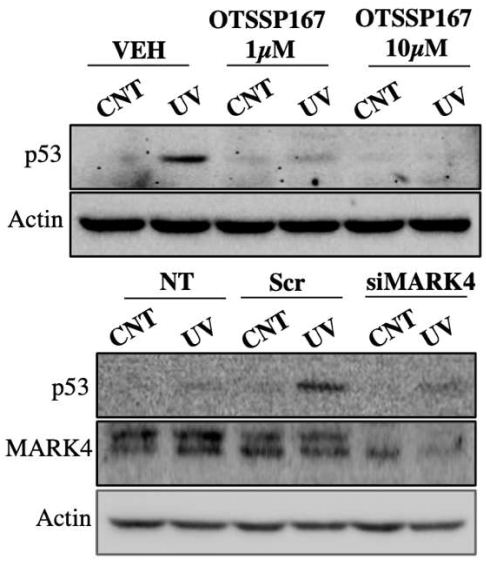

Fig. 5-7. P53 levels were measured after UV treatment in the presence and absence of OTSSP167 at 1μM or 10μM (upper blot), or siRNA for MARK4 (lower blot) using immunoblots. Actin is used as a loading control.

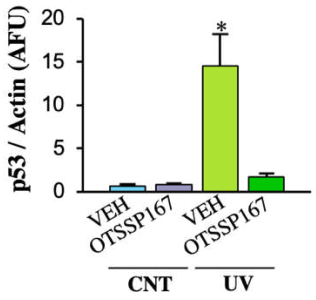

Fig. 5-8. Mean data of immunoblots measuring p53 in control and UV treated cells in the presence and absence of OTSS9167 showing increased p53 levels after UV which is prevented in the presence of OTSSP167. n=3, *p<0.05 compared to non-UV treated group. VEH = vehicle.

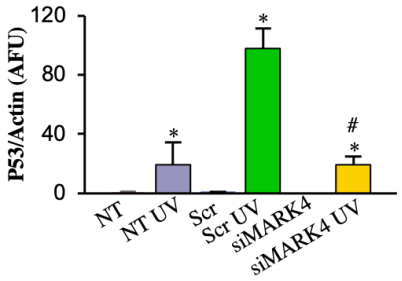

Fig. 5-9. Mean data of immunoblots measuring p53 in control and UV treated cells in the presence and absence of MARK4 siRNA showing increased p53 levels after UV which is prevented in the presence of MARK4 siRNA. n=3, *p<0.05 compared to non-UV treated group. NT= nontransfected. #p<0.05 compared to Scr UV group.

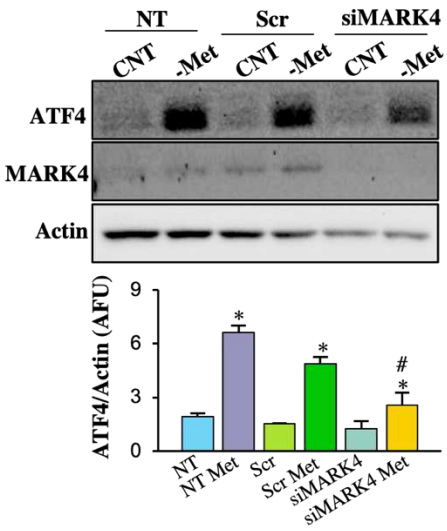

Fig. 5-10. ATF4 levels were measured after methionine deprivation in the presence and absence of siRNA for MARK4, using immunoblots. Actin was used as loading controls for immunoblots. n=3, *p<0.05 compared to non methionine deprived group. #p<0.05 compared to Scr Met (scrambled methionine deprived) group.

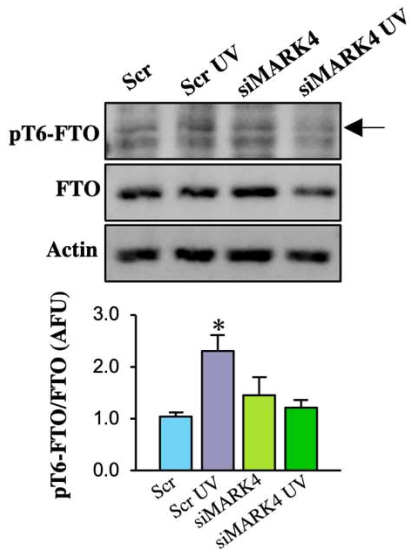

Fig. 5-11. FTO-T6 phosphorylation levels are measured in control and UV treated cells in the presence and absence of MARK4 using a phospho-T6 specific and immunoblots. Actin is used as a loading control. Mean data below show increased T6 phosphorylation with UV treatment which is prevented in the presence of MARK4 siRNA. n=3, *p<0.05 compared to Scr group.

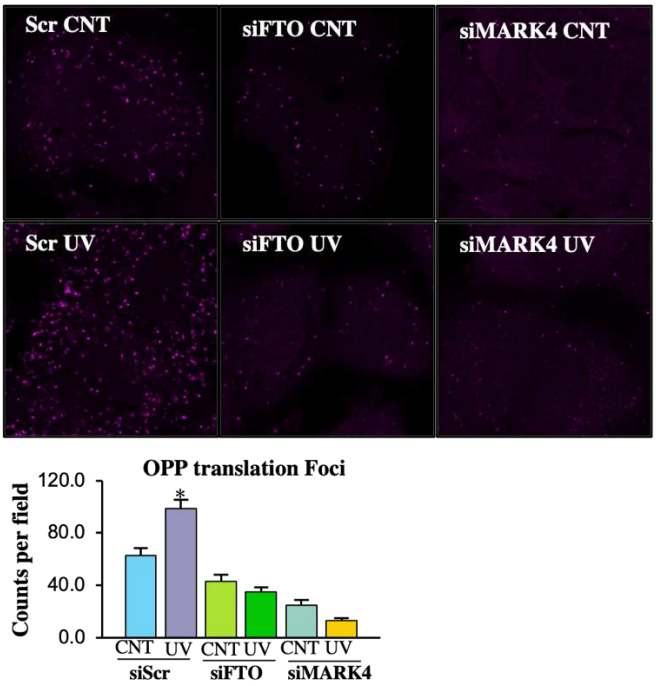

Fig. 5-12. Immunofluorescence staining of translation measured using OPP dye (in purple) in control and UV treated cells in the presence and absence of FTO and MARK4 siRNAs. Mean data below show a significant increase in translation foci after 20 min of UV stress in scrambled siRNA only, but not in the presence of FTO or MARK4 siRNA. n=3, *p<0.05 compared to control (CNT).

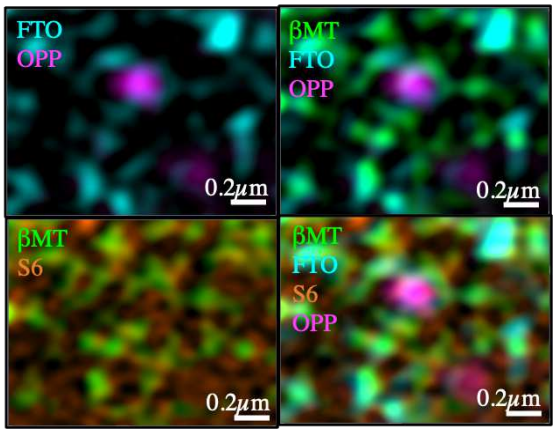

Fig. 5-13. Immunofluorescence staining showing OPP (purple), beta microtubules (green), FTO (blue) and S6 (orange) showing colocalization between all four components.

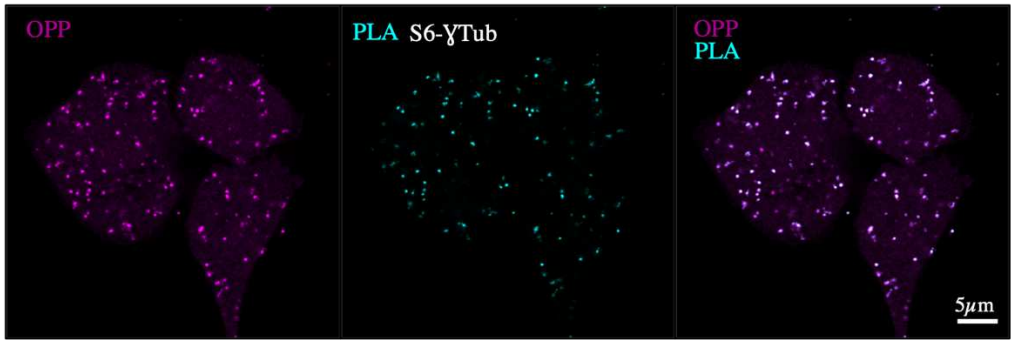

Fig. 5-14. Immunofluorescence staining of OPP (in purple) and PLA between S6 and gamma tubulin (in teal) in control and UV treated cells showing colocalization in the PLA signal and the dense translation foci.

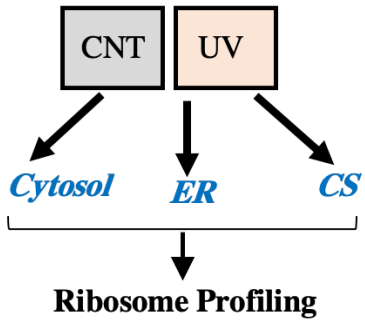

Fig. 5-15. Experimental design of ribosomal profiling experiment. Cells are either treated with UV or left untreated as a control, they are then fractionated to isolate 3 compartments, cytosol, ER, and CS, and ribosomal profiling is then done on each fractionated sample.

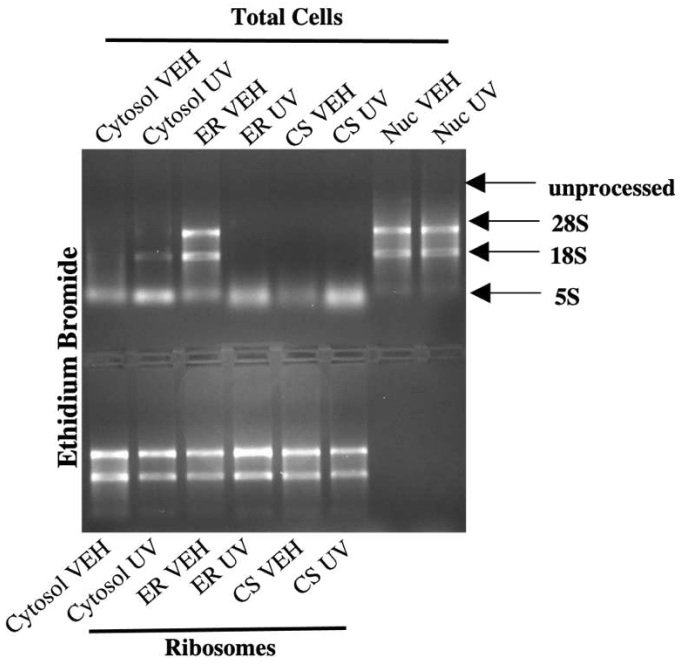

Fig. 5-16. RNA gel of total RNA isolated from total ribosomal isolation experiment from the input samples of each fraction and the ribosomes isolated in each fraction in control and UV treated cells. Samples are visualized using ethidium bromide staining. Arrows on side indicated the different ribosomal RNAs including the unprocessed ribosomal RNAs seen in nuclear fraction only.

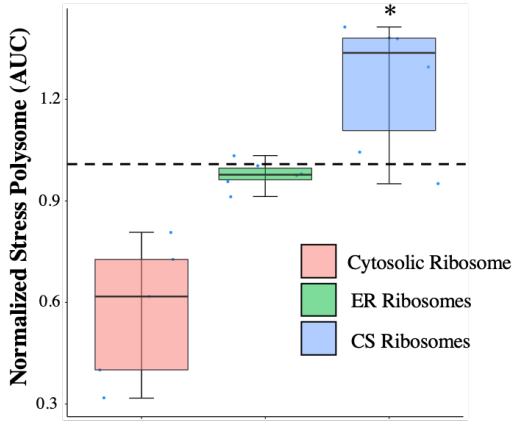

Fig. 5-17. Active translation of Cytosolic, ER, and CS ribosomal pools in UV treated cells, normalized to control measured as ratio of the areas under the curve of the polysomal curves using HPLC Ribo-SEC combined with cellular fractionation. n=5, *p<0.05 compared to Cytosol and ER Ribosomes.

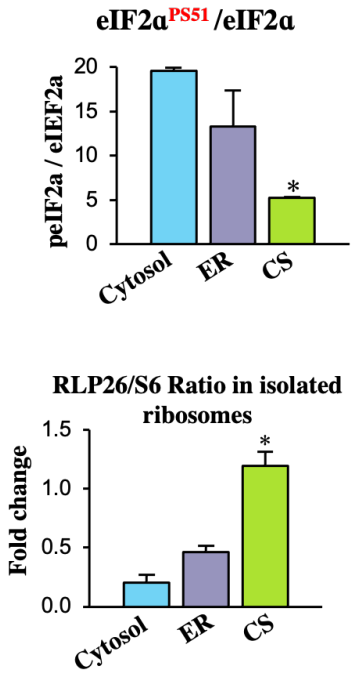

Fig. 5-18. Mean data of pS51-eIF2a levels normalized to total eIF2a, and RLP26 normalized to S6 ribosomal protein, measured in Cytosol, ER, or CS total ribosomal fraction in UV treated cells using immunoblots. Data show significantly lower pS51-eIF2a levels in the CS ribosomal pool compared to either Cytosol, or ER ribosomal pools, and significantly higher RLP26 enrichment in the CS ribosomal fraction compared to ER or cytosolic pools. n=3, *p<0.05 compared to cytosol and ER ribosomal fractions.

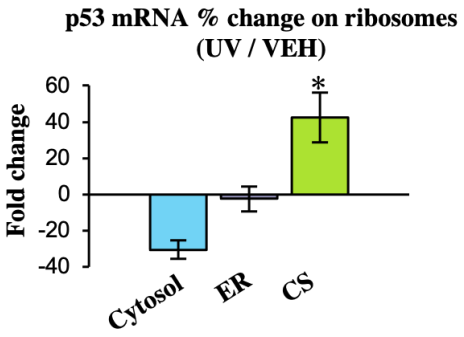

Fig. 5-19. P53 mRNA levels measured as fold change in UV treated cells compared to control cells in Cytosol, ER, or CS isolated ribosomes using qRT-PCR. 18S is used as a loading control. n=3, *p<0.05 compared to cytosol and ER groups.

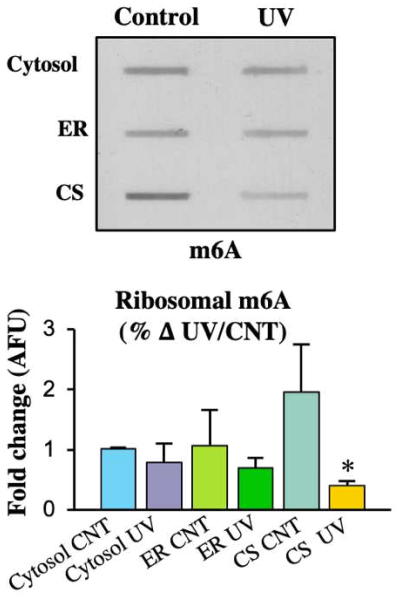

Fig. 5-20. RNA dot blot of isolated cytosol, ER, or CS ribosomal pools in control and UV treated cells. Mean data on side show change in m6A levels after UV treatment in each of the ribosomal fraction showing a decrease in m6A levels only in the CS fraction after 20 min of UV. n=3, *p<0.05 compared to control (CNT).

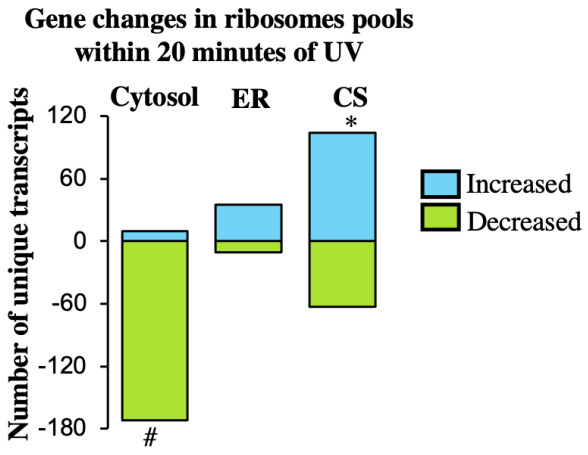

Fig. 5-21. Ribosome sequencing of ribosomal protected mRNA fragments in Cytosol, ER, and CS ribosomal pools, measured by differential sequencing analysis between UV and control within each ribosomal pool, showing that the largest number of increased translation occurs in the CS ribosomal pool, and the largest number of decreased translation in the Cytosolic ribosomal fraction after UV. n=3, *p<0.05 compared to cytosol and ER Increased groups. #p<0.05 compared to ER and CS Decreased groups.

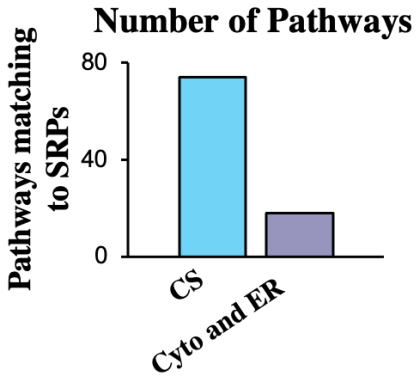

Fig. 5-22. Number of pathways of the significantly increased genes in the CS and Cyto-ER ribosomal pools compared to the pathways increased in the L-AHA mass

spectrometry quantification of the newly translated proteins, showing a significantly higher number (first chart), and percentage (second chart) of pathways detected in L-AHA experiment matching to the hits that are significantly increased in the CS ribosomal pool, but not in the Cytosol and ER ribosomal pools.

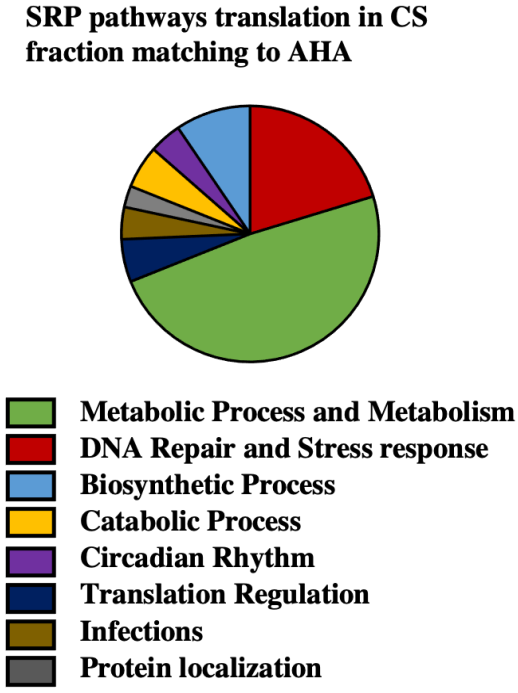

Fig. 5-23. Pie chart of the significant pathways of mRNA fragments sequenced in CS ribosomal fraction matching to significant pathways of the SRPs detected in AHA labelled experiment.

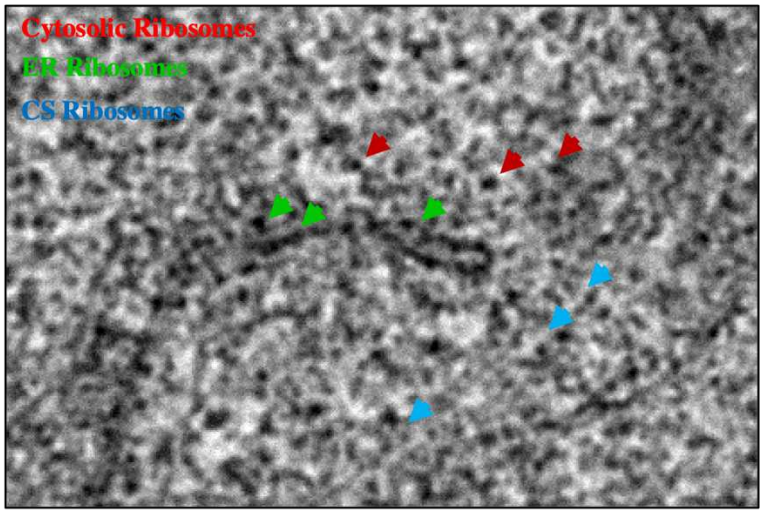

Fig. 5-24. Transmission electron microscopy (TEM) imaging of UV treated cells showing ribosomes in the cytosol (red arrow), ER sheets (green arrow), and along microtubule (blue arrow).

Chapter 6

PKR inhibits m6A-tagged SRP mRNAs at baseline

6.1. Introduction and Summary:

With the discovery of the activation (MARK4) signal upstream of FTO, via T6 phosphorylation, and the characterization of a distinct pool of ribosomes at microtubular branching points, a clearer image emerges of the details of the SRP translation system that provides a way to detect SRP mRNAs (with the bimodal m6A peaks in Chapter 3), and a way to selectively translate these mRNAs (on CS ribosomes). However the mechanism of going from inhibited translation at baseline to active translation after stress remained elusive. A few important questions remained unanswered, firstly, how does the bimodal m6A peak suppress translation of SRP mRNAs at baseline, and secondly, how does FTO demethylation remove this inhibitory signal to allow for the selective translation to occur. To address this important link, we focused on FTO again as it is the central node of regulation in this pathway. We looked at binding partners of FTO using mass spectrometry with a focus on proteins involved in the regulation of the translation machinery, and particularly in translation initiation, where the majority of translation regulation occurs. To our surprise, we found that PKR, and eIF2a kinase discussed in Chapter 1, was predicted to bind FTO, and this binding was further confirmed with subsequent experiments. PKR is known to bind viral double stranded RNAs, and it was intriguing that it may be a regulator of m6A-tagged mRNAs. We then show that PKR is potently activated by m6A-tagged mRNAs, a result that provides important links for SRP translation regulation. We also show that both PKR and FTO show a bimodal-binding distribution along the 3'UTRs of SRP mRNAs, a distribution that is very similar to m6A tags along these mRNAs. Moreover, we see that PKR shows colocalization with the stress translation foci, and the active form of PKR decreases binding with both gamma tubulin and the SRP translation foci in stress, coinciding with decreased peIF2a along these translation spots in stress. All together, these data

paint a clearer picture for the mechanism of SRP translation in stress. These suggest that PKR binds the bimodal m6A peaks along SRP mRNAs which results in phosphorylation of nearby peIF2a at S51 inhibiting their translation at baseline. Upon stress, MARK4 phosphorylates FTO at T6 which results in demethylation of one of the m6A peaks, a finding that is confirmed with PCR-based detection of m6A peaks along both p53 and SRSF7 mRNAs, which removes the PKR-mediated block on translation.

6.2. Results.

6.2.1. FTO removes inhibitory m6A translation brakes bound by the eIF2a kinase PKR

FTO phosphorylation by MARK4 and its subsequent activation appears to be required for p53 and SRSF7 translation, further linking microtubules in SRP translation during stress. However it remains unclear as to how the acute cytoskeletal-associated m6A demethylation mediates the selective translation of SRPs. Since demethylation involves removing a methyl tag, it suggests that m6A double peak methylation of the SRP mRNAs may serve as an inhibitor for translation, perhaps at baseline, and this translation brake would be removed by FTO via demethylation resulting in subsequent selective activation of translation. To test this, we looked for binding partners of FTO using co-immunoprecipitation and mass spectrometry that are involved directly in translation regulation, since FTO appears to be the central link in this pathway. Interestingly, we saw binding with eIF2a kinase PKR (Fig. 6-1), which was further confirmed with bidirectional co-immunoprecipitation and immunoblots suggesting a direct link to translation regulation (Fig. 6-2 , Fig. 6-3, Fig. 6-4). PKR is an eIF2a kinase that has been shown to be a stress sensor and mediator by inhibiting translation via phosphorylation of eIF2a activated by viral dsRNA, and some endogenous RNAs [212-214]. To assess the nature of the FTO-PKR interaction on SRP translation, we first inhibited PKR activity using C16 (or PKRi)

small molecule kinase inhibitor [215] which resulted in significant increase in SRP levels (p53, ATF4, and SRSF7) at baseline and after stress (Fig. 6-5, Fig. 6-6) suggesting that PKR may play a selective inhibitory role on SRP translation in cells. This finding means that active PKR at baseline, prior to stress, serves to suppress SRP translation, as it's inhibition results in active SRP translation at baseline, in the absence of stress. It also suggests that PKR serves as a translation brake for SRP mRNAs because its inhibition results in active translation both at baseline and after stress. This was further confirmed with selective knockdown of PKR with siRNA which also showed a significant increase in p53 levels measured at baseline and after stress (Fig. 6-7). All together, these data suggest a potential suppressive role for PKR in m6A-tagged SRP translation. Since PKR is an RNA-binding kinase which regulates translation (predominantly inhibiting translation) by phosphorylating eIF2a, we predicted that bimodal m6A-tagged SRP mRNAs may play a similar role to viral RNAs by binding to PKR, activating its kinase activity, and inhibiting their translation at baseline as a result. To test this, we first incubated purified PKR with either purified RNA or purified m6A-tagged RNA from the same cells and measured PKR activity in vitro using a kinase activity detection assay and by detecting autophosphorylation of PKR using immunoblots (Fig. 6-8). M6A-tagged mRNAs showed a significant and potent dose-dependent activation of PKR and its auto-phosphorylation which was not present in non-methylated RNAs isolated from the same cells (Fig. 6-8). These data suggest that cellular m6A-tagged SRP mRNAs may function as viral RNAs at baseline by recruiting PKR and selectively inhibiting their translation when not needed. This also suggests that the acute demethylation of SRP mRNAs by FTO may remove the PKR-mediated translation block allowing for translation to proceed. To test this, we measured the effect of FTO or MARK4, inhibition using siRNA, on PKR activity by detecting phosphorylated PKR. We see that while

PKR phosphorylation and its activity decrease acutely with stress, suggesting a decrease in its activity, knockdown of FTO or MARK4 result in an increase in PKR phosphorylation both at baseline and after stress suggesting that PKR activity inhibition after stress is likely mediated by FTO and MARK4 via m6A demethylation (Fig. 6-9). PLA immunofluorescence staining between pPKR, or active PKR, and gamma-tubulin shows a significant overlap at baseline which was significantly decreased within 20 minutes of UV, further confirming that activated PKR plays an inhibitory role on the stress translation-micro domains along the microtubule networks, and confirming the removal of this binding after stress (Fig. 6-10). Further assessment of P-eIF2a levels using immunofluorescence along the translation foci along the microtubule networks, which are the predicted sites of SRP translation, reveals a significant decrease in PeIF2a levels along the translation foci on the microtubule networks which is associated with an increase on other translation sites (Fig. 6-11). All together, these data confirm an important inhibitory role of PKR on the microtubule-linked selective translation of SRPs, which is removed acutely by FTO-mediated demethylation after stress, and highlight a novel role for PKR as a gatekeeper of SRP translation at baseline.

6.2.2. FTO and PKR show overlapping binding on methylation sites on SRP mRNAs

We previously detected a unique bimodal m6A peak pattern on acutely translated SRPs in stress which we predicted would be mediating their selective translation. However data so far suggest that the bimodal m6A peaks on SRP mRNAs may actually serve as an inhibitor of translation at baseline by activated PKR which subsequently phosphorylates eIF2a. To test this theory, we utilized PAR-CLIP sequencing [216], a protein-immunoprecipitation based experiment to sequence bound RNA fragments, to detect FTO and PKR binding sites on mRNAs

which we later factored using protein levels in stress measured using SILAC to elucidate the binding trends on translated SRP mRNAs (Fig. 6-12). This experiment would answer the question of where along the mRNAs do FTO and PKR bind, and whether SRP mRNAs show a unique binding pattern to FTO or PKR. An analysis of FTO binding sites along mRNA which were grouped based on protein levels post stress reveals a bimodal distribution along the increased protein groups, compared to maintained and decreased groups similar to the unique m6A pattern detected with meRIP (Fig. 6-13). Further analysis of PKR binding sites along cellular mRNAs using PAR-CLIP also reveals a similar bimodal peak distribution on SRP mRNAs (Fig. 6-13) with a significant overlap with FTO binding sites (Fig. 6-14). All together, these peak data reveal a significant and unique signature of SRP mRNAs marked by bimodal binding sites of FTO and PKR along m6A peaks in the 3'UTR. This finding confirms that PKR and FTO have a unique binding pattern to SRP mRNAs and the bimodal peak distribution parallels the m6A signature that marks SRP mRNAs, further linking m6A tagging to FTO-PKR regulation of SRP translation. Using a PCR-based quantitative assessment of methylation peaks along the p53 and SRSF7 3'UTRs corresponding to the predicted regions where FTO and PKR may bind, we see an FTO-dependent demethylation of the second peak within 20 minutes of UV in the extra-nuclear pool of mRNA suggesting an acute cytosolic role for FTO as an activation signal for selective translation of SRPs (Fig. 6-15). This further confirms the selective demethylation of SRP mRNAs along the second m6A peak, and further links the demethylation to acute translation of p53 and SRSF7. All together, these data suggest that PKR binds to predefined bimodal methylation peaks along the SRP mRNAs which are demethylated by FTO upon stress-induced MARK4 activation of FTO. This allows for translation to proceed thus explaining the mechanism for the selective translation of m6A-tagged SRPs along the MT

tubules via the cytoskeletal ribosomal pool (Fig. 6-16). Lastly, to see whether the m6A-mediated system regulates survival after stress, we measured cell survival and apoptosis, inferred by caspase-3 cleavage 24 hours UV stress in the presence and absence the central SRP translation mediator, FTO. Knockdown of FTO resulted in a significant increase in cell death as measured by caspase-3 further confirm the importance of m6A-mediated selective SRP translation for cell survival after stress (Fig. 6-17).

6.3. Figures.

Figure 6:

Accession	Description	Contaminant	Coverage	# Peptides	# PSMs	# Unique Peptides	# Protein Groups	# AAs	MW [kDa]	calc. pI	Found in Sample	Modifications	Area: F5: Sample	emPAI	Score Sequest HT	# Peptides Sequest HT
P19525	Interferon-induced, double-stranded RNA-activated protein kinase OS=Homo sapiens GN=EIF2AK2 PE=1 SV=2	FALSE	8.17	4	4	4	1	551	62.1	8.4	High		4.57E+05	0.425	10.84	4

Fig. 6-1. Mass spectrometric data of proteins co-immunoprecipitated with FTO in control cells, showing binding with eIF2a kinase PKR.

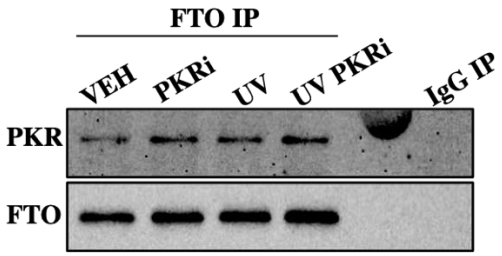

Fig. 6-2. FTO co-immunoprecipitation showing PKR binding in control and UV treated cells using immunoblots.

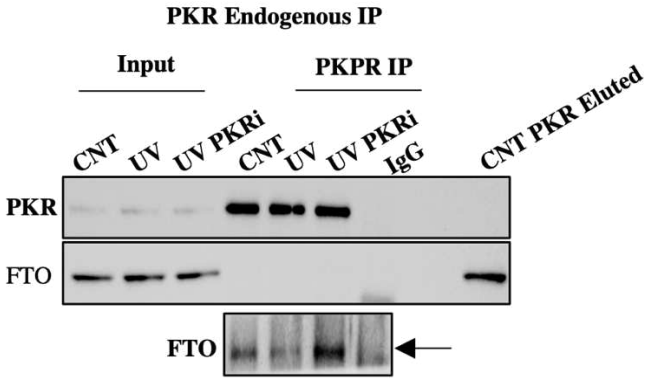

Fig. 6-3. PKR co-immunoprecipitation showing FTO binding in control and UV treated cells using immunoblots.

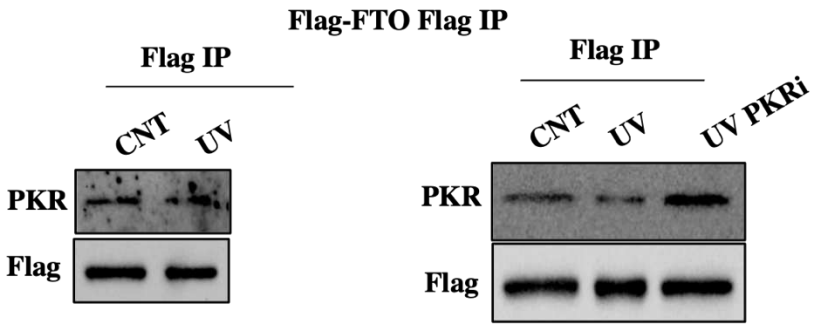

Fig. 6-4. Flag immunoprecipitation of Flag-tagged FTO confirming PKR binding in control and UV treated cells using immunoblots.

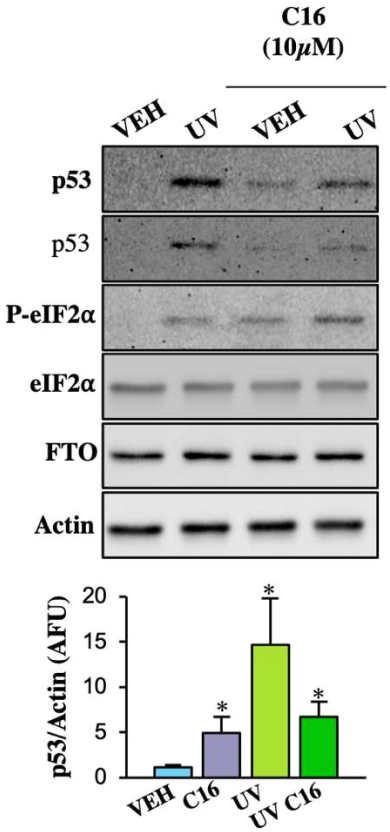

Fig. 6-5. Immunoblots of control and UV treated cells in presence and absence of C16, a PKR inhibitor, showing different protein cells. Actin is used as loading control. Mean

data below show increased p53 levels in UV as predicted with an increase in p53 levels in the presence of C16 both at baseline and UV. n=3, *p<0.05 compared to vehicle (VEH) group.

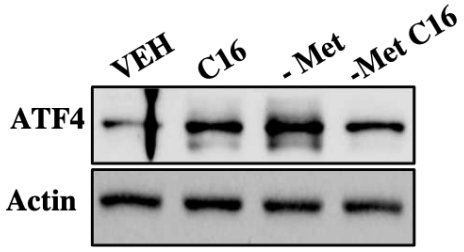

Fig. 6-6. ATF4 levels were measured after methionine deprivation in the presence and absence of C16, using immunoblots. Actin was used as loading controls for immunoblots.

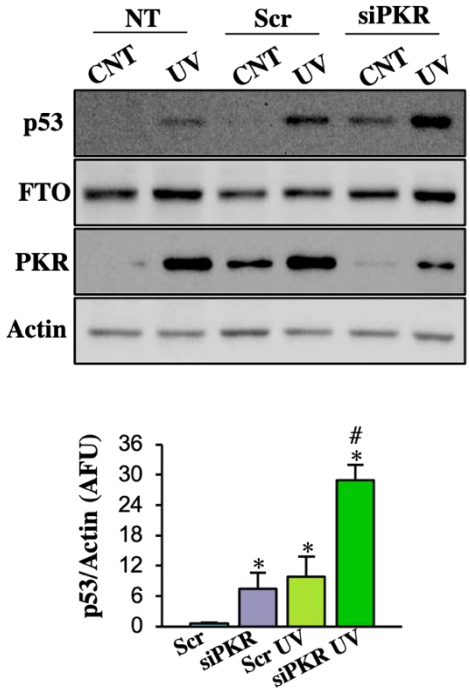

Fig. 6-7. P53 levels were measured after UV treatment in the presence and absence of siRNA for PKR, using immunoblots. Actin is used as loading control. Mean data below show that PKR siRNA increases p53 levels both at baseline and after UV treatment. n=3, *p<0.05 compared to Scr group. #p<0.05 compared to Scr UV.

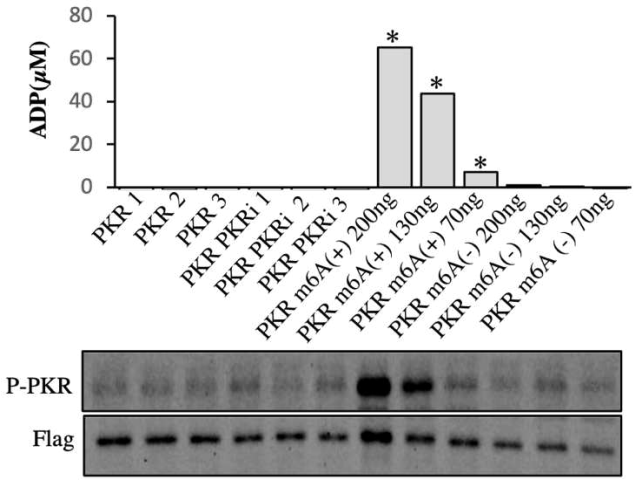

Fig. 6-8. Kinase assay measuring ADP levels detected from purified PKR kinase incubated with different amounts of either methylated or non-methylated RNA isolated from cells using m6A pull down assay showing a robust and dose-dependent activation of PKR kinase activity in the presence of m6A-tagged RNA. Immunoblots below show pPKR levels normalized to flag, from same samples in the kinase assay, confirming the m6A-mediated increased activity. n=3, *p<0.05 compared to PKR only, or PKR + non-methylated RNA groups.

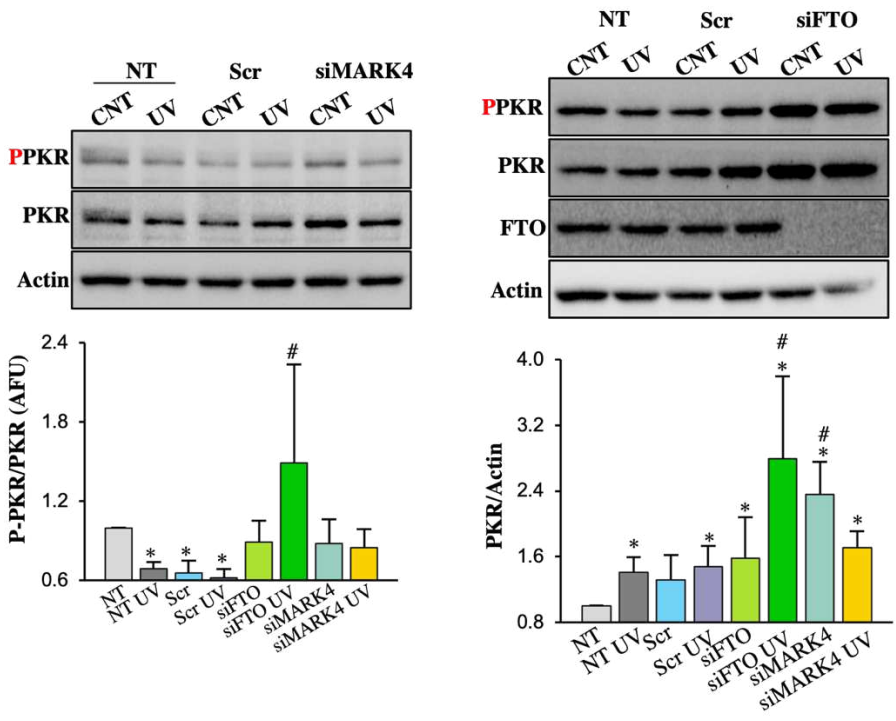

Fig. 6-9. pPKR levels were measured in control and UV treated cells in presence and absence of MARK4 (left blot) and FTO (right blot) siRNA using immunoblots. Actin is used as loading control. Mean data below show decreased pPKR levels after UV treatment which is lost in the presence of FTO or MARK4 siRNA, while total PKR levels increase with FTO and MARK4 siRNA. n=3-8, *p<0.05 compared to NT (non-transfected) group, #p<0.05 compared to Scr UV group.

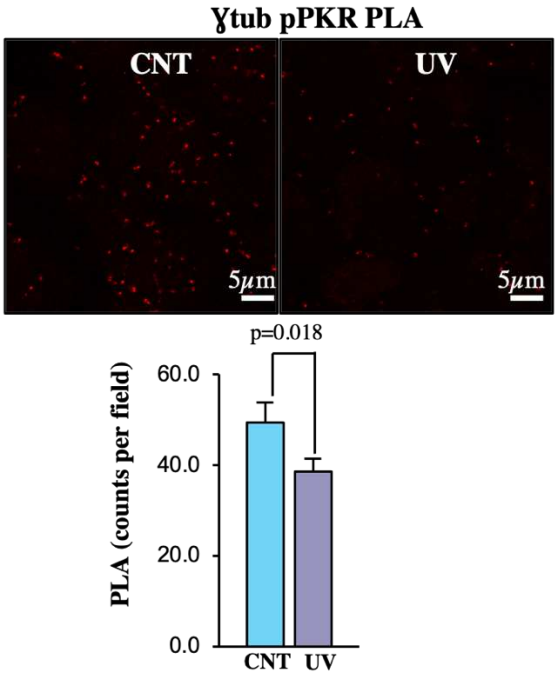

Fig. 6-10. Immunofluorescence staining of PLA between pPKR and gamma tubulin (in red) in control and UV treated cells with mean data on side showing a significant decrease in pPKR-colocalization with gamma tubulin after 20 min of UV treatment. n=3, p value is indicated.

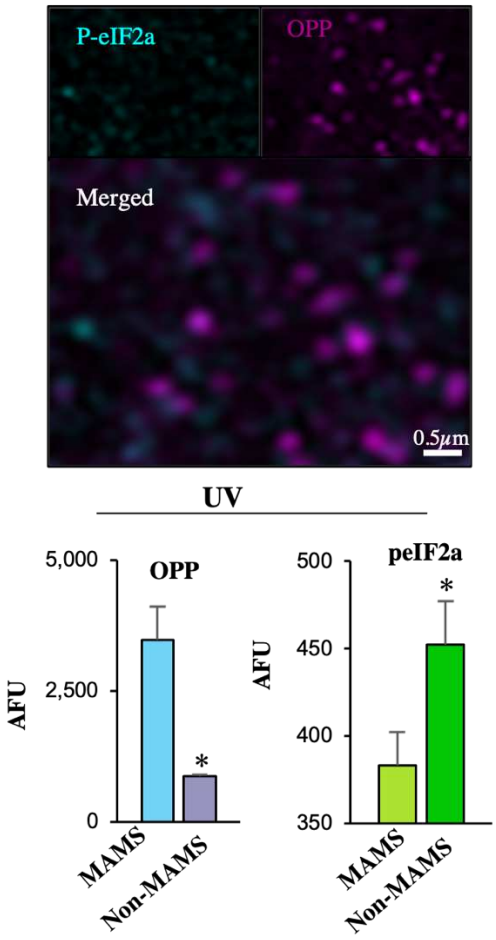

Fig. 6-11. Immunofluorescence staining of OPP (in purple) and pS51-eIF2a (in teal) in UV treated cells. Mean data on side show a significant dissociation in stress-induced OPP translation foci and pS51-eIF2a signal with a significant decrease in signal overlap after UV. n=3, *p<0.05 compared to control MAMS group.

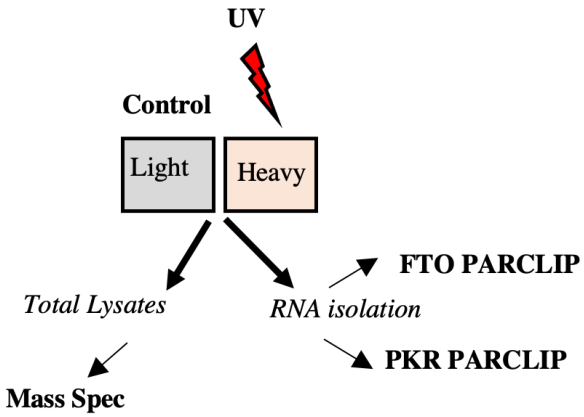

Fig. 6-12. Experimental design of FTO and PKR PAR-CLIP. RNA from control or UV treated cells was isolated from extra-nuclear fractions and FTO and PKR PAR-CLIP was performed as per methods section, and RNA is sequenced and analyzed.

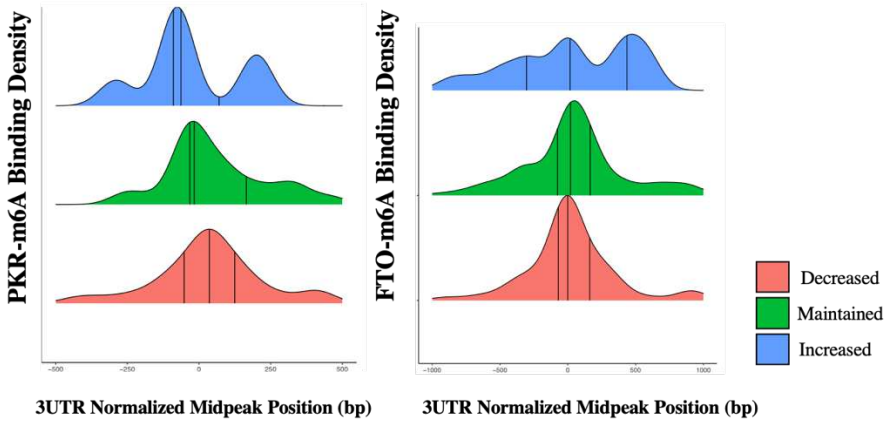

Fig. 6-13. Pooled PKR (top chart) and FTO (bottom chart)-bound mRNA peak locations from 3UTR of the increased, maintained, and decreased protein groups showing bimodal peak distribution downstream of the 3UTR of the increased protein groups in both PKR and FTO bound mRNA fragments.

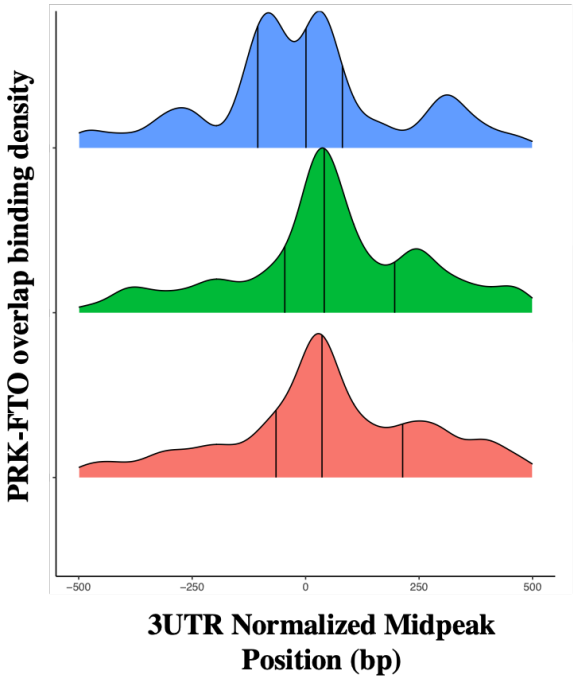

Fig. 6-14. Overlapping PKR-FTO bound mRNA peak locations from 3UTR of the increased, maintained, and decreased protein groups showing bimodal peak distribution downstream of the 3UTR of the increased protein groups in both PKR and FTO bound mRNA fragments.

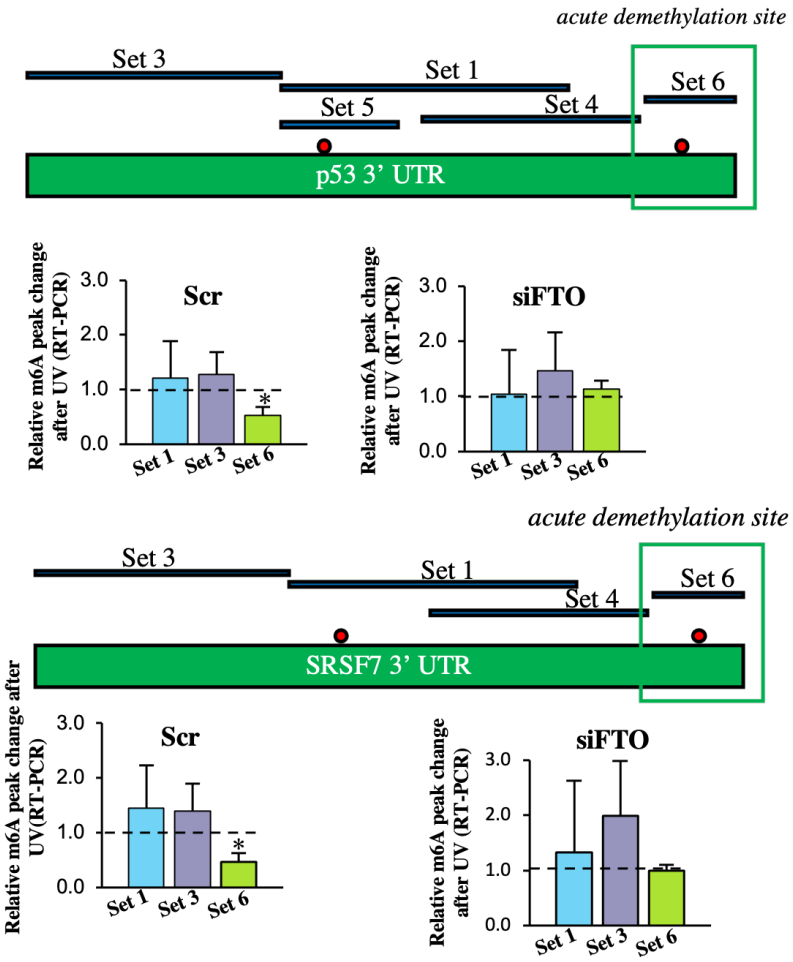

Fig. 6-15. Representation of the regions probed, and m6A peaks detected in p53 (left charts) and SRSF7 (right charts) 3'UTR using BST-MRT qRT enzyme assay for m6A detection. P53 and SRSF7 3'UTR region-specific methylation were measured in control and UV treated cells in the presence and absence of FTO siRNA. Mean data of methylated regions in charts below show demethylation in region set 6 of both p53 and SRSF mRNAs after UV, which is lost in the presence of FTO siRNA. Blue bars represent the areas spanned by the primer sets, red triangles indicated the location of the predicted

methylation site within a specific primer set region. Green box marks the region of demethylation that is observed after stress. n=4-5, *p<0.05 compared to Set 1 and 3.

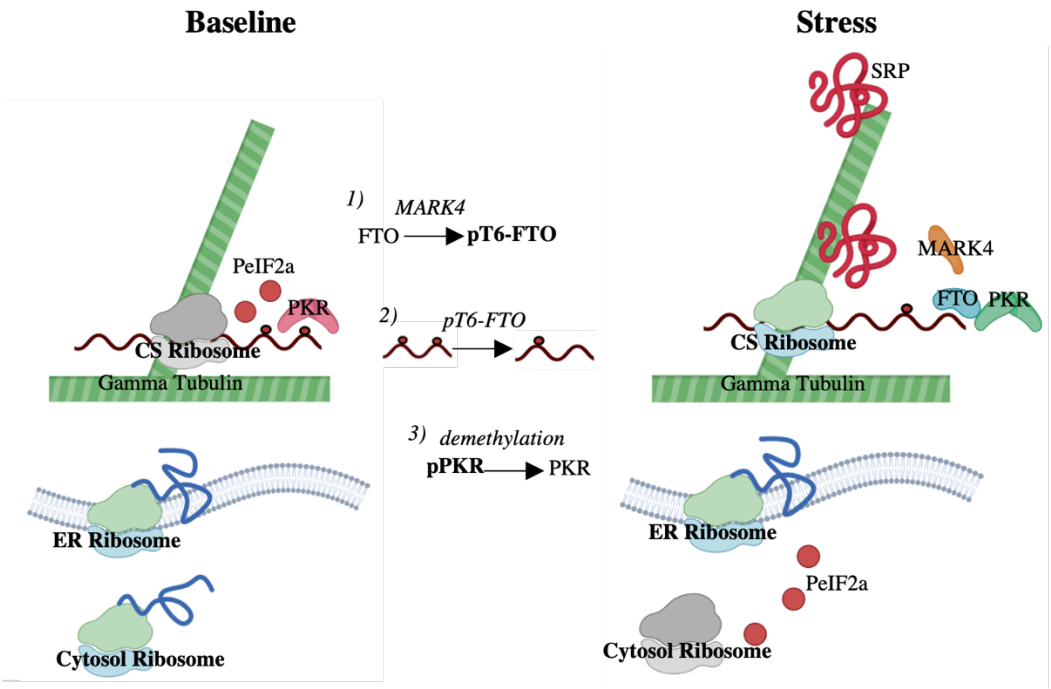

Fig. 6-16. Visual representation of CS-mediated SRP translation mechanism proposed. At baseline, cytosolic and ER ribosomes are actively translating transcripts while local PKR-mediated eIF2a phosphorylation along m6A peaks of SRPs maintains SRP translation suppressed in the CS ribosomal pool. After stress, eIF2a phosphorylation in the cytosolic ribosomal pool decreased translation in the cytosolic pool while MARK4-mediated phosphorylation of FTO on T6 activates the m6A peak demethylation along SRP mRNAs in the CS ribosomal pool, resulting in PKR inhibition and decreased eIF2a phosphorylation allowing for SRP translation to proceed on CS ribosomes. Gamma

tubulin provides the platform for the localized binding and translation along the CS-ribosomes.

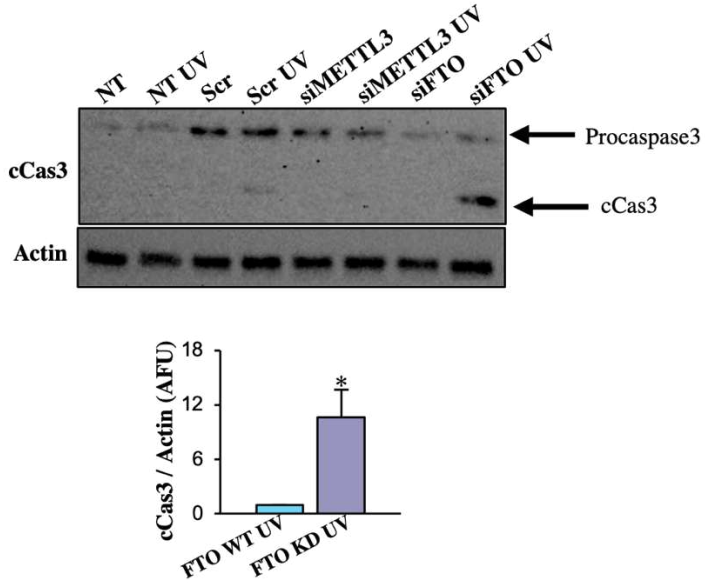

Fig. 6-17. Caspase 3 levels are measured in control and UV treated cells, 24 hours after treatment, in the presence and absence of METTL3 and FTO siRNA showing increased caspase cleavage in presence of FTO siRNA. Actin is used as a loading control. Mean data is shown on the right. n=3, *p<0.05 compared to FTO WT UV.

Chapter 7

General Discussion and Future Directions

7.1. Summary of Findings:

The complexities of the translation machinery seem to increase with every new discovery linking new systems, more heterogeneity in every component, and additional functions for most parts of the pathway. Nowhere is this more evident than during translation in stress where mRNA elements, ribosomal modifications, binding proteins, and other pathways have been shown to orchestrate two main events, one is shutting off global translation, and two, is simultaneously allow for selective translation. In this thesis, we propose and show evidence for a novel translation system for SRP mRNAs during stress since no comprehensive system that allows for translation of hundreds of proteins acutely after stress has been discovered to date. We start by outlining the challenges of the selective translation in stress and propose a logical approach to finding a proposed system to solve these challenges. We predicted that for translation machinery to be able to selectively translate SRP mRNAs, the mRNAs themselves would have to be marked by a signature which itself could serve the function of selective translation by binding to translation machinery-regulating proteins. Using this logic, we first show that firstly cells do in fact translate hundreds of proteins acutely (within 20 minutes) of UV and 2DG stress in an m6A-dependent manner. M6A is the most common modification on mRNAs and we predicted that it is likely used to mark SRPs, however, we predicted that SRP mRNAs would likely have a unique m6A signature that differentiates them so they can be preferentially translated during stress. Using meRIP-seq combined with SILAC, we identify a novel SRP mRNA signature consisting of a bimodal m6A peak along the 3'UTR, which was confirmed to be present on p53 and SRSF7 mRNAs using a PCR-based technique to quantify m6A peaks.

We then show that acute m6A demethylation occurs after stress mainly in cytoskeletal fraction, and using various experiments we show that FTO translocates outside the nucleus and associates with microtubule-associated proteins after stress resulting in demethylation of select mRNAs. We observe translation foci emerge acutely after stress on microtubule-branching points, marked by gamma-tubulin, which we predict are the active and selective SRP translation site. We then show that FTO is activated by phosphorylation on a hypermobile arm, via MARK4, a microtubule associated kinase, allowing for translation to proceed. Using various experiments and techniques we show that SRP translation occurs at microtubule-associated ribosomes which appear to be regulated differently from ER and cytosolic ribosomes after stress, and using Ribo-seq, we show that SRP mRNAs are preferentially translated on microtubule-associated ribosomes. Lastly, we show that PKR, an eIF2a kinase, binds to the bimodal m6A peaks on SRP mRNAs and inhibits their translation at baseline, and upon the removal of the second m6A peak by FTO (downstream of MARK4 activation), active PKR dissociates from the translation foci allowing for translation to proceed. Overall we present a novel model for selectively translating SRP mRNAs in this thesis. We propose that SRP mRNAs are tagged with bimodal m6A peaks which act as binding sites for PKR inhibiting their translation at baseline. Upon stress, MARK4 kinase activates an extranuclear FTO which demethylates the downstream (second) m6A peak removing the PKR block and allowing translation to proceed on microtubule-associated ribosomes.

7.2. new signature for SRPs:

Some of the important findings of this work are novel characteristics of SRPs. Stress response proteins are defined in this thesis as proteins that are recruited in stress by acute

translation, likely for repair and adaptation pathways. While many of those proteins may be present at baseline prior to stress, they are all increase significantly very early on in stress. Prior to this work, there has not been a characterization system to identify and group these proteins without extensive proteomics work. In this thesis we propose two novel ways of identifying and grouping SRPs. One is by the m6A bimodal signature in their 3'UTR, a finding that can be verified in any mRNA using a series of simple PCRs, and secondly is by association with novel microtubule-associated ribosomes. While the former finding provides an intriguing signature, and a novel way to group mRNAs, the latter finding would likely has major implications for SRP translation and other pathways and disease. We propose in this work the presence of functional and specialized microtubule-associated ribosomes which specialize in translating SRPs during stress. We predict that they mainly associate with gamma tubulin branching points of the microtubule as these sites are the most stable points of the microtubule system. This provides a sanctuary site for SRP translation during stress, but it also provides a quick and efficient way to transport required proteins anywhere in the cell within seconds using the microtubule system. We predict that the newly discovered microtubule-associated ribosomes likely play a very important role in cell adaptation and survival due to the unique characteristics mentioned above. While we provide no evidence for this in this work, we predict that CS ribosomes likely play very important roles in various human disease implicated in stress responses, which we will elaborate more on in section 7.4. Together, the bimodal m6A signature and the CS ribosomal association provide novel characterization system for mRNAs and SRPs that could prove useful in pathway analysis of diseases and cellular processes.

7.3 Novel assessment tools to assess stress and stress responses

This work also provides novel ways to assess stress and universal stress responses in cells and tissues. Firstly, we show that within minutes after stress, we see an increase in stress translation foci detected with a simple staining dye that labels newly made proteins (OPP). By quantifying the translation foci, we can detect stress-exposed cells, and stress-responsive cells. While this needs further validation, it is possible that this technique could be useful in further studies to quantify stress responses and stress-exposed cells and tissues.

Secondly, we show that CS ribosomes translation increases after stress using HPLC ribosome profiling. While this technique is very laboursome, making it difficult as a screening tool for stress responses in cells, the presence of CS ribosomes, which can be detected with simple immunofluorescence staining, could provide an indication for which cells and tissues are more stress-responsive. We predict that the presence of CS ribosomes in cells and tissues could make them better able to respond to stress, and it is very possible that the presence of CS ribosomes is highly variable among cells and tissues. While this needs further validation, just like the above suggestion, we predict that it is possible to use CS ribosome detection and quantification as a way to assess stress responsiveness and adaptation of a cell. We propose further experiments to characterize CS ribosomes in various tissues both in health and disease to allow for a better understanding of the role of CS ribosomes, and develop their usage as stress-detection methods.

Lastly, we show in this work that FTO, a central link in the SRP translation system proposed, leaves the nucleus and gets phosphorylated at threonine-6 to get activated and demethylase SRP mRNAs. We show that phospho-T6 FTO increases significantly after UV, and we predict that this modification could be a marker of stress responses as well. While further validation is required, a cytosolic pT6 FTO signal could be a marker of stress and stress responses, using a simple stain of cells and tissues.

7.4. Implications for human disease:

With the discovery of novel pathways come the excitement of possible new links to human disease. Stress and stress responses are well established links to a long list of human diseases. At the forefront of this list is ageing, cancer, and ischemic injuries, among others. As we age, our stress responses decrease, damage accumulates, and cells undergo senescence and eventual apoptosis. Similar processes occur that lead to cancer with the accumulation of DNA damage and mutations. Moreover, acute responses to ischemic injuries can determine life or death of an individual, and myocardial infarctions and strokes remain as one of the leading causes of death. We predict that this newly discovered SRP translation pathway plays important roles in various disease processes mentioned above due to the sheer number of SRPs implicated by this system and its effect on SRP translation and apoptosis. We show that among p53 is a long list of novel proteins that are affected by this system, some with known functions, and others that have yet to be discovered. Future directions for this work include looking at links between this novel SRP translation and ageing, cancer, and ischemic injuries to start. We predict that this system decreases with ageing, resulting in accumulation of damage leading to cancer, and other ageing-related diseases. While further research is required to confirm this link, the possible implications for major human diseases and possible novel drug targets, which will be discussed in more detail in section 7.5, make it one of the major future directions for this work. FTO and mRNA methylation have already been linked to various diseases such as cancer, neurodegenerative diseases, immune system function, and many others. The findings in the thesis would expand the possible links between m6A and FTO and human diseases, particularly stress-related diseases, providing new avenues for drug targets.

7.5. novel drug targets.

An important implication of this work and a promising future direction is the potential therapeutic targeting of the novel translation pathway discussed in this thesis. While hypothetical, we predict that this translation system and pathway could likely be implicated in ageing related diseases, which are particularly linked to accumulating cellular stress-related damage. Potential drugs that can increase or decrease the activity of this pathway could possibly alter the course of such diseases. For example we predict that the activity of the SRP translation system discussed here could decrease with age which would result in accumulating damage and senesce. If this turns out to be valid, drugs that can increase the activity of this system could theoretically delay stress-related damage and ageing. However more studies into how this system changes in response to stress and ageing are needed to develop selective drug targets. Therefore the most immediate future directions for this work is to understand how stress itself, and by extension ageing, affects this system so we can better understand how to prevent the predicted downregulation of this SRP translation system with ageing.

7.6. New understanding of Microtubule Targeting Agents (MTAs).

One of the most surprising findings in this work is the link between microtubules and translation where we see that microtubules, particularly gamma tubulin branching points, provide a site for selective translation on CS ribosomes. While this finding should be replicated and tested in other tissues to understand its true prevalence, it has immediate implications on our understanding of a large class of clinically used drugs that target the microtubule networks, collectively known as microtubule-targeting agents (or MTAs). These include microtubule stabilizers and destabilizers that are commonly used for conditions such as gout and other

autoimmune diseases, and in cancer therapeutics. It is thought that the mechanism of action of lots of drugs is destabilizing, or stabilizing the microtubules preventing normal cell functioning, such as proliferation and trafficking, and causing apoptosis. While this is certainly true, the new evidence we see in this work suggests that these drugs could also work in part by decreasing the cell's ability to respond to stress by destabilizing the CS ribosomes and the selective SRP translation, as we saw with colchicine and nocodazole in this work. A better understanding of the mechanism of action of such an important and large class of drugs could perhaps lead to improved generations of drugs where toxicity is decreased and desired effects are increased.

7.7. Remaining questions and recommended future directions

As with all discoveries in science, we end up with more unanswered questions than what we start with at the beginning, and below I outline some of the most pressing questions that emerge from this work which I believe warrant future funding and investigation.

7.7.1. How prevalent is this translation system, particularly in healthy damage-prone tissues with low regenerative potential such as the heart and brain? Tissues that have limited regeneration potential would rely more heavily on repair mechanism and pathways, such as the system described in this thesis, while other tissues that can regenerate easily would simply invest the energy in making new cells, which are periodically replaced. Therefore I would predict that this system could play important roles in heart and brain function, especially in ischemic injuries where stress is severe and time is tissue. If this system is present in heart and brain tissues and is functioning to preserve their integrity and improve repair after severe stress, it could provide an important novel target in preventing ischemic tissue injuries in MIs and strokes, by upregulating this system or increasing its activity. Therefore a future project could involve studying the CS

ribosomes, along with the m6A-mediated SRP translation pathway (MARK4-FTO-PKR) in heart and brain tissue, and monitoring its change after stress and with ageing. Studying the regulation of this system could perhaps enable us to increase its activity providing better protection for vital tissues.

7.7.2. Most of the studies done here are in cancer cells, particularly A549 cells confirming that this translation system is active in cancer, at least in A549 cells, providing significant protection against stresses, such as nutrient limitation and damaging agents, such as chemotherapeutics and radiation. This important finding suggests that if we are able to suppress this system, by either developing specific FTO inhibitors, or more general m6A demethylase inhibitors, or even by using biologics targeting FTO such as siRNA, we can potentially break down an important shield that cancer might be using to provide resistance against both immune system insults and chemotherapies and radiation. This suggests that lower doses of chemotherapies and radiation could be used to produce a more potent effect against cancer than currently used doses reducing therapy-associated toxicities.

7.7.3. As mentioned previously, defenses to stress decrease with ageing which leads to accumulation in damage. While this may appear to be a chicken an egg problem, where accumulating damage may decrease the defenses against stress, it very well likely acts in a positive feedback cycle. We see evidence for this in the rate of ageing in all species, we do not age at a steady rate starting from birth, instead we age in an exponential pattern with the rate of deterioration increasing further and further with time. This is an indication of a positive feedback loop suggesting that with time both the defenses against stress decrease and damage accumulates with decreased defenses, with each factor feeding into the other. Regardless of the positive feedback loop, bolstering the defenses, even early on in life, can potentially break the feedback

cycle, or simply slow down the inevitable progression. This is why one of the subsequent future directions for this work should be to investigate the function of the acute SRP translation system with ageing. I would predict a robust and exponential decrease with time coinciding with accumulating cellular damage. This important finding could elucidate the complex ageing process further and potential open up novel pathways for drug targets to decrease ageing related diseases. If this predicted decrease is true, the immediate question after that is what is causing the decrease in cell's ability to acutely translate SRPs. This would require extensive investigations into other cellular systems and into the mechanisms of regulation of all elements of the SRP translation system discussed in this work. However finding modulation targets with potential therapeutic benefits would require the detailed investigation of the mechanism of decrease of SRP translation system.

Final statement:

While the subsequent work is basic in nature, it lays the foundation for a myriad of studies with important therapeutic implications ranging from cancer treatments and ageing modulation to potentially protecting against more serious ischemic injuries in vital tissues such as the heart and the brain. I hope that subsequent studies continue the groundwork laid out in this thesis so we that the potential of this work can be fully realized.

References

1. Sauert, M., H. Temmel, and I. Moll, *Heterogeneity of the translational machinery: Variations on a common theme.* Biochimie, 2015. **114**: p. 39-47.
2. Walsh, M.J., J.E. Dodd, and G.M. Hautbergue, *Ribosome-inactivating proteins: potent poisons and molecular tools.* Virulence, 2013. **4**(8): p. 774-84.
3. Ricard-Blum, S., *The collagen family.* Cold Spring Harb Perspect Biol, 2011. **3**(1): p. a004978.
4. Liu, Y., A. Beyer, and R. Aebersold, *On the Dependency of Cellular Protein Levels on mRNA Abundance.* Cell, 2016. **165**(3): p. 535-50.
5. Mauro, V.P., S.A. Chappell, and J. Dresios, *Analysis of ribosomal shunting during translation initiation in eukaryotic mRNAs.* Methods Enzymol, 2007. **429**: p. 323-54.
6. Steward, O. and E.M. Schuman, *Compartmentalized synthesis and degradation of proteins in neurons.* Neuron, 2003. **40**(2): p. 347-59.
7. Reid, D.W. and C.V. Nicchitta, *Diversity and selectivity in mRNA translation on the endoplasmic reticulum.* Nat Rev Mol Cell Biol, 2015. **16**(4): p. 221-31.
8. Anders, M., et al., *Dynamic m(6)A methylation facilitates mRNA triaging to stress granules.* Life Sci Alliance, 2018. **1**(4): p. e201800113.
9. Boye, E. and B. Grallert, *eIF2alpha phosphorylation and the regulation of translation.* Curr Genet, 2020. **66**(2): p. 293-297.
10. Shi, Z., et al., *Heterogeneous Ribosomes Preferentially Translate Distinct Subpools of mRNAs Genome-wide.* Mol Cell, 2017. **67**(1): p. 71-83 e7.
11. Zhou, J., et al., *N(6)-Methyladenosine Guides mRNA Alternative Translation during Integrated Stress Response.* Mol Cell, 2018. **69**(4): p. 636-647 e7.
12. Dinman, J.D., *Pathways to Specialized Ribosomes: The Brussels Lecture.* J Mol Biol, 2016. **428**(10 Pt B): p. 2186-94.
13. Proud, C.G., *Signalling to translation: how signal transduction pathways control the protein synthetic machinery.* Biochem J, 2007. **403**(2): p. 217-34.
14. Reid, D.W. and C.V. Nicchitta, *Primary role for endoplasmic reticulum-bound ribosomes in cellular translation identified by ribosome profiling.* J Biol Chem, 2012. **287**(8): p. 5518-27.
15. Shibata, Y., G.K. Voeltz, and T.A. Rapoport, *Rough sheets and smooth tubules.* Cell, 2006. **126**(3): p. 435-9.
16. Xue, S. and M. Barna, *Specialized ribosomes: a new frontier in gene regulation and organismal biology.* Nat Rev Mol Cell Biol, 2012. **13**(6): p. 355-69.
17. Simsek, D., et al., *The Mammalian Ribo-interactome Reveals Ribosome Functional Diversity and Heterogeneity.* Cell, 2017. **169**(6): p. 1051-1065 e18.
18. Yamasaki, S. and P. Anderson, *Reprogramming mRNA translation during stress.* Curr Opin Cell Biol, 2008. **20**(2): p. 222-6.
19. Galluzzi, L., T. Yamazaki, and G. Kroemer, *Linking cellular stress responses to systemic homeostasis.* Nat Rev Mol Cell Biol, 2018. **19**(11): p. 731-745.

20. Dunand-Sauthier, I., et al., *Stress-activated protein kinase pathway functions to support protein synthesis and translational adaptation in response to environmental stress in fission yeast.* Eukaryot Cell, 2005. **4**(11): p. 1785-93.
21. Milo, R., *What is the total number of protein molecules per cell volume? A call to rethink some published values.* Bioessays, 2013. **35**(12): p. 1050-5.
22. Fonseca, B.D., et al., *The ever-evolving role of mTOR in translation.* Semin Cell Dev Biol, 2014. **36**: p. 102-12.
23. Rolfe, D.F. and G.C. Brown, *Cellular energy utilization and molecular origin of standard metabolic rate in mammals.* Physiol Rev, 1997. **77**(3): p. 731-58.
24. Buttgereit, F. and M.D. Brand, *A hierarchy of ATP-consuming processes in mammalian cells.* Biochem J, 1995. **312 (Pt 1)**: p. 163-7.
25. Topisirovic, I. and N. Sonenberg, *mRNA translation and energy metabolism in cancer: the role of the MAPK and mTORC1 pathways.* Cold Spring Harb Symp Quant Biol, 2011. **76**: p. 355-67.
26. Darmanis, S., et al., *Simultaneous Multiplexed Measurement of RNA and Proteins in Single Cells.* Cell Rep, 2016. **14**(2): p. 380-9.
27. Gingold, H. and Y. Pilpel, *Determinants of translation efficiency and accuracy.* Mol Syst Biol, 2011. **7**: p. 481.
28. Tuller, T., et al., *Translation efficiency is determined by both codon bias and folding energy.* Proc Natl Acad Sci U S A, 2010. **107**(8): p. 3645-50.
29. Zhou, J., et al., *Dynamic m(6)A mRNA methylation directs translational control of heat shock response.* Nature, 2015. **526**(7574): p. 591-4.
30. Komar, A.A. and M. Hatzoglou, *Cellular IRES-mediated translation: the war of ITAFs in pathophysiological states.* Cell Cycle, 2011. **10**(2): p. 229-40.
31. Wethmar, K., *The regulatory potential of upstream open reading frames in eukaryotic gene expression.* Wiley Interdiscip Rev RNA, 2014. **5**(6): p. 765-78.
32. Keene, J.D., *RNA regulons: coordination of post-transcriptional events.* Nat Rev Genet, 2007. **8**(7): p. 533-43.
33. Quinn, J.J. and H.Y. Chang, *Unique features of long non-coding RNA biogenesis and function.* Nat Rev Genet, 2016. **17**(1): p. 47-62.
34. Thelen, M.P. and M.J. Kye, *The Role of RNA Binding Proteins for Local mRNA Translation: Implications in Neurological Disorders.* Front Mol Biosci, 2019. **6**: p. 161.
35. Guo, H., *Specialized ribosomes and the control of translation.* Biochem Soc Trans, 2018. **46**(4): p. 855-869.
36. Andreev, D.E., et al., *Translation of 5' leaders is pervasive in genes resistant to eIF2 repression.* Elife, 2015. **4**: p. e03971.
37. Liu, B. and S.B. Qian, *Translational reprogramming in cellular stress response.* Wiley Interdiscip Rev RNA, 2014. **5**(3): p. 301-15.
38. Ryoo, H.D. and D. Vasudevan, *Two distinct nodes of translational inhibition in the Integrated Stress Response.* BMB Rep, 2017. **50**(11): p. 539-545.
39. Edupuganti, R.R., et al., *N(6)-methyladenosine (m(6)A) recruits and repels proteins to regulate mRNA homeostasis.* Nat Struct Mol Biol, 2017. **24**(10): p. 870-878.
40. Wang, X., et al., *N6-methyladenosine-dependent regulation of messenger RNA stability.* Nature, 2014. **505**(7481): p. 117-20.

41. Griseri, P. and G. Pages, *Regulation of the mRNA half-life in breast cancer.* World J Clin Oncol, 2014. **5**(3): p. 323-34.
42. Ross, J., *mRNA stability in mammalian cells.* Microbiol Rev, 1995. **59**(3): p. 423-50.
43. Zheng, G., et al., *ALKBH5 is a mammalian RNA demethylase that impacts RNA metabolism and mouse fertility.* Mol Cell, 2013. **49**(1): p. 18-29.
44. Wei, J., et al., *Differential m(6)A, m(6)Am, and m(1)A Demethylation Mediated by FTO in the Cell Nucleus and Cytoplasm.* Mol Cell, 2018. **71**(6): p. 973-985 e5.
45. Liu, J., et al., *A METTL3-METTL14 complex mediates mammalian nuclear RNA N6-adenosine methylation.* Nat Chem Biol, 2014. **10**(2): p. 93-5.
46. Jia, G., et al., *N6-methyladenosine in nuclear RNA is a major substrate of the obesity-associated FTO.* Nat Chem Biol, 2011. **7**(12): p. 885-7.
47. Li, H., et al., *FTO is involved in Alzheimer's disease by targeting TSC1-mTOR-Tau signaling.* Biochem Biophys Res Commun, 2018. **498**(1): p. 234-239.
48. Wang, C.Y., et al., *FTO modulates circadian rhythms and inhibits the CLOCK-BMAL1-induced transcription.* Biochem Biophys Res Commun, 2015. **464**(3): p. 826-32.
49. Annapoorna, P.K., et al., *FTO: An Emerging Molecular Player in Neuropsychiatric Diseases.* Neuroscience, 2019. **418**: p. 15-24.
50. Wang, X., et al., *N(6)-methyladenosine Modulates Messenger RNA Translation Efficiency.* Cell, 2015. **161**(6): p. 1388-99.
51. Zou, S., et al., *N(6)-Methyladenosine: a conformational marker that regulates the substrate specificity of human demethylases FTO and ALKBH5.* Sci Rep, 2016. **6**: p. 25677.
52. Liu, N. and T. Pan, *N6-methyladenosine-encoded epitranscriptomics.* Nat Struct Mol Biol, 2016. **23**(2): p. 98-102.
53. Fu, Y., et al., *N6-methyldeoxyadenosine marks active transcription start sites in Chlamydomonas.* Cell, 2015. **161**(4): p. 879-892.
54. Xiang, Y., et al., *RNA m(6)A methylation regulates the ultraviolet-induced DNA damage response.* Nature, 2017. **543**(7646): p. 573-576.
55. Gulati, P., et al., *Fat mass and obesity-related (FTO) shuttles between the nucleus and cytoplasm.* Biosci Rep, 2014. **34**(5).
56. Patil, D.P., B.F. Pickering, and S.R. Jaffrey, *Reading m(6)A in the Transcriptome: m(6)A-Binding Proteins.* Trends Cell Biol, 2018. **28**(2): p. 113-127.
57. Genuth, N.R. and M. Barna, *Heterogeneity and specialized functions of translation machinery: from genes to organisms.* Nat Rev Genet, 2018. **19**(7): p. 431-452.
58. Lerner, R.S., et al., *Partitioning and translation of mRNAs encoding soluble proteins on membrane-bound ribosomes.* RNA, 2003. **9**(9): p. 1123-37.
59. Kaneko, M., et al., *ER Stress and Disease: Toward Prevention and Treatment.* Biol Pharm Bull, 2017. **40**(9): p. 1337-1343.
60. Strzyz, P., *Translation: RAPping with ribosomes.* Nat Rev Mol Cell Biol, 2017. **18**(7): p. 406.
61. Wilson, D.N. and K.H. Nierhaus, *Ribosomal proteins in the spotlight.* Crit Rev Biochem Mol Biol, 2005. **40**(5): p. 243-67.

62. Klein, D.J., P.B. Moore, and T.A. Steitz, *The roles of ribosomal proteins in the structure assembly, and evolution of the large ribosomal subunit.* J Mol Biol, 2004. **340**(1): p. 141-77.
63. Lecompte, O., et al., *Comparative analysis of ribosomal proteins in complete genomes: an example of reductive evolution at the domain scale.* Nucleic Acids Res, 2002. **30**(24): p. 5382-90.
64. *Tribute to Professor George E. Palade.* J Cell Mol Med, 2007. **11**(1): p. 2-3.
65. Ford, D., *Ribosomal heterogeneity - A new inroad for pharmacological innovation.* Biochem Pharmacol, 2020. **175**: p. 113874.
66. Williams, M.E. and I.M. Sussex, *Developmental regulation of ribosomal protein L16 genes in Arabidopsis thaliana.* Plant J, 1995. **8**(1): p. 65-76.
67. Pedder, C.M., D. Ford, and J.E. Hesketh, *Targeting of transcripts encoding membrane proteins in polarized epithelia: RNA-protein binding studies of the SGLT1 3'-UTR.* Biochem Soc Trans, 2008. **36**(Pt 3): p. 525-7.
68. Knight, Z.A., et al., *Molecular profiling of activated neurons by phosphorylated ribosome capture.* Cell, 2012. **151**(5): p. 1126-37.
69. Meyuhas, O., *Ribosomal Protein S6 Phosphorylation: Four Decades of Research.* Int Rev Cell Mol Biol, 2015. **320**: p. 41-73.
70. Takagi, M., et al., *Regulation of p53 translation and induction after DNA damage by ribosomal protein L26 and nucleolin.* Cell, 2005. **123**(1): p. 49-63.
71. Cai, Y., N. Singh, and H. Li, *Essential role of Ufm1 conjugation in the hematopoietic system.* Exp Hematol, 2016. **44**(6): p. 442-6.
72. Hamilton, E.M.C., et al., *UFM1 founder mutation in the Roma population causes recessive variant of H-ABC.* Neurology, 2017. **89**(17): p. 1821-1828.
73. Martin, I., et al., *Ribosomal protein s15 phosphorylation mediates LRRK2 neurodegeneration in Parkinson's disease.* Cell, 2014. **157**(2): p. 472-485.
74. Roundtree, I.A., et al., *Dynamic RNA Modifications in Gene Expression Regulation.* Cell, 2017. **169**(7): p. 1187-1200.
75. Simsek, D. and M. Barna, *An emerging role for the ribosome as a nexus for post-translational modifications.* Curr Opin Cell Biol, 2017. **45**: p. 92-101.
76. Sloan, K.E., et al., *Tuning the ribosome: The influence of rRNA modification on eukaryotic ribosome biogenesis and function.* RNA Biol, 2017. **14**(9): p. 1138-1152.
77. Moor, A.E., et al., *Global mRNA polarization regulates translation efficiency in the intestinal epithelium.* Science, 2017. **357**(6357): p. 1299-1303.
78. Gold, V.A., et al., *Visualization of cytosolic ribosomes on the surface of mitochondria by electron cryo-tomography.* EMBO Rep, 2017. **18**(10): p. 1786-1800.
79. Walker, P.R. and J.F. Whitfield, *Cytoplasmic microtubules are essential for the formation of membrane-bound polyribosomes.* J Biol Chem, 1985. **260**(2): p. 765-70.
80. Kim, S. and P.A. Coulombe, *Emerging role for the cytoskeleton as an organizer and regulator of translation.* Nat Rev Mol Cell Biol, 2010. **11**(1): p. 75-81.
81. Chudinova, E.M. and E.S. Nadezhdina, *Interactions between the Translation Machinery and Microtubules.* Biochemistry (Mosc), 2018. **83**(Suppl 1): p. S176-S189.
82. Kim, S., P. Wong, and P.A. Coulombe, *A keratin cytoskeletal protein regulates protein synthesis and epithelial cell growth.* Nature, 2006. **441**(7091): p. 362-5.

83. Ramaekers, F.C., et al., *Polyribosomes associated with microfilaments in cultured lens cells.* Biochim Biophys Acta, 1983. **740**(4): p. 441-8.
84. Traub, P., et al., *Colocalization of single ribosomes with intermediate filaments in puromycin-treated and serum-starved mouse embryo fibroblasts.* Biol Cell, 1998. **90**(4): p. 319-37.
85. Toh, B.H., et al., *Association of mitochondria with intermediate filaments and of polyribosomes with cytoplasmic actin.* Cell Tissue Res, 1980. **211**(1): p. 163-9.
86. Murti, K. and R. Goorha, *Synthesis of frog virus 3 proteins occurs on intermediate filament-bound polyribosomes.* Biol Cell, 1989. **65**(3): p. 205-14.
87. Horne, Z. and J. Hesketh, *Increased association of ribosomes with myofibrils during the skeletal-muscle hypertrophy induced either by the beta-adrenoceptor agonist clenbuterol or by tenotomy.* Biochem J, 1990. **272**(3): p. 831-3.
88. Medalia, O., et al., *Macromolecular architecture in eukaryotic cells visualized by cryoelectron tomography.* Science, 2002. **298**(5596): p. 1209-13.
89. Hesketh, J.E. and I.F. Pryme, *Evidence that insulin increases the proportion of polysomes that are bound to the cytoskeleton in 3T3 fibroblasts.* FEBS Lett, 1988. **231**(1): p. 62-6.
90. Moon, R.T., et al., *The cytoskeletal framework of sea urchin eggs and embryos: developmental changes in the association of messenger RNA.* Dev Biol, 1983. **95**(2): p. 447-58.
91. Fulton, A.B., K.M. Wan, and S. Penman, *The spatial distribution of polyribosomes in 3T3 cells and the associated assembly of proteins into the skeletal framework.* Cell, 1980. **20**(3): p. 849-57.
92. Lenk, R., et al., *A cytoskeletal structure with associated polyribosomes obtained from HeLa cells.* Cell, 1977. **10**(1): p. 67-78.
93. Howe, J.G. and J.W. Hershey, *Translational initiation factor and ribosome association with the cytoskeletal framework fraction from HeLa cells.* Cell, 1984. **37**(1): p. 85-93.
94. Liu, G., et al., *F-actin sequesters elongation factor 1alpha from interaction with aminoacyl-tRNA in a pH-dependent reaction.* J Cell Biol, 1996. **135**(4): p. 953-63.
95. Kandl, K.A., et al., *Identification of a role for actin in translational fidelity in yeast.* Mol Genet Genomics, 2002. **268**(1): p. 10-8.
96. Gross, S.R. and T.G. Kinzy, *Improper organization of the actin cytoskeleton affects protein synthesis at initiation.* Mol Cell Biol, 2007. **27**(5): p. 1974-89.
97. Morelli, J.K., et al., *Actin depolymerization affects stress-induced translational activity of potato tuber tissue.* Plant Physiol, 1998. **116**(4): p. 1227-37.
98. Stapulionis, R., S. Kolli, and M.P. Deutscher, *Efficient mammalian protein synthesis requires an intact F-actin system.* J Biol Chem, 1997. **272**(40): p. 24980-6.
99. Owen, C.H., D.J. DeRosier, and J. Condeelis, *Actin crosslinking protein EF-1a of Dictyostelium discoideum has a unique bonding rule that allows square-packed bundles.* J Struct Biol, 1992. **109**(3): p. 248-54.
100. Yang, F., et al., *Identification of an actin-binding protein from Dictyostelium as elongation factor 1a.* Nature, 1990. **347**(6292): p. 494-6.
101. Sotelo-Silveira, J., et al., *Myelinated axons contain beta-actin mRNA and ZBP-1 in periaxoplasmic ribosomal plaques and depend on cyclic AMP and F-actin integrity for in vitro translation.* J Neurochem, 2008. **104**(2): p. 545-57.

102. Ostroff, L.E., et al., *Polyribosomes redistribute from dendritic shafts into spines with enlarged synapses during LTP in developing rat hippocampal slices.* Neuron, 2002. **35**(3): p. 535-45.
103. Fukazawa, Y., et al., *Hippocampal LTP is accompanied by enhanced F-actin content within the dendritic spine that is essential for late LTP maintenance in vivo.* Neuron, 2003. **38**(3): p. 447-60.
104. Bramham, C.R., *Local protein synthesis, actin dynamics, and LTP consolidation.* Curr Opin Neurobiol, 2008. **18**(5): p. 524-31.
105. Rodriguez, A.J., et al., *Mechanisms and cellular roles of local protein synthesis in mammalian cells.* Curr Opin Cell Biol, 2008. **20**(2): p. 144-9.
106. Smart, F.M., G.M. Edelman, and P.W. Vanderklish, *BDNF induces translocation of initiation factor 4E to mRNA granules: evidence for a role of synaptic microfilaments and integrins.* Proc Natl Acad Sci U S A, 2003. **100**(24): p. 14403-8.
107. Tiedge, H. and J. Brosius, *Translational machinery in dendrites of hippocampal neurons in culture.* J Neurosci, 1996. **16**(22): p. 7171-81.
108. Deitch, J.S. and G.A. Banker, *An electron microscopic analysis of hippocampal neurons developing in culture: early stages in the emergence of polarity.* J Neurosci, 1993. **13**(10): p. 4301-15.
109. Steward, O. and W.B. Levy, *Preferential localization of polyribosomes under the base of dendritic spines in granule cells of the dentate gyrus.* J Neurosci, 1982. **2**(3): p. 284-91.
110. St Johnston, D., *Moving messages: the intracellular localization of mRNAs.* Nat Rev Mol Cell Biol, 2005. **6**(5): p. 363-75.
111. Shiina, N., et al., *Microtubule severing by elongation factor 1 alpha.* Science, 1994. **266**(5183): p. 282-5.
112. Hamill, D., et al., *Polyribosome targeting to microtubules: enrichment of specific mRNAs in a reconstituted microtubule preparation from sea urchin embryos.* J Cell Biol, 1994. **127**(4): p. 973-84.
113. Puhka, M., et al., *Endoplasmic reticulum remains continuous and undergoes sheet-to-tubule transformation during cell division in mammalian cells.* J Cell Biol, 2007. **179**(5): p. 895-909.
114. English, A.R. and G.K. Voeltz, *Endoplasmic reticulum structure and interconnections with other organelles.* Cold Spring Harb Perspect Biol, 2013. **5**(4): p. a013227.
115. Schwarz, D.S. and M.D. Blower, *The endoplasmic reticulum: structure, function and response to cellular signaling.* Cell Mol Life Sci, 2016. **73**(1): p. 79-94.
116. Jagannathan, S., et al., *Multifunctional roles for the protein translocation machinery in RNA anchoring to the endoplasmic reticulum.* J Biol Chem, 2014. **289**(37): p. 25907-24.
117. Shibata, Y., et al., *Mechanisms determining the morphology of the peripheral ER.* Cell, 2010. **143**(5): p. 774-88.
118. Hu, J., W.A. Prinz, and T.A. Rapoport, *Weaving the web of ER tubules.* Cell, 2011. **147**(6): p. 1226-31.
119. West, M., et al., *A 3D analysis of yeast ER structure reveals how ER domains are organized by membrane curvature.* J Cell Biol, 2011. **193**(2): p. 333-46.
120. Gurel, P.S., A.L. Hatch, and H.N. Higgs, *Connecting the cytoskeleton to the endoplasmic reticulum and Golgi.* Curr Biol, 2014. **24**(14): p. R660-R672.

121. Dehmelt, L. and S. Halpain, *The MAP2/Tau family of microtubule-associated proteins.* Genome Biol, 2005. **6**(1): p. 204.
122. Matsuno, A., et al., *Modulation of protein kinases and microtubule-associated proteins and changes in ultrastructure in female rat pituitary cells: effects of estrogen and bromocriptine.* J Histochem Cytochem, 1997. **45**(6): p. 805-13.
123. Schulman, H., *Phosphorylation of microtubule-associated proteins by a Ca2+/calmodulin-dependent protein kinase.* J Cell Biol, 1984. **99**(1 Pt 1): p. 11-9.
124. Huang, Y.A., et al., *Microtubule-associated type II protein kinase A is important for neurite elongation.* PLoS One, 2013. **8**(8): p. e73890.
125. Drewes, G., et al., *MARK, a novel family of protein kinases that phosphorylate microtubule-associated proteins and trigger microtubule disruption.* Cell, 1997. **89**(2): p. 297-308.
126. Seger, R., et al., *Microtubule-associated protein 2 kinases, ERK1 and ERK2, undergo autophosphorylation on both tyrosine and threonine residues: implications for their mechanism of activation.* Proc Natl Acad Sci U S A, 1991. **88**(14): p. 6142-6.
127. Drewes, G., et al., *Microtubule-associated protein/microtubule affinity-regulating kinase (p110mark). A novel protein kinase that regulates tau-microtubule interactions and dynamic instability by phosphorylation at the Alzheimer-specific site serine 262.* J Biol Chem, 1995. **270**(13): p. 7679-88.
128. Scarborough, E.A., et al., *Microtubules orchestrate local translation to enable cardiac growth.* Nat Commun, 2021. **12**(1): p. 1547.
129. Giannakakou, P., et al., *Enhanced microtubule-dependent trafficking and p53 nuclear accumulation by suppression of microtubule dynamics.* Proc Natl Acad Sci U S A, 2002. **99**(16): p. 10855-60.
130. Parker, A.L., M. Kavallaris, and J.A. McCarroll, *Microtubules and their role in cellular stress in cancer.* Front Oncol, 2014. **4**: p. 153.
131. Giannakakou, P., et al., *p53 is associated with cellular microtubules and is transported to the nucleus by dynein.* Nat Cell Biol, 2000. **2**(10): p. 709-17.
132. Allen, M.A., et al., *Global analysis of p53-regulated transcription identifies its direct targets and unexpected regulatory mechanisms.* Elife, 2014. **3**: p. e02200.
133. Beckerman, R. and C. Prives, *Transcriptional regulation by p53.* Cold Spring Harb Perspect Biol, 2010. **2**(8): p. a000935.
134. Sullivan, K.D., et al., *Mechanisms of transcriptional regulation by p53.* Cell Death Differ, 2018. **25**(1): p. 133-143.
135. Guha, T. and D. Malkin, *Inherited TP53 Mutations and the Li-Fraumeni Syndrome.* Cold Spring Harb Perspect Med, 2017. **7**(4).
136. Masuda, K., K. Abdelmohsen, and M. Gorospe, *RNA-binding proteins implicated in the hypoxic response.* J Cell Mol Med, 2009. **13**(9A): p. 2759-69.
137. Raspaglio, G., et al., *HuR regulates beta-tubulin isotype expression in ovarian cancer.* Cancer Res, 2010. **70**(14): p. 5891-900.
138. Raspaglio, G., et al., *Hypoxia induces class III beta-tubulin gene expression by HIF-1alpha binding to its 3' flanking region.* Gene, 2008. **409**(1-2): p. 100-8.
139. Valen, G., et al., *Hydrogen peroxide induces endothelial cell atypia and cytoskeleton depolymerization.* Free Radic Biol Med, 1999. **26**(11-12): p. 1480-8.

140. Bisig, C.G., et al., *Incorporation of 3-nitrotyrosine into the C-terminus of alpha-tubulin is reversible and not detrimental to dividing cells.* Eur J Biochem, 2002. **269**(20): p. 5037-45.
141. Eiserich, J.P., et al., *Microtubule dysfunction by posttranslational nitrotyrosination of alpha-tubulin: a nitric oxide-dependent mechanism of cellular injury.* Proc Natl Acad Sci U S A, 1999. **96**(11): p. 6365-70.
142. Joe, P.A., A. Banerjee, and R.F. Luduena, *The roles of cys124 and ser239 in the functional properties of human betaIII tubulin.* Cell Motil Cytoskeleton, 2008. **65**(6): p. 476-86.
143. Carre, M., et al., *Tubulin is an inherent component of mitochondrial membranes that interacts with the voltage-dependent anion channel.* J Biol Chem, 2002. **277**(37): p. 33664-9.
144. Zala, D., et al., *Vesicular glycolysis provides on-board energy for fast axonal transport.* Cell, 2013. **152**(3): p. 479-91.
145. Aon, M.A. and S. Cortassa, *Coherent and robust modulation of a metabolic network by cytoskeletal organization and dynamics.* Biophys Chem, 2002. **97**(2-3): p. 213-31.
146. Durrieu, C., F. Bernier-Valentin, and B. Rousset, *Microtubules bind glyceraldehyde 3-phosphate dehydrogenase and modulate its enzyme activity and quaternary structure.* Arch Biochem Biophys, 1987. **252**(1): p. 32-40.
147. Vertessy, B.G., et al., *Pyruvate kinase as a microtubule destabilizing factor in vitro.* Biochem Biophys Res Commun, 1999. **254**(2): p. 430-5.
148. Maldonado, E.N., et al., *Voltage-dependent anion channels modulate mitochondrial metabolism in cancer cells: regulation by free tubulin and erastin.* J Biol Chem, 2013. **288**(17): p. 11920-9.
149. Rostovtseva, T.K., et al., *Tubulin binding blocks mitochondrial voltage-dependent anion channel and regulates respiration.* Proc Natl Acad Sci U S A, 2008. **105**(48): p. 18746-51.
150. Azuma, K., et al., *Expression of ERCC1 and class III beta-tubulin in non-small cell lung cancer patients treated with carboplatin and paclitaxel.* Lung Cancer, 2009. **64**(3): p. 326-33.
151. Srivastava, R.K., et al., *Involvement of microtubules in the regulation of Bcl2 phosphorylation and apoptosis through cyclic AMP-dependent protein kinase.* Mol Cell Biol, 1998. **18**(6): p. 3509-17.
152. Puthalakath, H., et al., *The proapoptotic activity of the Bcl-2 family member Bim is regulated by interaction with the dynein motor complex.* Mol Cell, 1999. **3**(3): p. 287-96.
153. Knipling, L. and J. Wolff, *Direct interaction of Bcl-2 proteins with tubulin.* Biochem Biophys Res Commun, 2006. **341**(2): p. 433-9.
154. Guzun, R., et al., *Mitochondria-cytoskeleton interaction: distribution of beta-tubulins in cardiomyocytes and HL-1 cells.* Biochim Biophys Acta, 2011. **1807**(4): p. 458-69.
155. Ferlini, C., et al., *Bcl-2 down-regulation is a novel mechanism of paclitaxel resistance.* Mol Pharmacol, 2003. **64**(1): p. 51-8.
156. Andre, N., et al., *Paclitaxel induces release of cytochrome c from mitochondria isolated from human neuroblastoma cells'.* Cancer Res, 2000. **60**(19): p. 5349-53.
157. Reszka, A.A., et al., *Association of mitogen-activated protein kinase with the microtubule cytoskeleton.* Proc Natl Acad Sci U S A, 1995. **92**(19): p. 8881-5.

158. McCarroll, J.A., et al., *betaIII-tubulin is a multifunctional protein involved in drug sensitivity and tumorigenesis in non-small cell lung cancer.* Cancer Res, 2010. **70**(12): p. 4995-5003.
159. Lee, K.M., et al., *Class III beta-tubulin, a marker of resistance to paclitaxel, is overexpressed in pancreatic ductal adenocarcinoma and intraepithelial neoplasia.* Histopathology, 2007. **51**(4): p. 539-46.
160. Ferrandina, G., et al., *Class III beta-tubulin overexpression is a marker of poor clinical outcome in advanced ovarian cancer patients.* Clin Cancer Res, 2006. **12**(9): p. 2774-9.
161. Kavallaris, M., *Microtubules and resistance to tubulin-binding agents.* Nat Rev Cancer, 2010. **10**(3): p. 194-204.
162. Oakley, B.R., V. Paolillo, and Y. Zheng, *gamma-Tubulin complexes in microtubule nucleation and beyond.* Mol Biol Cell, 2015. **26**(17): p. 2957-62.
163. Goshima, G., et al., *Augmin: a protein complex required for centrosome-independent microtubule generation within the spindle.* J Cell Biol, 2008. **181**(3): p. 421-9.
164. Chumova, J., et al., *Microtubular and Nuclear Functions of gamma-Tubulin: Are They LINCed?* Cells, 2019. **8**(3).
165. Alvarado-Kristensson, M., *gamma-tubulin as a signal-transducing molecule and meshwork with therapeutic potential.* Signal Transduct Target Ther, 2018. **3**: p. 24.
166. Kultz, D., *Molecular and evolutionary basis of the cellular stress response.* Annu Rev Physiol, 2005. **67**: p. 225-57.
167. Hotamisligil, G.S. and R.J. Davis, *Cell Signaling and Stress Responses.* Cold Spring Harb Perspect Biol, 2016. **8**(10).
168. Fulda, S., et al., *Cellular stress responses: cell survival and cell death.* Int J Cell Biol, 2010. **2010**: p. 214074.
169. Hetz, C., *The unfolded protein response: controlling cell fate decisions under ER stress and beyond.* Nat Rev Mol Cell Biol, 2012. **13**(2): p. 89-102.
170. Moseley, P., *Stress proteins and the immune response.* Immunopharmacology, 2000. **48**(3): p. 299-302.
171. Bahrami, S. and F. Drablos, *Gene regulation in the immediate-early response process.* Adv Biol Regul, 2016. **62**: p. 37-49.
172. Schreiber, S.S., et al., *Activation of immediate early genes after acute stress.* Neuroreport, 1991. **2**(1): p. 17-20.
173. Song, P., et al., *The regulation of protein translation and its implications for cancer.* Signal Transduct Target Ther, 2021. **6**(1): p. 68.
174. Hershey, J.W., N. Sonenberg, and M.B. Mathews, *Principles of translational control: an overview.* Cold Spring Harb Perspect Biol, 2012. **4**(12).
175. Senft, D. and Z.A. Ronai, *Adaptive Stress Responses During Tumor Metastasis and Dormancy.* Trends Cancer, 2016. **2**(8): p. 429-442.
176. Rios-Fuller, T.J., et al., *Translation Regulation by eIF2alpha Phosphorylation and mTORC1 Signaling Pathways in Non-Communicable Diseases (NCDs).* Int J Mol Sci, 2020. **21**(15).
177. Rajesh, K., et al., *Phosphorylation of the translation initiation factor eIF2alpha at serine 51 determines the cell fate decisions of Akt in response to oxidative stress.* Cell Death Dis, 2015. **6**: p. e1591.

178. Baird, T.D., et al., *Selective mRNA translation during eIF2 phosphorylation induces expression of IBTKalpha.* Mol Biol Cell, 2014. **25**(10): p. 1686-97.
179. Muaddi, H., et al., *Phosphorylation of eIF2alpha at serine 51 is an important determinant of cell survival and adaptation to glucose deficiency.* Mol Biol Cell, 2010. **21**(18): p. 3220-31.
180. Morris, D.R. and A.P. Geballe, *Upstream open reading frames as regulators of mRNA translation.* Mol Cell Biol, 2000. **20**(23): p. 8635-42.
181. Calvo, S.E., D.J. Pagliarini, and V.K. Mootha, *Upstream open reading frames cause widespread reduction of protein expression and are polymorphic among humans.* Proc Natl Acad Sci U S A, 2009. **106**(18): p. 7507-12.
182. Vattem, K.M. and R.C. Wek, *Reinitiation involving upstream ORFs regulates ATF4 mRNA translation in mammalian cells.* Proc Natl Acad Sci U S A, 2004. **101**(31): p. 11269-74.
183. Taniuchi, S., et al., *Integrated stress response of vertebrates is regulated by four eIF2alpha kinases.* Sci Rep, 2016. **6**: p. 32886.
184. Guo, L., et al., *Phosphorylated eIF2alpha predicts disease-free survival in triple-negative breast cancer patients.* Sci Rep, 2017. **7**: p. 44674.
185. Smit, E., J.C.S. Kleinjans, and T. van den Beucken, *Phosphorylation of eIF2alpha promotes cell survival in response to benzo[a]pyrene exposure.* Toxicol In Vitro, 2019. **54**: p. 330-337.
186. Stephens, S.B. and C.V. Nicchitta, *Divergent regulation of protein synthesis in the cytosol and endoplasmic reticulum compartments of mammalian cells.* Mol Biol Cell, 2008. **19**(2): p. 623-32.
187. Danan, C., S. Manickavel, and M. Hafner, *PAR-CLIP: A Method for Transcriptome-Wide Identification of RNA Binding Protein Interaction Sites.* Methods Mol Biol, 2016. **1358**: p. 153-73.
188. Castellanos-Rubio, A., et al., *A novel RT-QPCR-based assay for the relative quantification of residue specific m6A RNA methylation.* Sci Rep, 2019. **9**(1): p. 4220.
189. Pazarentzos, E. and T.G. Bivona, *Adaptive stress signaling in targeted cancer therapy resistance.* Oncogene, 2015. **34**(45): p. 5599-606.
190. Rastogi, R.P., et al., *Molecular mechanisms of ultraviolet radiation-induced DNA damage and repair.* J Nucleic Acids, 2010. **2010**: p. 592980.
191. Cipponi, A., et al., *MTOR signaling orchestrates stress-induced mutagenesis, facilitating adaptive evolution in cancer.* Science, 2020. **368**(6495): p. 1127-1131.
192. Verma, N., et al., *DNA Damage Stress: Cui Prodest?* Int J Mol Sci, 2019. **20**(5).
193. Zander, G., et al., *mRNA quality control is bypassed for immediate export of stress-responsive transcripts.* Nature, 2016. **540**(7634): p. 593-596.
194. Meyer, K.D., et al., *5' UTR m(6)A Promotes Cap-Independent Translation.* Cell, 2015. **163**(4): p. 999-1010.
195. Protter, D.S.W. and R. Parker, *Principles and Properties of Stress Granules.* Trends Cell Biol, 2016. **26**(9): p. 668-679.
196. Belyi, V.A., et al., *The origins and evolution of the p53 family of genes.* Cold Spring Harb Perspect Biol, 2010. **2**(6): p. a001198.
197. Blanco, S. and M. Frye, *Role of RNA methyltransferases in tissue renewal and pathology.* Curr Opin Cell Biol, 2014. **31**: p. 1-7.

198. Engel, M., et al., *The Role of m(6)A/m-RNA Methylation in Stress Response Regulation.* Neuron, 2018. **99**(2): p. 389-403 e9.
199. Nadezhdina, E.S., et al., *Microtubules govern stress granule mobility and dynamics.* Biochim Biophys Acta, 2010. **1803**(3): p. 361-71.
200. Brock, A., S. Huang, and D.E. Ingber, *Identification of a distinct class of cytoskeleton-associated mRNAs using microarray technology.* BMC Cell Biol, 2003. **4**: p. 6.
201. Rossello, C.A., et al., *gamma-Tubulin(-)gamma-Tubulin Interactions as the Basis for the Formation of a Meshwork.* Int J Mol Sci, 2018. **19**(10).
202. Trinczek, B., et al., *MARK4 is a novel microtubule-associated proteins/microtubule affinity-regulating kinase that binds to the cellular microtubule network and to centrosomes.* J Biol Chem, 2004. **279**(7): p. 5915-23.
203. Heidary Arash, E., et al., *MARK4 inhibits Hippo signaling to promote proliferation and migration of breast cancer cells.* EMBO Rep, 2017. **18**(3): p. 420-436.
204. Oba, T., et al., *Microtubule affinity-regulating kinase 4 with an Alzheimer's disease-related mutation promotes tau accumulation and exacerbates neurodegeneration.* J Biol Chem, 2020. **295**(50): p. 17138-17147.
205. Clement, M., et al., *MARK4 (Microtubule Affinity-Regulating Kinase 4)-Dependent Inflammasome Activation Promotes Atherosclerosis-Brief Report.* Arterioscler Thromb Vasc Biol, 2019. **39**(8): p. 1645-1651.
206. Timm, T., et al., *Structure and regulation of MARK, a kinase involved in abnormal phosphorylation of Tau protein.* BMC Neurosci, 2008. **9 Suppl 2**: p. S9.
207. Mohammad, T., et al., *Identification and evaluation of bioactive natural products as potential inhibitors of human microtubule affinity-regulating kinase 4 (MARK4).* J Biomol Struct Dyn, 2019. **37**(7): p. 1813-1829.
208. Noma, K., et al., *Microtubule-dependent ribosome localization in C. elegans neurons.* Elife, 2017. **6**.
209. Stephens, S.B., et al., *Analysis of mRNA partitioning between the cytosol and endoplasmic reticulum compartments of mammalian cells.* Methods Mol Biol, 2008. **419**: p. 197-214.
210. Yoshikawa, H., et al., *Efficient analysis of mammalian polysomes in cells and tissues using Ribo Mega-SEC.* Elife, 2018. **7**.
211. Ingolia, N.T., et al., *The ribosome profiling strategy for monitoring translation in vivo by deep sequencing of ribosome-protected mRNA fragments.* Nat Protoc, 2012. **7**(8): p. 1534-50.
212. Kim, Y., et al., *PKR Senses Nuclear and Mitochondrial Signals by Interacting with Endogenous Double-Stranded RNAs.* Mol Cell, 2018. **71**(6): p. 1051-1063 e6.
213. Williams, B.R., *PKR; a sentinel kinase for cellular stress.* Oncogene, 1999. **18**(45): p. 6112-20.
214. Tang, Y., et al., *Role of PKR in the Inhibition of Proliferation and Translation by Polycystin-1.* Biomed Res Int, 2019. **2019**: p. 5320747.
215. Jammi, N.V., L.R. Whitby, and P.A. Beal, *Small molecule inhibitors of the RNA-dependent protein kinase.* Biochem Biophys Res Commun, 2003. **308**(1): p. 50-7.

216. Spitzer, J., et al., *PAR-CLIP (Photoactivatable Ribonucleoside-Enhanced Crosslinking and Immunoprecipitation): a step-by-step protocol to the transcriptome-wide identification of binding sites of RNA-binding proteins.* Methods Enzymol, 2014. **539**: p. 113-61.